Versatile synthesis and properties of sulfonated polyphenylene derivatives

A Doctoral Thesis

Presented to

Special Doctoral Program for Green Energy Conversion Science and Technology

Integrated Graduate School of Medicine, Engineering and Agricultural Science

University of Yamanashi

March 2020

Ibuki Hosaka

Contents

Chapter 1: Introduction

1.1 General introduction

Since the industrial revolution, several countries centered upon the United Kingdom had achieved economic, industrial and agricultural development. In particular, energy revolution from the natural energy to fossil fuel such as petroleum and coal significantly improved the productivity of manufactured product, which made the rich and convenient life.[1] However, economic development with the fossil fuel was a burden to environment due to the emission of a large amount of greenhouse gases such as CO_2, NOx and SOx. In 1896, Arrhenius reported that concentration of CO_2 in the atmosphere impacted on the temperature of the ground.[2] It has been reported so far that the globally averaged combined land and ocean surface temperature increased by 0.85 ^{o}C from 1880 to 2012, and CO_2 concentration in the atmosphere have also increased by 40% since pre-industrial times.[3] Therefore, increase of CO_2 concentration in the atmosphere is considered as matter of major cause for global warming. To investigate the detail of correlation between the CO_2 concentration in atmosphere and global warming, ministry of the environment, national institute for environmental studies (NIES) and Japan aerospace exploration agency (JAXA) developed the greenhouse gases observing satellite (GOSAT) called as "IBUKI" and started the measurement of CO_2 concentration in the atmosphere.[4] As shown in Figure 1-1, CO_2 concentration has been increasing by approximately 2 ppm per year from 2009, despite improved energy conversion system with low emission of CO_2.[5] To reduce the CO_2 concentration in the atmosphere, the several innovative energy conversion systems without fossil fuels such as solar, hydro, wind and geothermal are developed. In particular, proton

exchange membrane fuel cells using hydrogen as a fuel have attracted much attention to create the low carbon societies.

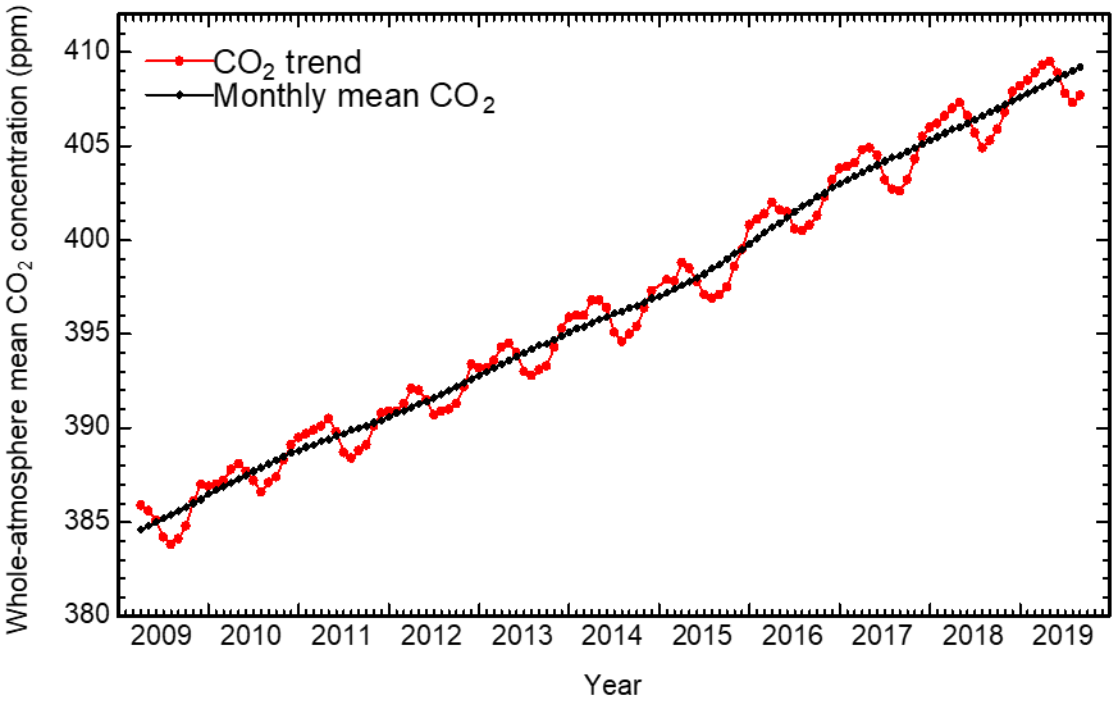

Figure 1-1. Trend of whole-atmosphere mean CO_2 concentration measured by IBUKI.[5]

1.2 Proton exchange membrane fuel cells (PEMFCs)

1.2.1 Current status and issues of PEMFCs

Proton exchange membrane fuel cells (PEMFCs) have attracted considerable attention as alternative energy devices to traditional thermal power generation and internal combustion engines because PEMFCs operated with pure H_2 emit only water as a by-product, i.e., zero-carbon energy conversion system.[6-9] In 2009, co-generation fuel cell systems (CG-FCs) have been commercialized in Japan, which provided not only electric power but also hot water at the household. Thus, energy conversion efficiency of CG-FCs is at least 80% and significantly

higher than that of thermal power plant. The vehicles that installed PEMFCs (FCVs) instead of gasoline engine were also developed and started into market from 2014 in Japan. Ministry of economy, trade and industry (METI) set a binding target to introduce 5,300,000 units of CG-FCs and 800,000 units of FCVs until 2030 in Japan.[10] As of March of 2019, 276,217 units[11] of CG-FCs and 3,056 units[12] of FCVs have already been introduced in Japan; however, these numbers are far from achievement of target due to delaying in the spread by the technical issues for PEMFCs. Therefore, several technical challenges for PEMFCs such as lifetime, safety, mass productivity, filling time of fuel and infrastructure e.g., hydrogen production, storage, transportation and distribution (gas station) have to be solved to achieve the above target. Among them, cost reduction of PEMFCs is especially big agenda for dissemination of PEMFCs in the market. Figure 1-2 shows the cost analysis of the 2017 projected fuel cell stack at 100,000 system per year. The proton exchange membrane occupies 12% of the total cost of PEMFCs and incurs the high cost of the system.[13] Therefore, cost effective proton exchange membranes with improved properties are strongly required.

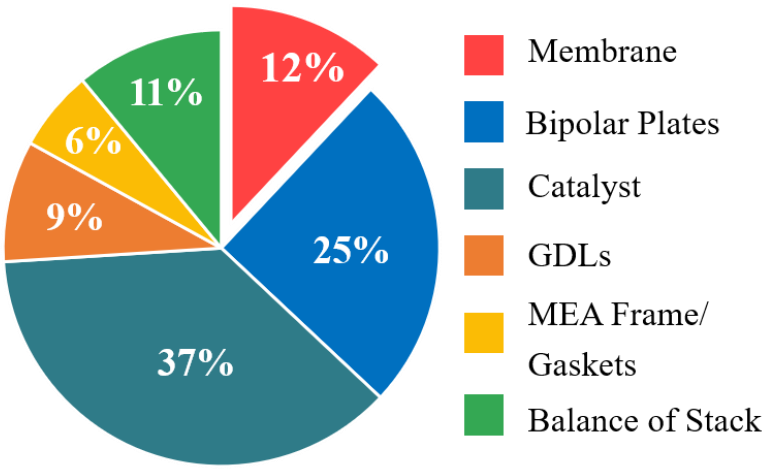

Figure 1-2. Breakdown of the 2017 projected fuel cell stack cost at 100,000 system per year[13]

1.2.2 Perfluorosulfonic acid ionomers as proton exchange membrane

Perfuluorosulfonic acid (PFSA) ionomers such as Nafion is generally used as proton exchange membrane in the PEMFCs because PFSA ionomers show 0.1~0.01 S cm^{-1} of proton conductivity at 80 ^{o}C due to high acid dissociation constant of the perfluorosulfonic acid groups (p*K*a: -5.5 to -6). Generally, the strong electron-withdrawing nature of fluorine atoms leads to stabilization of $–CF_2\text{-}SO_3^-$ as the conjugate base, thus protons of sulfonic acid groups can easily dissociate in the presence of water and become a good source of the proton.[14] Furthermore, the hydrophilic side-chain with super acidity promotes the formation of ionic clusters and well-connected ionic path way within the hydrophobic matrix, resulting in the improvement of the proton conductivity. Currently, PFSA ionomer reinforced with PTFE called as Nafion XL has been developed and exhibited approximately two times higher storage modulus (E') than that of commercial Nafion 212.[15] Y. Oshiba et al. also reported that the pore-filled membrane consisting of prepared PFSA ionomer and ultra-high molecular weight polyethylene (UHMWPE) showed much higher tensile strength value (70.0 MPa) than that of commercial Nafion 211 (29.4 MPa).[16] Gore and associates also developed the reinforced PFSA ionomer with the expanded polytetrafluoroethylene (ePTFE) called as GORE-SELECT membrane which has been made as thin as approximately 5 μm, resulting in minimizing ohmic losses of fuel cell.[14,17]

However, there still remain problems associated with PFSA membranes. PFSA membranes suffer from some disadvantages such as low environmental compatibility, high production cost, and high gas permeability. As mentioned above, in order for wider spread commercialization of PEMFCs, the cost of proton exchange membrane should be reduced, specifically from

$1000 m^{-2} (present) to $10 m^{-2} (final target). To overcome these drawbacks of PFSA ionomers, one of the attractive candidates is sulfonated aromatic ionomers because of potentially low cost, high versatility of molecular structure and high gas barrier properties.

1.2.3 Current trends and issues of sulfonated aromatic ionomers

To replace state-of-the-art PFSA ionomers, sulfonated aromatic ionomers have been researched and developed all over the world. As representatives, poly(arylene ether)s (SPAEs),[18] poly(arylene sulfide)s (SPASs)[19], polyimides (SPIs)[20], and polybenzimidazoles (PBIs)[21] have been studied and some were claimed to show the superior mechanical and thermal stability compared with PFSA ionomers because of their rigid polymer backbone structures. In particular, SPAE ionomers which could be synthesized from inexpensive raw materials via simple synthetic route (e.g., nucleophilic aromatic substitution reaction) have attracted much attention to replace PFSA ionomers. Kim et al. reported that pendant dual-sulfonated poly(arylene ether ketone)s (SPEEKs) multiblock copolymers with 1.92 meq g^{-1} of ion exchange capacity (IEC) estimated by inverse titration method exhibited the excellent proton conductivity (80 mS cm^{-1}) at 80 ^{o}C and 80% RH due to the well-developed phase-separation with well-connected hydrophilic ionic channel (Figure 1-3).[22]

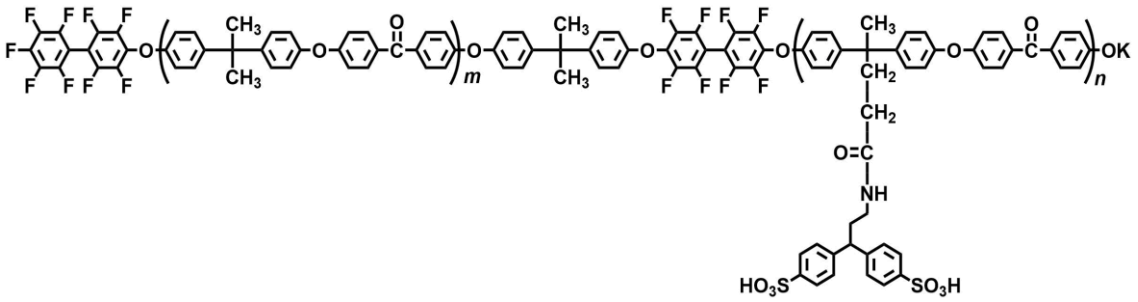

Figure 1-3. Chemical structure of pendant dual-sulfonated poly(arylene ether ketone)s.[22]

McGrath et al. clarified that the longer block length of hydrophilic and hydrophobic repeating units in the polymer main chain induced more distinct nanophase separation and better connectivity among the ionic domains i.e., the primary structure (or sequence of the components) of the polymer chain affected the membrane morphology and proton conductivity (Figure 1-4).[23] However, most sulfonated aromatic ionomers showed the low chemical stability to radial species derived from hydrogen peroxide, accordingly indicating the lower cell performance and lifetime for FC stacks.

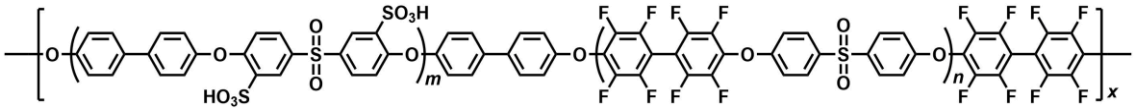

Figure 1-4. Chemical structure of BisSF-BPSH multiblock copolymer.[23]

1.2.4 Chemical degradation mechanism of SPAE ionomers

Radical species such as hydroxyl and hydroperoxyl radicals are produced as by-product in the operating PEMFCs conditions at both electrode sides. In the anode side, oxygen permeated through the membrane from the cathode to the anode directly reacts with H_2, which generates the hydrogen peroxide followed by incomplete reduction at the surface of the anode catalyst. On the other hand, oxygen reduction at the cathode proceeds not only four-electron process but also two-electron process, resulting in the generation of hydrogen peroxide. Radical species are known to form by homolytic and heterolytic dissociation of hydrogen peroxide, in particular, in the presence of Fe ions. [24]

In general, radical species which are produced as by-product in FC operating conditions cause the chemical degradation of the proton exchange membrane, which lead to the increase

of the electric resistance and the gas permeability of hydrogen. As a result, decrease of fuel utilization and electrical short circuit of FCs are caused.[25-27] Currently, Mukerjee et al. reported the chemical degradation mechanism of SPAE ionomers as shown in scheme 1-1. Hydroxyl radical attacks to the positions of the aromatic ring next to the ether linkage because of high electron density provided from the unshared electron pair of oxygen. After the addition of hydroxyl radical, the scission of the ether bonds might take place by *ipso*-attack of hydroxyl radical to the -OR groups, due to the activating effect of hydroxyl substituents in the *ortho* position to -OR (Scheme 1-1 (a)).[28] Another possibility is the direct *ipso*-attack of hydroxyl radicals to the -OR groups of typical poly(arylene ether)s as shown in Scheme 1-1 (b).[28]

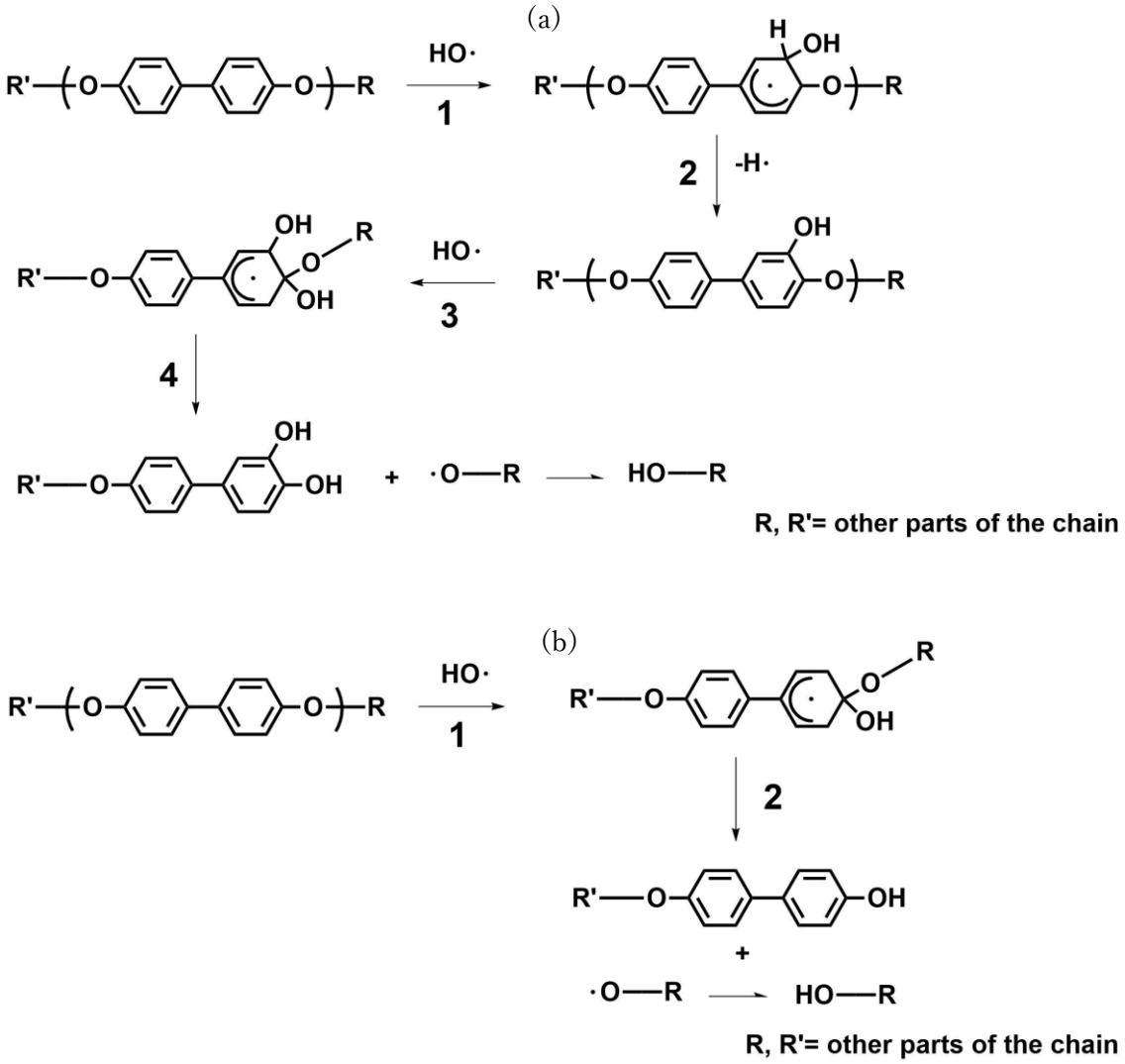

Scheme 1-1. Chemical degradation process of SPAE ionomers.[28]

1.2.5 Approach for improvement of the chemical stability

As mentioned above, sulfonated aromatic ionomers containing the ether linkage are vulnerable to radical species because of high electron density provided from the unshared electron pair of oxygen. Therefore, many researchers have studied to improve the chemical stability of sulfonated aromatic ionomers, and there seemed two major approaches as follows to overcome these issues

1) Addition of the radical scavengers in the membranes

Cerium ion is a typical additive to quench the radical species. Kim et al. suggested the radical quenching mechanism through reversible oxidation and reduction of Ce^{3+} and Ce^{4+} as follows.[29] Endoh et al. also reported that the use of Ce^{3+} as radical quencher enhanced the chemical stability of PFSA ionomer by a factor of 100 to 1,000. Moreover, fuel cell with Ce^{3+} composite PFSA ionomer could operate for 6,000 hours at 120 °C and 50% relative humidity condition.[30]

$$Ce^{3+} + \cdot OH + H^{+} \rightarrow Ce^{4+} + H_2O \quad (1)$$

$$Ce^{3+} + \cdot OOH + H^{+} \rightarrow Ce^{4+} + H_2O_2 \quad (2)$$

$$Ce^{4+} + H_2O_2 \rightarrow Ce^{3+} + \cdot OOH + H^{+} \quad (3)$$

$$Ce^{4+} + \cdot OOH \rightarrow Ce^{3+} + O_2 + H^{+} \quad (4)$$

Kim et al. reported that the weight loss of cerium composite SPEEKs after Fenton's test at room temperature is only 27%, where pristine sulfonated aromatic ionomer showed 100% of weight loss.[29]

However, the cerium ion composite membrane system has two disadvantages. First, cerium ion deactivates (or neutralizes) the ion conduction groups and leads to decrease the number

of the proton, decreasing the proton conductivity and the cell performance. Second, cerium ions are mobile in the operating PEMFCs conditions and thus easy to leach out from the membrane by diffusion process.

2) Elimination of ether linkages from the polymer backbone

As discussed in the section 1.2.4, chemical degradation by radical species occurs at the or near the polar linkage such as ether. Holdcroft et al. reported that a sulfophenylated terphenylene copolymer membrane without ether linkage having IEC of 3.70 meq g^{-1} displayed no practical weight loss and chemical degradation in the oxidative stability test (at 80 °C in Fenton's reagent (Figure 1-5).[31]

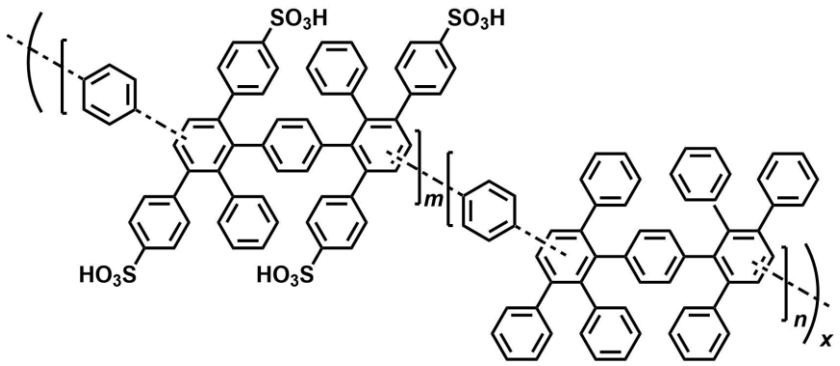

Figure 1-5. Chemical structure of sulfonated phenylated poly(phenylene) (sPPP).[31]

Our laboratory has also developed a series of sulfonated aromatic ionomers without the ether linkage in polymer main chain composed of sulfo-1,4-phenylene groups as the hydrophilic component, and hexafluoroisopropylidene (SBAF)[32], or quinquephenylene (SPP-QP)[33] groups as the hydrophobic component. As shown in Table 1, these membranes had significantly high chemical stability in the oxidative stability test.[32,33] However, these

sulfonated aromatic copolymers required costly, air- and moisture-sensitive Ni(0) complex, bis(1,5-cyclooctadiene)nickel(0) ($Ni(COD)_2$), as a promoter for efficient C-C coupling copolymerization reactions to obtain high molecular weight polymers, which undermines the advantages of potentially inexpensive hydrocarbon-based materials.

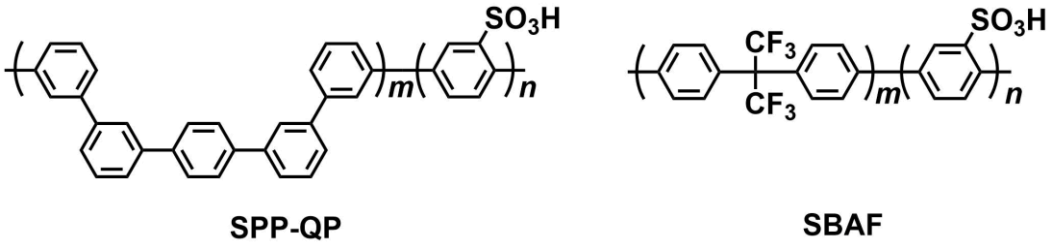

Figure 1-6. Chemical structure of SPP-QP and SBAF copolymers.[32,33]

Table 1-1. Oxidative stability of SPP-QP and SBAF membranes.[32,33]

Copolymer	IEC[a](meq g^{-1})	Residue[b] (%)		
		Weight	Molecular weight[c]	IEC[a]
SPP-QP	2.4	99	99	100
SBAF	1.5	100	100	100
SBAF	2.5	100	100	100
SBAF	3.0	100	100	100

a: Calculated from back titration b: After Fenton's test at 80 °C for 1 h.

c: Determined by GPC analyses (calibrated with polystyrene standards).

1.3 Objective of this PhD research

For all of these reasons, sulfonated aromatic ionomer membranes are greatly demanded as alternatives to the PFSA ionomers, however, chemically stable sulfonated aromatic ionomer with cost-effectiveness has not been developed yet. Therefore, the objective of this PhD research is to develop a highly proton conductive sulfonated aromatic ionomer with high chemical stability in consideration of mass production and dissemination. To accomplish this objective, two approaches, i.e., effect of radical quencher and elimination of ether linkage, have been tried and investigated as explained in chapter 1.2.5. in this doctoral thesis.

In chapter 2, the phosphine oxide moiety serving as a radical quencher is focused to improve the oxidative stability and by direct introduction into polymer main chain of SPAE with low cost and simply synthetic procedure. The effect of triphenyl phosphine oxide moieties in hydrophilic components on oxidative stability is explained.

In chapter 3, new versatile synthesis method for sulfonated aromatic copolymers using commercially available and low-cost $NiBr_2$ is investigated. Moreover, effect of difference in the synthetic route between conventional method with Ni(0) complex and new method with $NiBr_2$ on the membrane properties such as proton conductivity, mechanical property and membrane morphology is also investigated in detail in chapter 4.

1.4 References

1 J. R. McNeill, S*omething New Under the Sun An Environmental History of the Twentieth-Century World*, (2001)

2 S. Arrhenius, *Lond. Edinb. Dublin Phil. Mag. J. Sci. (5th ser.)*. **1896**, *41*, 237.

3 IPCC "*Climate Change 2013 - The Physical Science Basis*" https://www.ipcc.ch/site/assets/uploads/2018/02/WG1AR5_SPM_FINAL.pdf

4 Satellite Observation Center "*Global Greenhouse Gas Observation by Satellite GOSAT Project*" http://www.gosat.nies.go.jp/eng/GOSAT_pamphlet_en.pdf

5 National Institute for Environmental Studies "*Whole-atmosphere monthly mean CO2 concentration based on GOSAT observations -Recent data-*" http://www.gosat.nies.go.jp/en/recentglobalghg.html

6 E4tech Strategy Energy Sustainability "The *Fuel Cell Industry Review 2018*" https://www.californiahydrogen.org/wp-content/uploads/2019/01/TheFuelCellIndustryReview2018.pdf

7 F. Baldi, L. Wang, M. Pérez-Fortes, F. Marechal, *Frontiers in Energy Research* **2018**, *6*, 139.

8 A. Arshad, H.M. Ali, A. Habib, M.A. Bashir, M. Jabbal, Y. Yan, *Therm. Sci. Eng. Prog.* **2019**, *9*, 308.

9 I. Staffell, D. Scamman, A.V. Abad, P. Balcombe, P.E. Dodds, P. Ekins, N. Shah, K.R. W ard, *Energy Environ. Sci.* **2019**, *12*,463.

10 METI "The Strategic Road Map for Hydrogen and Fuel Cells ～Industry-academia-

government action plan to realize Hydrogen Society～”

https://www.meti.go.jp/press/2018/03/20190312001/20190312001-1.pdf

11 Enefarm Partners

https://www.gas.or.jp/user/comfortable-life/enefarm-partners/common/data/20190423_web.pdf

12 METI “Progress of The Strategic Road Map for Hydrogen and Fuel Cells”

https://www.meti.go.jp/shingikai/energy_environment/suiso_nenryo/roadmap_hyoka_wg/pdf/001_04_00.pdf

13 DOE Hydrogen and Fuel Cells Program Record “Fuel Cell System Cost -2017-“

https://www.hydrogen.energy.gov/pdfs/17007_fuel_cell_system_cost_2017.pdf

14 A. Kusoglu, A. Z. Weber, *Chem. Rev.* **2017**, *117*, 987.

15 S. Shi, A.Z. Weber, A. Kusoglu, *J. Membr. Sci.* **2016**, *516*, 123.

16 Y. Oshiba, J. Tomatsu, T. Yamaguchi, *J. Power Sources* **2018**, *394*, 67.

17 W. Liu, T. Suzuki, H. Mao, T. Schmiedel, *ECS Trans.* **2012**, *50*, 51..

18 D.W. Shin, M.D. Guiver, Y.M. Lee, Chem. Rev. **2017**, *117*, 4759.

19 Z. Wang, H.Z. Ni, C.J. Zhao, M.Y. Zhang, H. Na, *J. Appl. Polym. Sci.* **2009**, *112*, 858.

20 K.H. Lee, S.Y. Lee, D.W. Shin, C. Wang, S.-H. Ahn, K.-J. Lee, M.D. Guiver, Y.M. Lee, *Polymer* **2014**, *55*, 1317.

21 X. Qiu, M. Ueda, H. Hu, Y. Sui, X. Zhang, L. Wang, *ACS Appl. Mater. Interfaces* **2017**, *9*, 33049.

22 K. Kang, D. Kim, *J. Membr. Sci.* **2019**, *578*, 103.

23 H. Lee, A.S. Badami, A. Roy, J.E. McGrath, *J. Polym. Sci. Part A Polym. Chem.*, **2007**, *45*,

4879.

24 M. Ghelichi, P.-É.A. Melchy, M.H. Eikerling, *J. Phys. Chem. B* **2014**, *118*, 11375.

25 J.R. Yu, B.L. Yi, D.M. Xing, F.Q. Liu, Z.G. Shao, Y.Z. Fu, H.M. Zhang, *Phys. Chem. Chem. Phys.* **2003**, *5*, 611.

26 A.B. LaConti, H. Liu, C. Mittelsteadt, R.C. McDonald, *ECS Trans.* **2006**, *1*, 199.

27 D.A. Schiraldi, D. Savant, C. Zhou, *ECS Trans.* **2010**, *33*, 883.

28 L. Zhang, S. Mukerjee, *J. Electrochem. Soc.* **2006**, *153*, A1062.

29 S. Yang, D. Kim, *J. Power Sources* **2018**, *393*, 11.

30 E. Endoh, N. Onoda, Y. Kaneko, Y. Hasegawa, S. Uchiike, Y. Takagi, T. Take, *ECS Electrochem. Lett.* **2013**, *2*, F73.

31 T. J. G. Skalski, M. Adamski, B. Britton, E. M. Schibli, T. J. Peckham, T. Weissbach, T. Moshisuki, S. Lyonnard, B. J. Frisken, S. Holdcroft, *ChemSusChem* **2018**, *11*, 4033.

32 J. Ahn, R. Shimizu, K. Miyatake, *J. Mater. Chem. A* **2018**, *6*, 24625.

33 J. Miyake, R. Taki, T. Mochizuki, R. Shimizu, R. Akiyama, M. Uchida, K. Miyatake, *Sci. Adv.* **2017**, *3*, eaao0476.

Chapter 2: Effect of Sulfonated Triphenylphosphine Oxide Groups in Aromatic Block Copolymers as Proton-exchange Membranes

2.1 Introduction

Proton-exchange membranes (PEMs) are one of the key components in proton-exchange membrane fuel cells.[1] Currently, perfluorinated (PFSA) ionomer membranes are state-of-the-art because they show very high proton conductivity and good mechanical and chemical stability under fuel cell operating conditions. However, there has been great demand for fluorinefree PEMs in order to lower the production cost and the environmental impact.

Sulfonated poly(arylene ether)s (SPAEs) are one of the most studied alternative PEMs due to the easy synthetic process, molecular design versatility, and good film forming capability.[2-10] Among them, the multiblock copolymers composed of sulfonated and un-sulfonated blocks showed improved proton conductivity due to a well-developed hydrophilichydrophobic phase-separated morphology with interconnected ionic channels.[11-15] Most SPAE based PEMs, however, suffer from insufficient mechanical stability under wet/dry cycle conditions. Furthermore, the poor oxidative stability of SPAE-based PEMs is also a critical issue.

To address these issues, our laboratory has demonstrated that the introduction of sulfonated triphenylphosphine oxide moieties contributes to the improvement of the oxidative stability of SPAE-based PEMs (PK,[16] Figure 2-1). Although the position and content of the sulfonated triphenylphosphine oxide moieties must affect the oxidative and mechanical stability of the membranes, a study on such detailed structure properties relationships is yet to be

demonstrated. In this paper, I report the synthesis of novel SPAE-based PEMs having dense sulfonated triphenylphosphine oxide moieties (PP, Figure 2-1). The properties of the PP membranes are compared with those of the PK membrane sharing similar hydrophobic blocks but with a different density of the sulfonated triphenylphosphine oxide moieties.

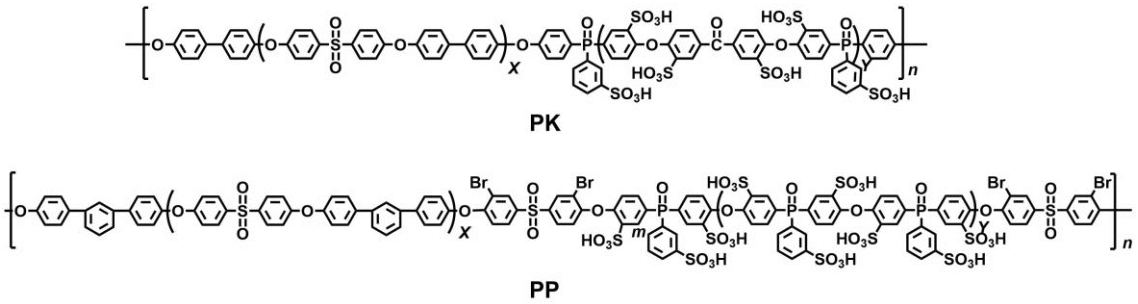

Figure 2-1. Chemical structure of the PP copolymer and the reference copolymer PK.

2.2 Experimental

2.2.1 Materials

N,N-Dimethylacetamide (DMAc), dimethyl sulfoxide (DMSO), *N*-methyl-2-pyrrolidinone (NMP), toluene (dehydrated), 30 wt% oleum, sulfuric acid (96%), hydrochloric acid (35-37%), potassium carbonate (K_2CO_3), calcium carbonate ($CaCO_3$), and sodium chloride (NaCl) were purchased from Kanto Chemical Co. and used as received. Bis(4-fluorophenyl)sulfone (FPS) and N-bromosuccinimide (NBS) were purchased from TCI Inc. and used as received. Methanol was purchased from Wako and used as received. DMSO-d_6 (0.03% tetramethylsilane (TMS) and 99.9 atom% D) and 1,1,2,2-tetrachloroethane-d_2 (TCE-d_2, 99 atom% D) were purchased from Acros Organics and used as received. Spectra/Por 6 dialysis tubing (1,000 Da MWCO) was purchased from Spectrum Laboratories, Inc. and used as received. Bis(4-fluorophenyl)phenylphosphine oxide (FPPO) was purchased

from Aldrich and used as received. *m*-Terphenyl (MTP) monomer, 1,3-bis(4-hydroxyphenyl)benzene, was provided by Honshu Chemical Industry Co., Ltd. and used as received. Bis(4-hydroxyphenyl)phenylphosphine oxide (BHPPO)[17] and bis(3-bromo-4-fluorophenyl)sulfone (BrFPS)[18] were synthesized according to the literature.

2.2.2 Measurements

^{1}H (500 MHz), ^{19}F (471 MHz), and ^{31}P (202 MHz) NMR spectra were obtained on a JEOL JNM-ECA 500 using DMSO-d_6 or TCE-d_2. Apparent molecular weight was estimated from gel permeation chromatography (GPC) system with a Jasco 805 UV detector. DMF containing 0.01 M LiBr was used as eluent. A Shodex K-805L column was used for sulfonated compounds and a Shodex SB-803HQ column was used for un-sulfonated compounds, respectively. Molecular weight was calibrated with standard polystyrene samples. Ion exchange capacity (IEC) values of membranes were calculated from back-titration method. Water uptake and proton conductivity were measured at 80 °C with a solid electrolyte analyzer system (MSBAD-V-FC, Bel Japan Co.) equipped with a temperature and humidity controllable chamber. Weight of the membranes was measured by magnetic suspension balance at given humidity, and then water uptake ((weight of hydrated membrane) – (weight of dry membrane) / weight of dry membrane × 100) was obtained. Vacuum drying for 3 h at 80 °C gave the weight of dry membranes and exposure to a targeted humidity for at least 2 h gave the weight of hydrated membranes. Proton conductivity was measured using four-probe conductivity cell attached with impedance spectroscopy (Solartron 1255B and 1287) simultaneously in the same chamber. Ion conducting resistances (R) were determined from

the impedance plot obtained in the frequency range from 1 to 105 Hz. The proton conductivity (σ) was calculated from the equation $\sigma = l / (A \times R)$, where l and A are the distance between the two inner Au wires and the conducting area, respectively. Dynamic mechanical analysis (DMA) was carried out with an ITK DVA-225 dynamic viscoelastic analyzer. Humidity dependence of storage modulus (E'), loss modulus (E''), and tan δ at 80 ^{o}C was investigated for membranes (5 mm × 30 mm) at a humidification rate of 1% relative humidity (RH) per minute. Oxidative stability of membranes was checked by immersing membranes in Fenton's reagent (3% H_2O_2, 2 ppm $FeSO_4$) at 80 ^{o}C for 1 h. Loss of weight and molecular weight were checked for the samples after the stability test. For TEM observations, the membranes were stained with lead ions by ion exchange of the sulfonic acid groups in 0.5 M lead (II) acetate aqueous solution, rinsed with deionized water, and dried. The stained membranes were embedded in epoxy resin, sectioned to 50 nm thickness with Leica microtome Ultracut UCT, and placed on copper grids. Images were taken on a Hitachi H-9500 TEM with an accelerating voltage of 200 kV.

2.2.3 Synthesis of the hydroxy (OH)-terminated telechelic oligomers 1

A typical procedure is as follows (X=3). A 100 mL three-necked round bottom flask equipped with a magnetic stirring bar, a condenser, a Dean-Stark trap, and a nitrogen inlet/outlet, was charged with MTP monomer (3.81 mmol), FPS (2.86 mmol), K_2CO_3 (9.52 mmol), DMAc (6.7 mL), and toluene (0.5 mL). The mixture was heated at 140 ^{o}C for 3 h. After the reaction, the reaction mixture was poured into a 1 M hydrochloric acid to precipitate a solid. The crude product was washed with hot deionized water and hot methanol several

times. Drying in a vacuum oven gave oligomer in 89% yield (X values; targeted = 3.0, ^{1}H NMR = 5.1, GPC = 7.5).

X=6 was prepared under the condition similar to that for X = 3. MTP monomer (5.72 mmol), FPS (4.90 mmol), K_2CO_3 (14.3 mmol), DMAc (10 mL), and toluene (0.5 mL) were used. 93% yield (X values; targeted = 6.0, ^{1}H NMR = 10, GPC = 12).

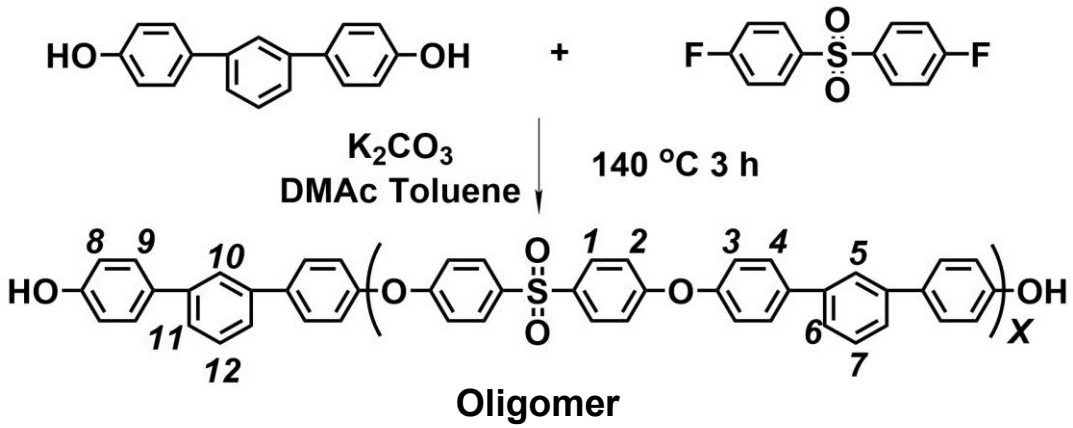

Scheme 2-1. Synthesis of the hydroxy (OH)-terminated telechelic oligomers 1

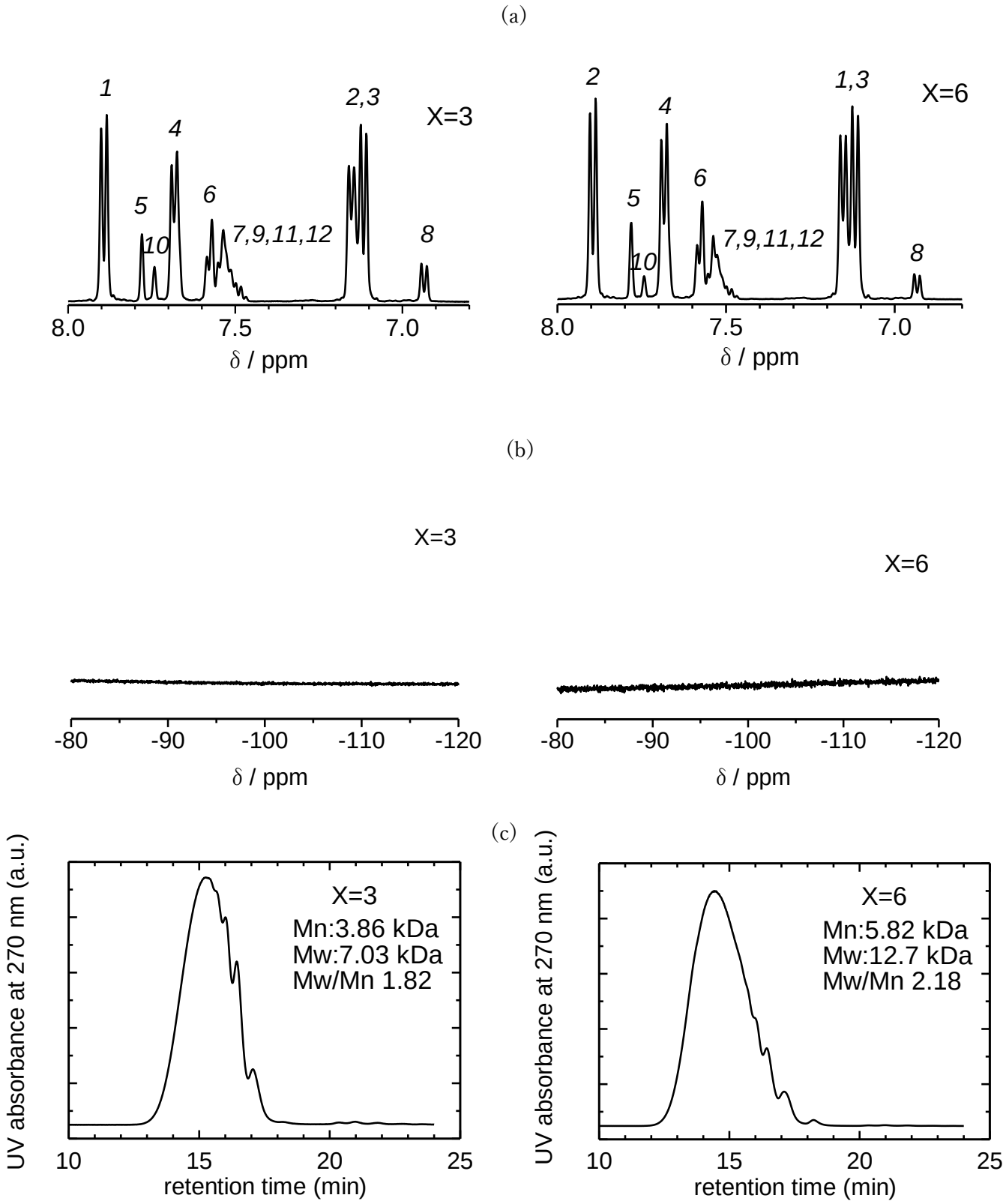

Figure 2-2. (a) ^{1}H, (b) ^{19}F NMR spectra (TCE-d_2, 80 °C), and (c) GPC profile of 1 oligomer.

2.2.4 Synthesis of the hydrophilic oligomer containing the phosphine oxide moiety [BHPPO-terminated oligomer]

A 100 mL three-necked round bottom flask equipped with a magnetic stirring bar, a condenser, a Dean-Stark trap, and a nitrogen inlet/outlet, was charged with BHPPO (4.83 mmol), FPPO (2.42 mmol), K_2CO_3 (12.1 mmol), DMAc (8 mL), and toluene (1.6 mL). After the reaction was conducted at 160 °C for 20 h, the reaction mixture was poured into a 1 M hydrochloric acid to precipitate a solid. The crude product was washed with hot deionized water several times. Drying in a vacuum oven gave oligomer in 87% yield (Y values; targeted = 1.0, ^{1}H NMR = 1.6).

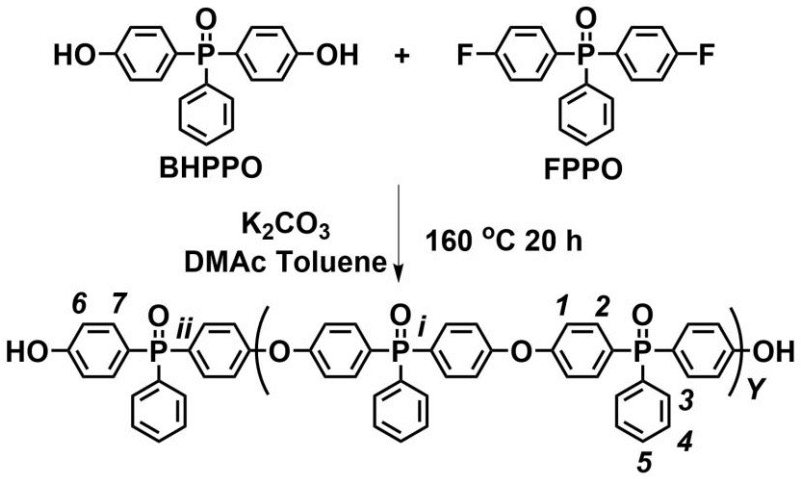

Scheme 2-2. Synthesis of the hydrophilic oligomer containing the phosphine oxide moiety [BHPPO-terminated oligomer]

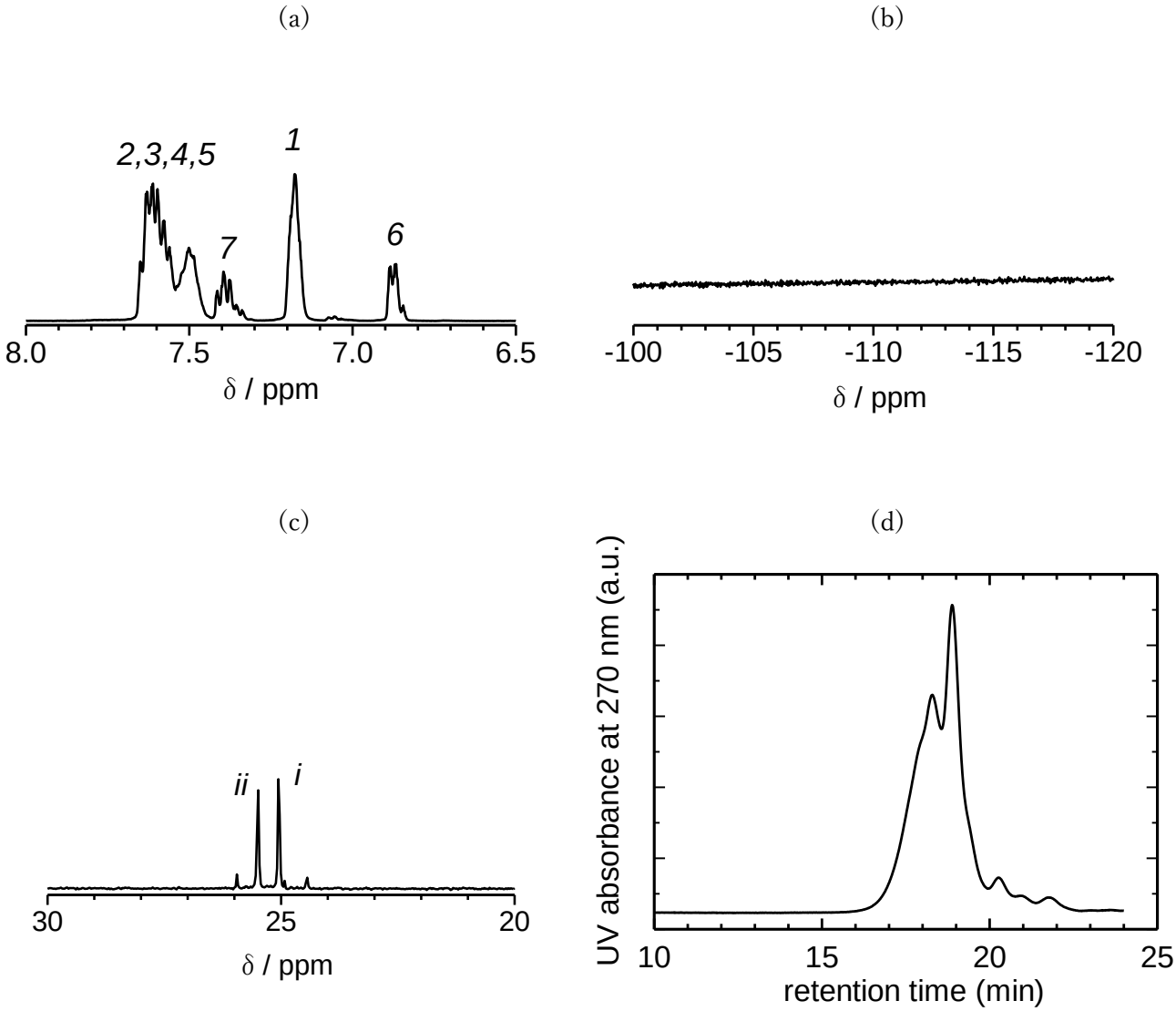

Figure 2-3. (a) ^{1}H, (b) ^{19}F, (c) ^{31}P NMR spectra (DMSO-d_6, 80 °C), and (d) GPC profile of BHPPO-terminated oligomer.

[Hydrophilic oligomer precursor]

A 100 mL three-necked round bottom flask equipped with a magnetic stirring bar, a condenser, a Dean-Stark trap, and a nitrogen inlet/outlet, was charged with BHPPO-terminated oligomer (1.58 mmol), BrFPS (4.74 mmol), K_2CO_3 (4.74 mmol), DMAc (25 mL), and toluene (5 mL). After the reaction was conducted at 160 °C for 3 h, the reaction mixture was poured into a 1 M hydrochloric acid to precipitate a solid. The resulting solid was washed with hot deionized water several times. Drying in a vacuum oven gave oligomer.

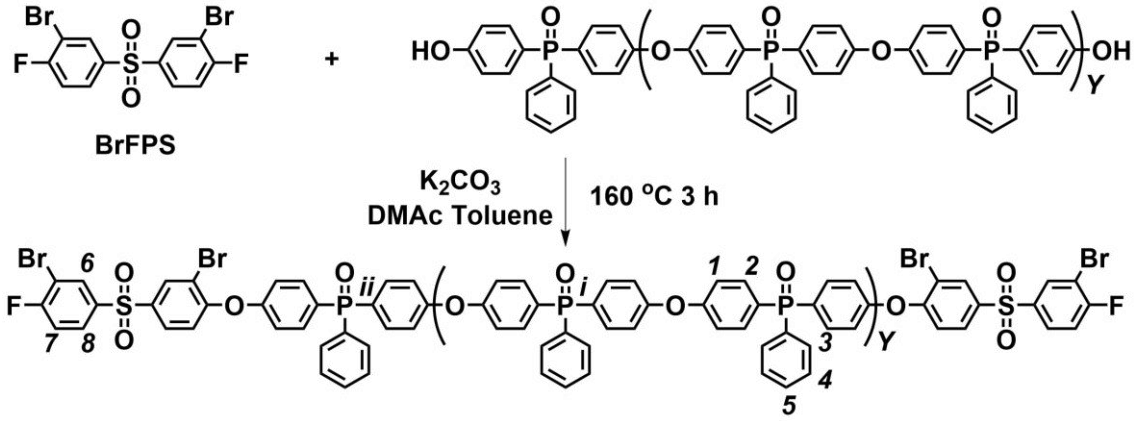

Scheme 2-3. Synthesis of hydrophilic oligomer precursor.

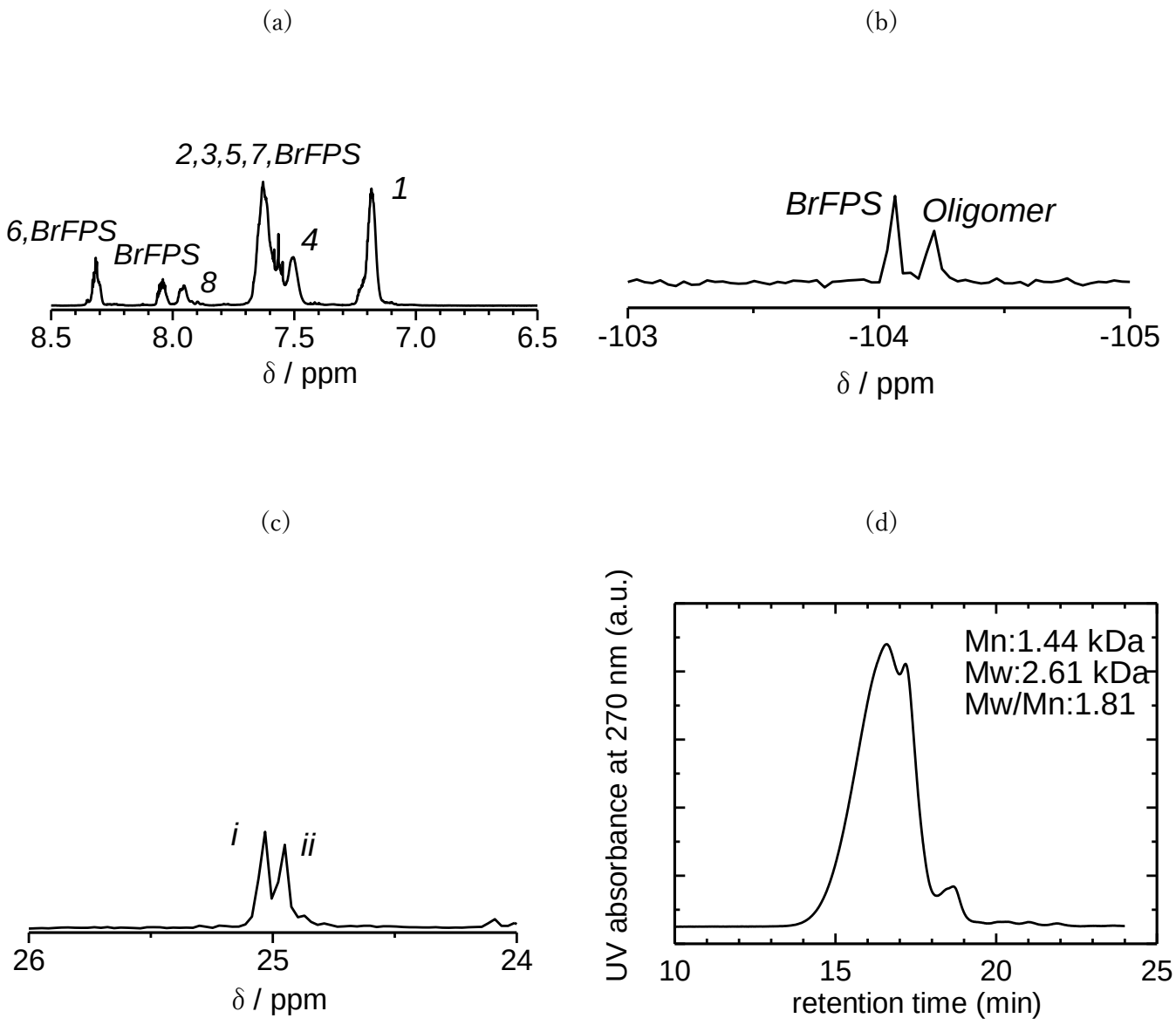

Figure 2-4. (a) ^{1}H, (b) ^{19}F, (c) ^{31}P NMR spectra (DMSO-d_6, 80 ^{o}C), and (d) GPC profile of hydrophilic oligomer precursor.

[Hydrophilic oligomer (2)]

A 100 mL round bottom flask equipped with a magnetic stirring bar was charged with hydrophilic oligomer precursor (1.50 mmol) and 30 wt% oleum (18 mL). The amount of 30 wt% oleum was adjusted to be 5 excess equimolar of SO_3 to the phenyl rings in the oligomer. After the sulfonation reaction at r.t. for 48 h, the reaction mixture was poured into H_2O, basified with NaOH aqueous solution, dialyzed, and dried to give the targeted oligomer 2 in 73% yield. (Y value; ^{1}H NMR = 1.9).

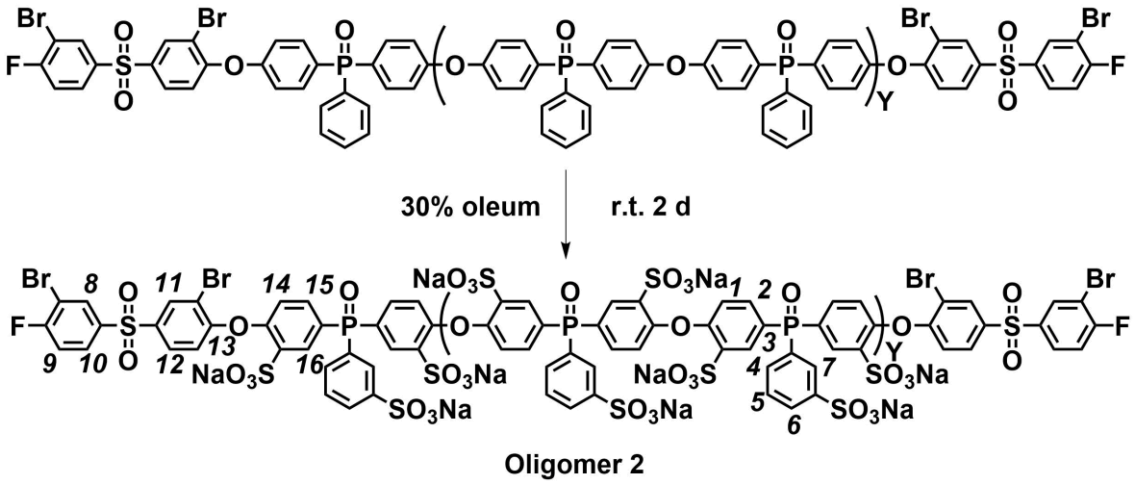

Scheme 2-4. Synthesis of hydrophilic oligomer (2)

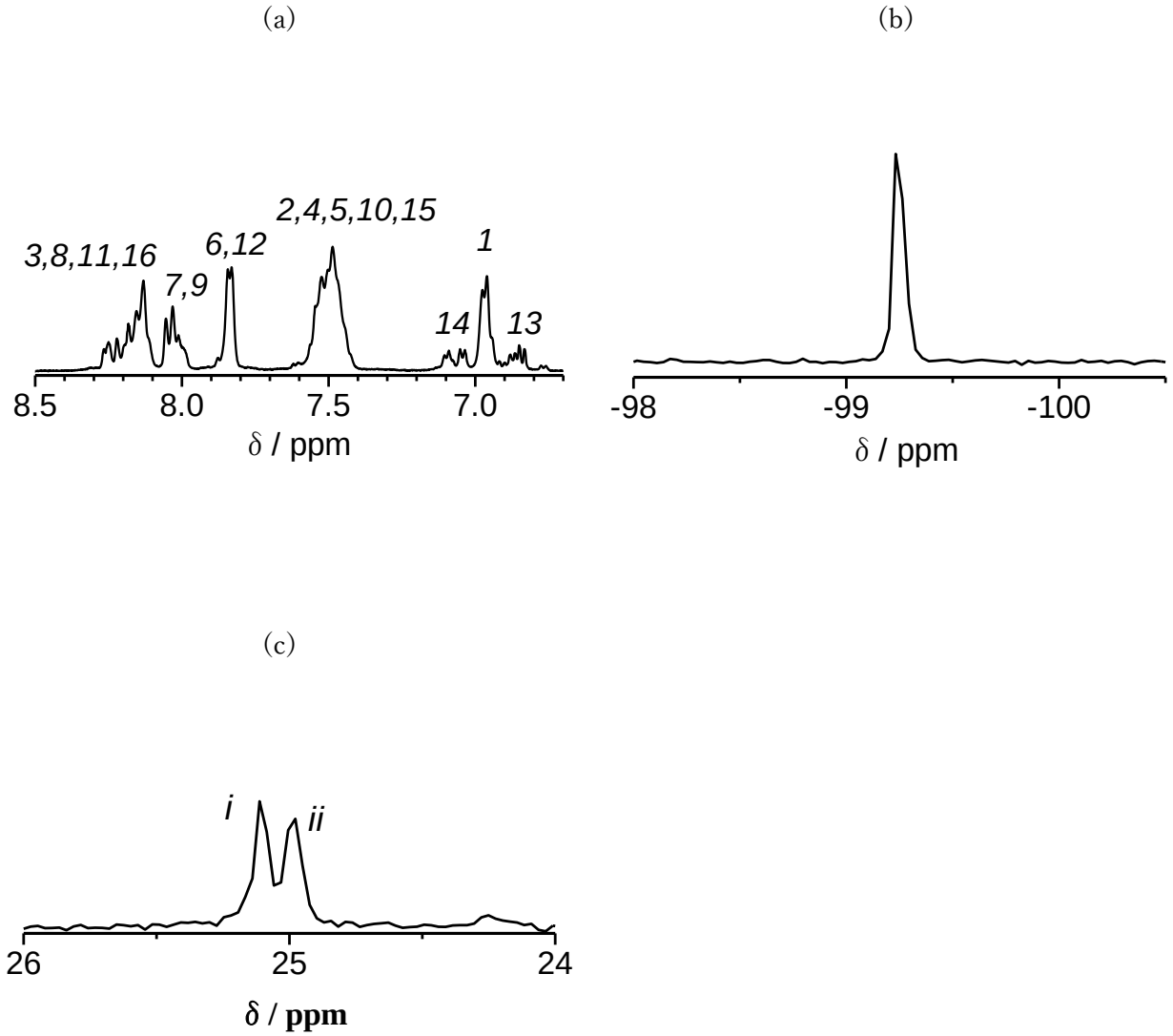

Figure 2-5. (a) ^{1}H, (b) ^{19}F, and (c) ^{31}P NMR spectra (DMSO-d_6, 80 °C) of oligomer 2.

2.2.5 Synthesis of multiblock copolymers (PP)

A typical procedure is as follows (X5Y2). A 100 mL three-necked round bottom flask equipped with a magnetic stirring bar, a condenser, a Dean-Stark trap, and a nitrogen inlet/outlet, was charged with oligomer 1 (0.142 mmol), oligomer 2 (0.142 mmol), K_2CO_3 (0.568 mmol), $CaCO_3$ (1.42 mmol), DMSO (5 mL), and toluene (1 mL). After the mixture was conducted at 140 °C for 21 h, the reaction mixture was poured into a 1 M hydrochloric acid. The crude mixture was dialyzed and dried to give the targeted polymer PP in 67% yield.

X10Y2 was synthesized under the conditions similar to those for X5Y2. Oligomer 1 (0.142 mmol), oligomer 2 (0.142 mmol), K_2CO_3 (0.568 mmol), $CaCO_3$ (1.42 mmol), DMSO (5 mL), and toluene (1 mL). 71% yield.

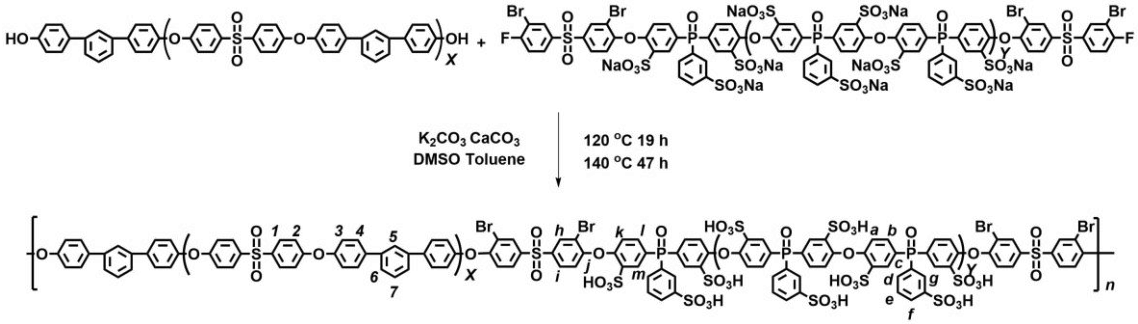

Scheme 2-5. Synthesis of multiblock copolymers (PP)

(a)

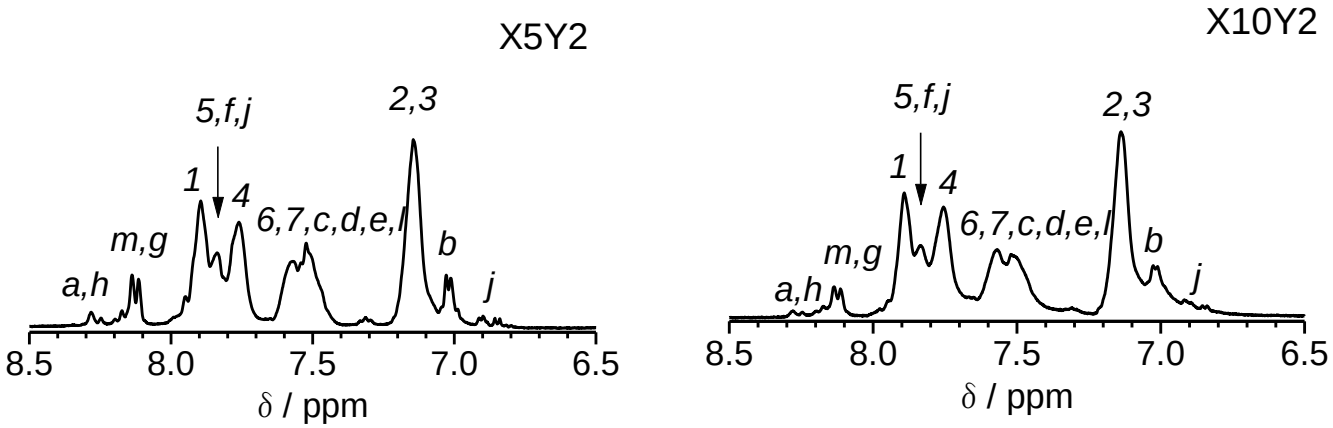

(b)

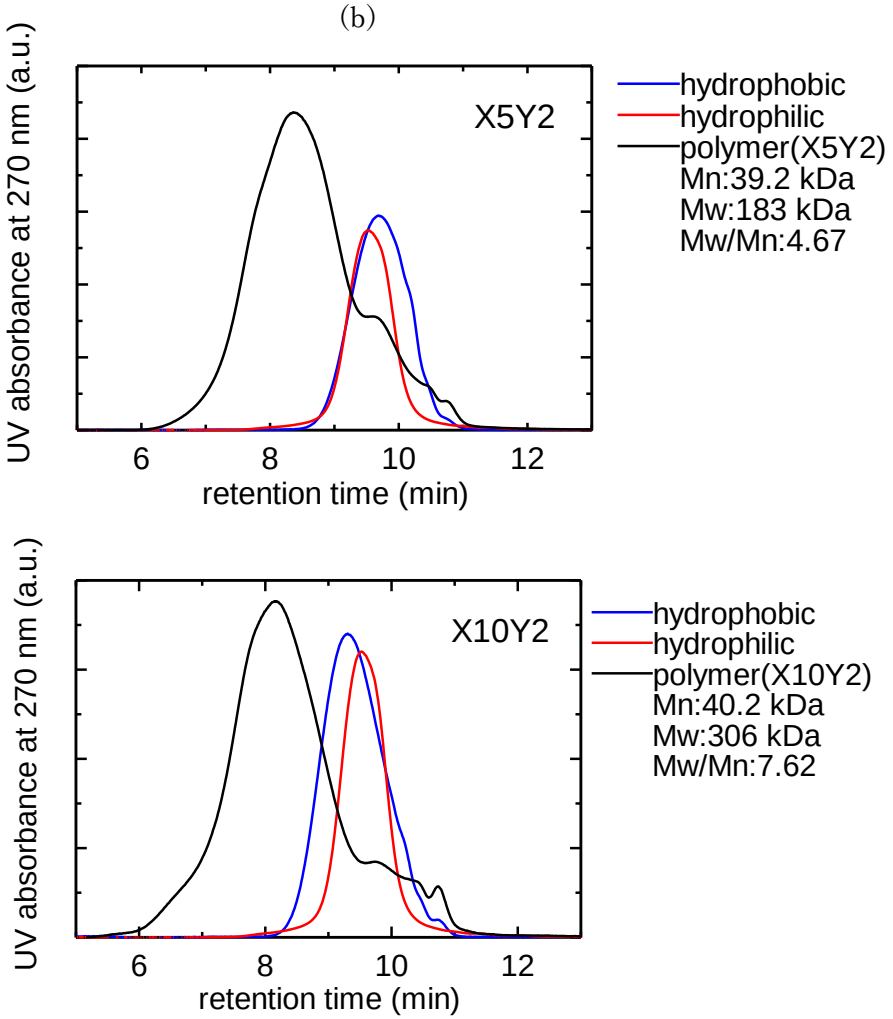

Figure 2-6. (a) ^{1}H NMR spectrum (DMSO-d_6 80 °C) and (b) GPC profiles

2.3 Result and discussion

2.3.1 Synthesis of the hydroxy (OH)-terminated telechelic oligomers 1

Scheme 1a represents the synthetic route for the title block copolymers PP. First of all, the hydrophobic oligomers 1 were prepared according to the literature (Scheme 2-1).[15] The nucleophilic substitution polymerization of a slight excess of 1,3-bis(4-hydroxyphenyl)benzene (MTP) with bis(4-fluorophenyl)sulfone (FPS) under basic conditions provided the hydroxy (OH)-terminated telechelic oligomers 1. The number of repeat units (X = 3 and 6) was controlled by the feed comonomer ratio. The chemical structure of oligomers 1 was confirmed by ^{1}H and ^{19}F NMR spectra (Figure 2-2), in which all signals were well-assigned to the supposed chemical structure. The X values obtained by ^{1}H NMR spectra (ca. 5 and 10) were slightly higher than the targeted values (X = 3 and 6). The X values estimated from GPC analyses (ca. 8 and 12) were even higher than those above, probably because the oligomers 1 comprise a rigid molecular structure and are eluted faster in our GPC system than the standard polystyrene samples. Therefore, the values (X = 5, 10) determined by ^{1}H NMR spectra were used as the number of repeat units of the oligomers 1 for the following block copolymerization reaction.

2.3.2 Synthesis of the hydrophilic oligomer containing the phosphinoxide moiety

The hydrophilic oligomer 2 was synthesized in three steps, i.e., nucleophilic substitution polymerization reaction, endcapping with bis(3-bromo-4-fluorophenyl)sulfone (BrFPS), followed by sulfonation reaction. First, the OH-terminated telechelic oligomer was prepared in a similar manner as described for the oligomers 1 (Scheme 2-2). A slight excess of bis(4-

hydroxyphenyl)phenylphosphine oxide (BHPPO) gave the targeted oligomer. The chemical structure of the oligomer was confirmed by ^{1}H, ^{19}F, and ^{31}PNMR spectra (Figure 2-3), in which all signals were well-assigned. GPC data, however, showed much lower values than expected. This result is consistent with our previous work, in which the oligomers containing triphenylphosphine oxide moieties had some interaction with our GPC columns, resulting in underestimation of the molecular weights.[16] Since the oligomer in this study carries more triphenylphosphine oxide groups than the previous oligomer, the interaction might become more prominent. On the contrary, the Y value (2) obtained from the ^{1}H NMR spectrum was reasonable (targeted Y = 1).

Then, the endcapping reaction with BrFPS was carried out in a similar manner as described for the oligomer (Scheme 2-3). Endcapping with the brominated compound was carried out to increase the reactivity in the following block copolymerization reaction.[19] The ^{1}H, ^{19}F, and ^{31}P NMR spectra suggested the formation of the targeted BrFPS-terminated oligomer (Figure 2-4). Although the monomeric BrFPS was contaminated (two ^{19}F NMR signals), this could be easily removed in the next step.

The sulfonation reaction of the BrFPS-terminated oligomer was conducted to synthesize hydrophilic oligomer 2 (Scheme 2-4). The ^{1}H, ^{19}F, and ^{31}P NMR spectra suggested the formation of targeted oligomer 2 (Figure 2-5). In the ^{31}P NMR spectrum, two signals were observed, which can be assigned as phosphorous atoms in the repeat unit and at the chain terminals, respectively. In the ^{19}F NMR spectrum, the hydrophilic oligomer 2 showed a single peak at -99.3 ppm, which was significantly shifted to the lower magnetic field compared to that of the non-endcapped hydrophilic oligomer having bis(4-fluorophenyl)phenylphosphine

oxide (FPPO) terminals (-107.2 ppm).[16] The result suggests that 2 would be more reactive than the non-endcapped hydrophilic oligomer.[20] Furthermore, the single ^{19}F NMR peak supported the successful removal of the BrFPS contaminant.

2.3.3 Synthesis of multiblock copolymers (PP)

Block copolymerization of 1 and 2 was carried out under conditions similar to that for the oligomerization reaction (Scheme 2-5). The obtained copolymers 3 possessed high molecular weights (apparent Mw = 183-306 kDa, Table 1) and were soluble in polar organic solvents. Casting from NMP solutions provided thin bendable membranes (ca. 30 μm thick). The ^{1}H NMR spectra of the copolymers confirmed the hydrophilic and hydrophobic components without detectable terminal groups. The experimental ion exchange capacity (IEC) values obtained by ^{1}H NMR spectra (Figure 2-6) were comparable to or slightly lower than those calculated from the feed ratios (Table 1). On the other hand, IEC values obtained by titration were much lower than these IEC values, suggesting that part of the sulfonic acid groups embedded in the rather hydrophobic environment did not function as ion exchangeable groups. Similar behavior was previously observed for the other series of sulfonated block copolymer membranes having a rigid main chain structure.[21]

Table 1-1. Molecular weight, IEC, water uptake, and oxidative stability of PP and PK membranes

PEMs	Composition	Molecular weight[a] (kDa)		IEC (meq g^{-1})			Residue[b] (%)	
		Mn	Mw	Target	NMR	Titration	Weight	Mw[a]
PP	X5Y2	39	183	2.36	1.90	1.15	80	75
PP	X10Y2	40	306	1.71	1.63	0.92	88	74
PK[c]	X30Y4	90	204	1.30	1.06	0.92	96	94

a: Determined by GPC analyses (calibrated with polystyrene standards).

b: After Fenton's test at 80 °C for 1 h. c: See ref 16.

2.3.4 Morphology

Figure 2-7 shows a TEM image of the PP-X5Y2 membrane stained with lead ions. While the effect of counter cations might not be negligible, TEM images often provide useful information on the morphology of ionomer membranes. The PP membrane showed phase-separated morphology with hydrophilic (black domain) and hydrophobic (white domain) components. The hydrophilic domain of the PP membrane was narrow with a string-like structure, which was similar to that of the reference copolymer PK, probably because both copolymers contained similar, rigid, and linear hydrophilic blocks. The difference lies in their size, i.e., the width of the hydrophilic parts of the PP membrane was ca. 3 nm, which was slightly smaller than that of the PK (ca. 5 nm) membrane. The shorter hydrophilic chain length of PP (Y = 2) compared to PK (Y = 4) must be responsible. The connectivity of the hydrophilic domains in the PP membrane was somewhat lower than that in the PK membrane.

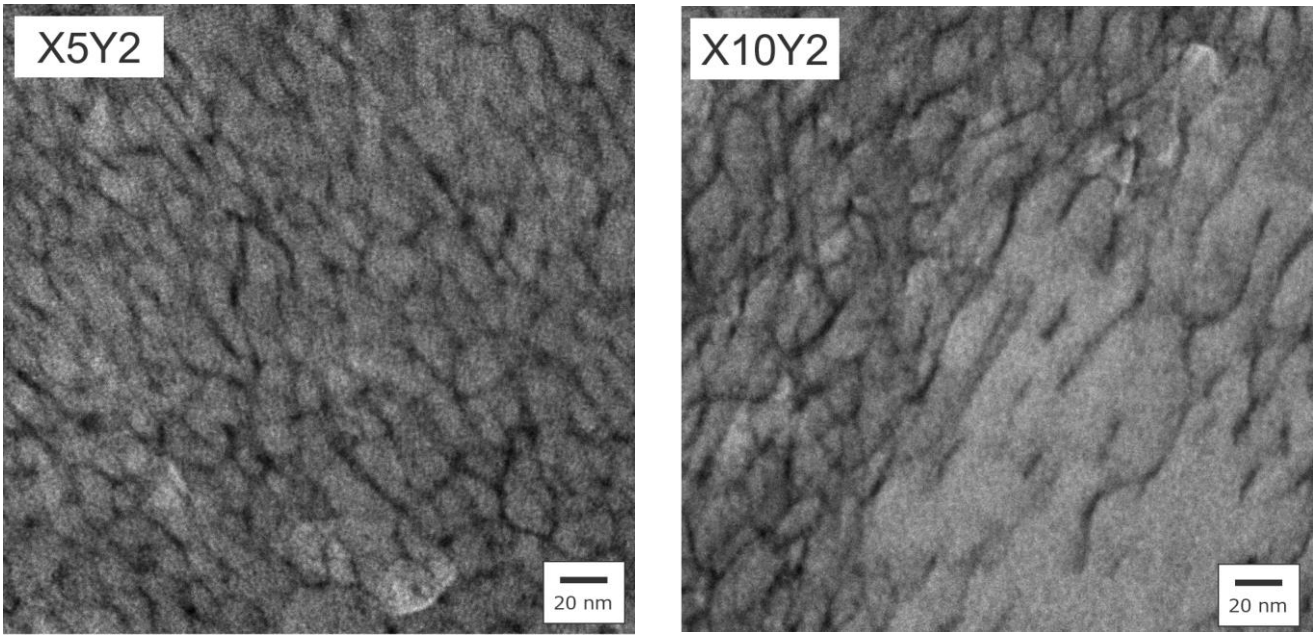

Figure 2-7. TEM images of PP X5Y2 and X10Y2 membrane in lead ion form.

2.3.5 Proton conductivity and water uptake

The water uptake and proton conductivity of the PP membranes was investigated at 80 °C as a function of relative humidity (RH). For comparison, data for Nafion NRE 212 and PK (sharing similar hydrophobic blocks but with a different density of the sulfonated triphenylphosphine oxide moieties) membranes are also included in Figure 2-8. The water uptake and proton conductivity of these membranes were dependent on RH, i.e., a higher RH caused higher water uptake and proton conductivity. The PP membrane with the higher IEC value (X5Y2, 1.15 meq g^{-1}) showed much higher proton conductivity than that the reference PK (0.92 meq g^{-1}) membrane due to the former's higher IEC value. Comparison of PP-X10Y2 (0.92 meq g^{-1}) with PK (0.92 meq g^{-1}) revealed that these two membranes showed comparable proton conductivity at a wide range of humidities (the PP membrane showed only slightly lower proton conductivity than PK at 20% RH). Although the PP and PK membranes showed much lower proton conductivity than the Nafion NRE 212 membrane at low RH, all membranes showed comparable proton conductivity at high RH, probably due to the higher water uptake of PP and PK compared to Nafion NRE 212.

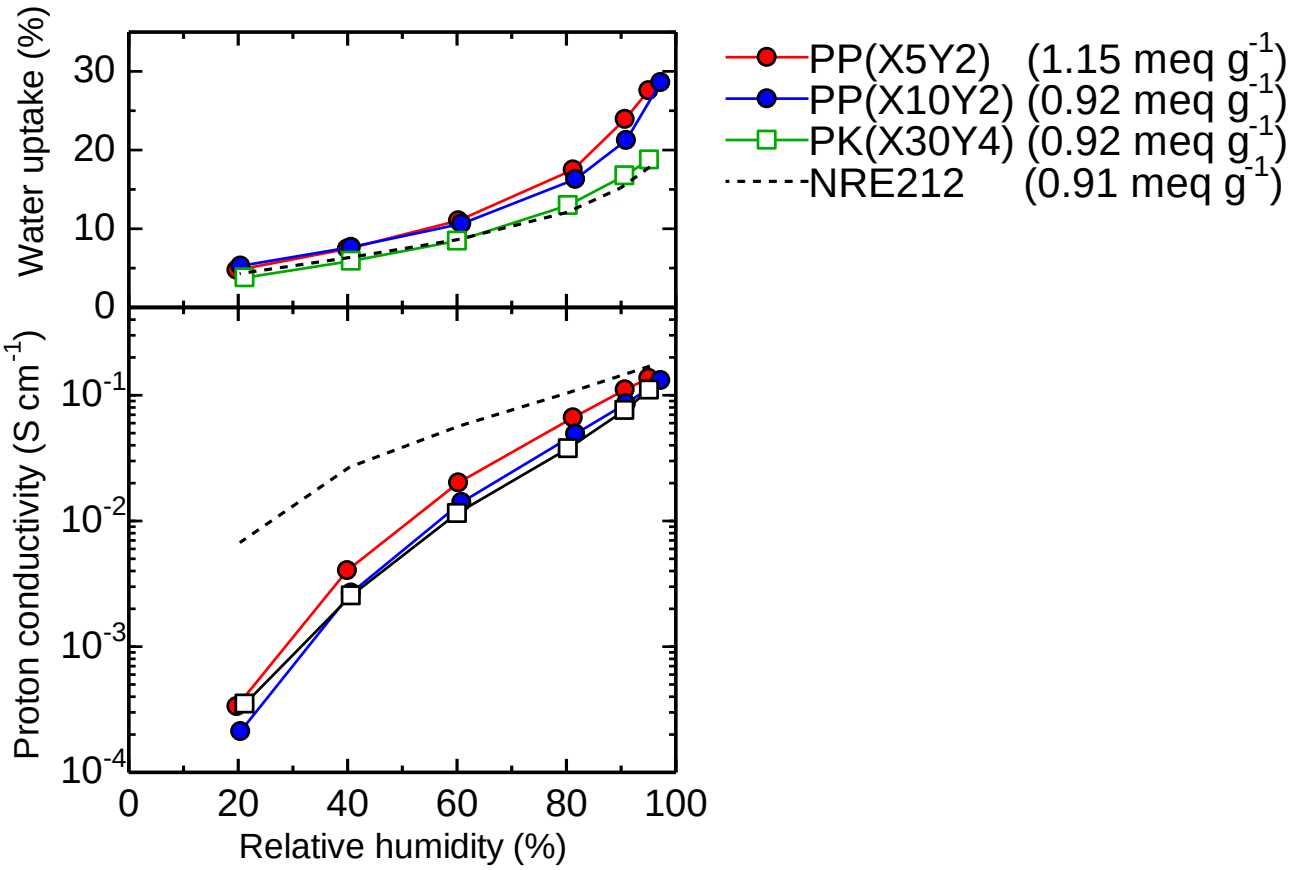

Figure 2-8. Water uptake and proton conductivity of the membranes (IEC values obtained by titration in parentheses) at 80 °C as a function of RH.

2.3.6 DMA

The mechanical properties of the membranes were investigated via dynamic mechanical analyses (DMA) under the same conditions as that for water uptake and proton conductivity measurements (at 80 °C as a function of RH) (Figure 2-9). All membranes showed similar humidity dependence on storage moduli (E'), loss moduli (E''), and tan δ , i.e., distinct peaks at ca. 50-60% RH in the E'' and tan δ curves were observed. These peaks could be ascribed to the glass transition of the copolymers, in which the absorbed water acts as a plasticizer.[22] The similar behavior indicated that the structural difference (or the content of triphenylphosphine oxide groups) within this study (PP and PK) did not affect the humidity-dependent viscoelastic properties.

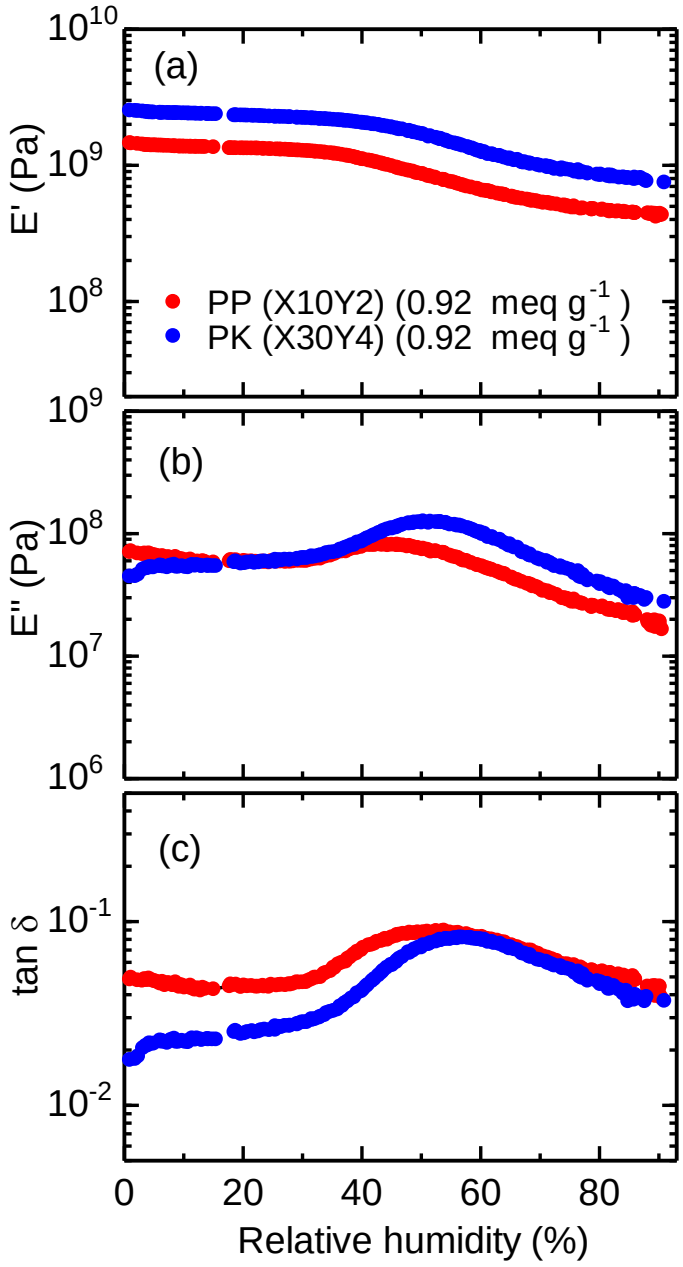

Figure 2-9. DMA analyses of membranes; (a) E' (storage moduli), (b) E'' (loss moduli), and (c) tan δ at 80 °C as a function of RH.

2.3.7 Oxidative stability

The oxidative stability was tested under accelerated conditions in Fenton's reagent at 80 °C for 1 h, and is summarized in Table 1. Under such harsh conditions, most SPAE-based membranes degrade significantly. In our previous work, membranes without phosphine oxide groups degraded severely (residual weight and M_w are 57% and 56%, respectively) despite the similar titration IEC (1.06 meq g^{-1}) and water uptake (18.2%) values.[21] In contrast, two PP membranes exhibited good oxidative stability, retaining more than 80% of the weight and 74% of the weight-averaged molecular weight. The oxidative stability of the PK membrane with the smaller content of triphenylphosphine oxide groups was even better. This result indicated that not only the density of the sulfonated triphenylphosphine oxide moieties but also other factors such as water affinity might affect the oxidative stability of the membranes. Although the PP membranes have highly dense sulfonated triphenylphosphine oxide moieties, those of the water uptake were also high. The higher water uptake of the PP membranes might provide more chances of attack by water-soluble radical species, resulting in degradation of the PP membranes. Since the post-test-analysis of the PP membranes revealed that degradation occurred mainly at the hydrophilic parts (Figure 2-10), optimization of the molecular design in the hydrophilic parts (e.g., the position and density of the sulfonated triphenylphosphine oxide moieties) should be further investigated.

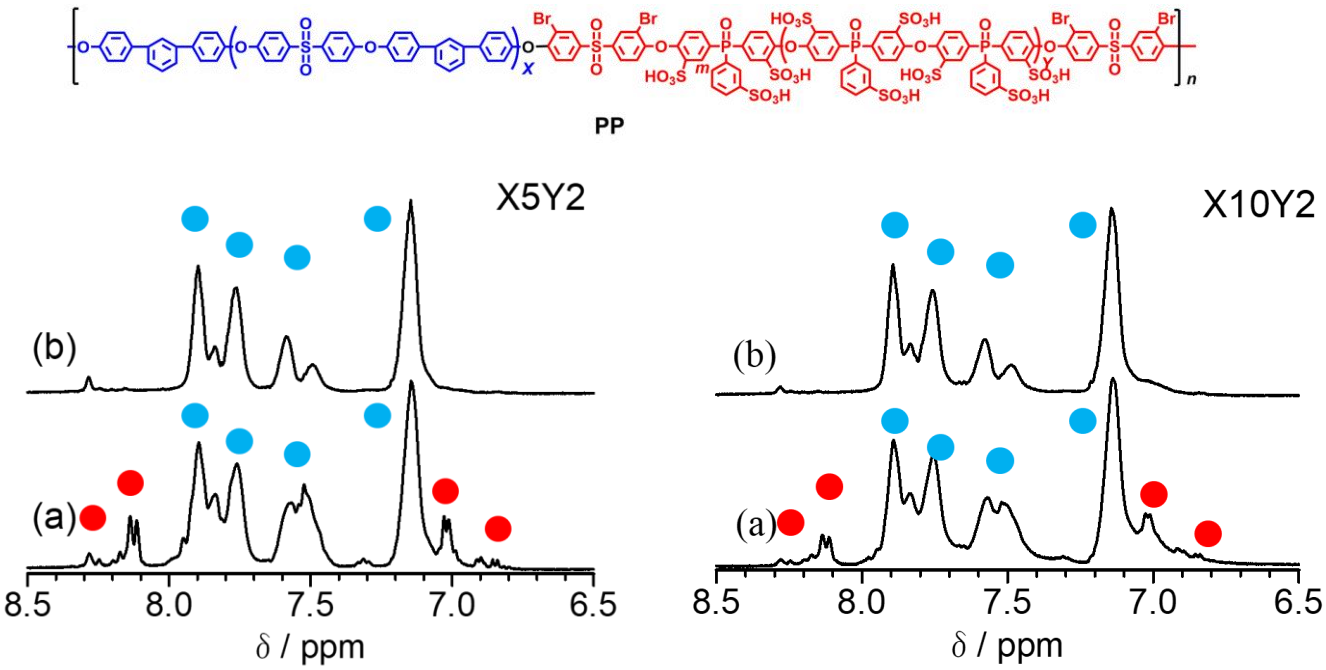

Figure 2-10. ^{1}H NMR spectra (DMSO-d_6, 80 °C) of the PP-X5Y2 sand PP-X10Y2 membranes (a) before and (b) after Fenton's test.

2.4 Conclusion

In conclusion, I have synthesized a new type of aromatic block copolymer PP containing dense sulfonated triphenylphosphine oxide moieties in the hydrophilic blocks. The obtained copolymer PP possessed high molecular weight and good solubility in polar organic solvents. Solution casting produced self-standing and bendable PP membranes. It is indicated that the introduction of sulfonated triphenylphosphine oxide moieties is effective in improving the oxidative stability of the membranes. However, detailed comparison with the PK membrane sharing similar hydrophobic blocks but a smaller content of sulfonated triphenylphosphine oxide moieties revealed that the dense introduction of sulfonated triphenylphosphine oxide moieties led to higher water uptake, resulting in the decrease in the oxidative stability of the membranes. Thus, the position and content of the sulfonated triphenylphosphine oxide moieties should be optimized for further improving the properties.

2.5 Reference

1 H. Zhang, P. K. Shen, *Chem. Rev.* **2012**, *112*, 2780.

2 M.A.Hickner, H. Ghassemi, Y. S. Kim, B. R. Einsla, J. E. McGrath, *Chem. Rev.* **2004**, *104*, 4587.

3 Y. Chen, Y. Meng, S. Wang, S. Tian, Y. Chen, A. S. Hay, *J. Membr. Sci.* **2006**, *280*, 433.

4 K.Miyatake, Y. Chikashige, E. Higuchi, M. Watanabe, *J. Am. Chem. Soc.* **2007**, *129*, 3879.

5 T. J. Peckham, S. Holdcroft, *Adv. Mater.* **2010**, *22*, 4667.

6 C. H. Park, C. H. Lee, M. D. Guiver, Y. M. Lee, Prog. *Polym. Sci.* **2011**, *36*, 1443.

7 Y.A.Elabd, M. A. Hickner, *Macromolecules* **2011**, *44*, 1.

8 S. Takamuku, P. Jannasch, *Macromolecules* **2012**, *45*, 6538.

9 E.A.Weiber, S. Takamuku, P. Jannasch, *Macromolecules* **2013**, *46*, 3476.

10 K. Si, R. Wycisk, D. Dong, K. Cooper, M. Rodgers, P. Brooker, D. Slattery, M. Litt, *Macromolecules* **2013**, *46*, 422.

11 B. Bae, T. Yoda, K. Miyatake, H. Uchida, M. Watanabe, *Angew. Chem., Int. Ed.* **2010**, *49*, 317.

12 B. Bae, T. Hoshi, K. Miyatake, M. Watanabe, *Macromolecules* **2011**, *44*, 3884.

13 T. Miyahara, T. Hayano, S. Matsuno, M. Watanabe, K. Miyatake, *ACS Appl. Mater. Interfaces* **2012**, *4*, 2881.

14 J. Miyake, M. Watanabe, K. Miyatake, *RSC Adv.* **2014**, *4*, 21049.

15 J. Miyake, M. Sakai, M. Sakamoto, M. Watanabe, K. Miyatake, *J. Membr. Sci.* **2015**, *476*, 156.

16 J. Miyake, M. Watanabe, K. Miyatake, *ACS Appl. Mater. Interfaces* **2013**, *5*, 5903.

17 L. Fu, G. Xiao, D. Yan, *ACS Appl. Mater. Interfaces* **2010**, *2*, 1601.

18 N. Li, D. W. Shin, D. S. Hwang, Y. M. Lee, M. D. Guiver, *Macromolecules* **2010**, *43*, 9810.

19 J. Miyake, M. Saito, R. Akiyama, M. Watanabe, K. Miyatake, *Chem. Lett.* **2015**, *44*, 964.

20 K. R. Carter, *Macromolecules* **1995**, *28*, 6462.

21 K. Miyatake, D. Hirayama, B. Bae, M. Watanabe, *Polym. Chem.* **2012**, *3*, 2517.

22 J.Miyake, T. Mochizuki, K. Miyatake, *ACS Macro Lett.* **2015**, *4*, 750.

Chapter 3: Versatile Synthesis of Sulfonated Aromatic Copolymers Using NiBr2

3.1 Introduction

Proton exchange membrane fuel cells (PEMFCs) have received considerable attention as a clean energy device using hydrogen due to high efficiency and low environment load for the realization of low-carbon society. PEMFCs have been already commercialized for electric vehicles and residential power sources. To further improve the fuel cell performance and reduce the cost, proton exchange membranes (PEMs) need to be more addressed. Currently, perfluorosulfonic acid polymer membranes (*e.g.*, Nafion) are most used as PEMs because of their high proton conductivity, high mechanical properties, and excellent chemical stability.[1-3] However, there are several disadvantages for the perfluorinated materials such as high gas permeability, low environmental compatibility, and high production cost; all these are related with the perfluorinated polymer structure. Therefore, there has been a great demand for alternative PEMs without containing fluorine atoms to overcome these issues.

Aromatic polymer based ionomers are an attractive candidate for the purpose. A number of studies on proton conductive aromatic ionomers can be found in the literature in the last decade.[4-6] Recently, our laboratory has developed a novel series of sulfonated aromatic copolymers (SPP-*bl*-1) composed of sulfo-1,4-phenylene as hydrophilic component and oligo(phenylene ether sulfone) as hydrophobic component.[7] The copolymer membranes exhibited high proton conductivity and mechanical stability under the conditions simulating fuel cell operation. In fact, good fuel cell performance was achieved with SPP-*bl*-1 membrane.

SPP-*bl*-1 copolymer, however, requires costly and air-sensitive Ni(0), bis(1,5-cyclooctadiene)nickel(0) or $Ni(cod)_2$, for the efficient C-C coupling copolymerization reaction, which undermines the advantages of potentially inexpensive aromatic polymers. Several research groups have reported more versatile synthetic method using Ni(II) compounds such as $NiCl_2(PPh_3)_2$ as an alternative to Ni(0) in the presence of Zn or Mg as a reducing agent for the synthesis of polyphenylenes, polythienylenes, and poly(phenylene ether ketone)s.[8-12] Relatively high molecular weight polymers and copolymers were obtained. Okamoto et al. reported synthesis of sulfonated polyphenylene block copolymers with $NiBr_2$, wherein sulfonated monomer was activated with electron-withdrawing carbonyl groups.[13] In the present study, I have investigated the applicability of Ni(II) promoted polymerization reaction (in the presence of Zn) to our sulfonated copolymers (SPP-*bl*-1) with simpler sulfonated monomer (2,5-dichlorobenzenesulfonic acid). Optimization of the polymerization conditions and characterization of the resulting copolymers are reported.

3.2 Experimental

3.2.1 Materials

Bis(4-chlorophenyl)sulfone, 4,4'-dihydroxybenzophenone, tetraethylammonium iodide, 2,5-dichlorobenzenesulfonic acid, 2,5-dichlorobenzenesulfonyl chloride, and 2,2-dimethyl-1-propanol were purchased from TCI, Inc. and used as received. Potassium carbonate (K_2CO_3), pyridine, 2,2'-bipyridyl, sodium sulfate (Na_2SO_4), sodium hydrogen carbonate ($NaHCO_3$), sodium chloride (NaCl), lithium bromide (LiBr), ethanol, methanol, 2-propanol, ethyl acetate, toluene dehydrated, deuterated dimethyl sulfoxide (DMSO-d_6), 0.01 M sodium hydroxide

aqueous solution, and hydrochloric acid were purchased from Kanto Chemical Co. and used as received. Nickel(II) bromide ($NiBr_2$) and sodium iodide (NaI) were purchased from Wako and used as received. N,N-dimethylacetamide (DMAc) was purchased from Kanto Chemical Co. and dehydrated with solvent purification system (Nikko Hansen & co., LTD) prior to use. Sodium 2,5-dichlorobenzenesulfonate was prepared by neutralizing 2,5-dichlorobenzenesulfonic acid with Amberlite IR-120 Na ion-exchange resin (ACROS). Zn powder was purchased from Wako and washed with 1.0 M hydrochloric acid, ethanol, and acetone prior to use. Oligo(phenylene ether sulfone) (the average number of repeat unit was 9.9) was prepared according to the literature.[14]

3.2.2 Measurements

^{1}H NMR spectra were obtained on a JEOL JNM-ECA 500 using DMSO-d_6 as a solvent and tetramethylsilane (TMS) as an internal reference. Molecular weight of the copolymers was measured with gel permeation chromatography (GPC) equipped with a Jasco 805 UV detector and a Shodex K-805L column. DMF containing 0.01 M LiBr was used as eluent. Molecular weight was calibrated with standard polystyrene samples. Ion exchange capacity (IEC) of the copolymer membranes was determined by back-titration. A piece of the membrane (ca. 30 mg) was equilibrated in 60 mL of 2 M NaCl aqueous solution for 12 h. HCl released by the ion exchange reaction was titrated with standard 0.01 M NaOH aqueous solution at r.t. Water uptake and proton conductivity of the membranes were measured at 80 °C with a solid electrolyte analyzer system (MSBAD-V-FC, Bel Japan Co.) equipped with a temperature and humidity controllable chamber. Weight of the membrane was measured by

magnetic suspension balance at a given humidity, then water uptake was calculated using the following equation; (weight of hydrated membrane - weight of dry membrane) / weight of dry membrane × 100. Vacuum drying for 3 h at 80 °C gave the weight of dry membranes and exposure to a given humidity for at least 2 h gave the weight of hydrated membranes. Proton conductivity was measured using a four probe conductivity cell equipped with a Solartron 1255B and SI 1287 impedance analyzers with the same chamber. Ion conducting resistances (R) were determined from the impedance plot obtained in the frequency range from 1 to 10^5 Hz. The proton conductivity (σ) was calculated from the equation $\sigma = l / (A \times R)$, where A and l are the conducting area and the electrode distance, respectively.

3.2.3 Synthesis of Protected Monomer (1)

A 200 mL three neck flask equipped with a magnetic stirring bar and a nitrogen inlet/outlet was charged with 2,5-dichlorobenzenesulfonyl chloride (102 mmol, 25.0 g) and pyridine (106 mL). The mixture was cooled to 0 °C, and 2,2-dimethyl-1-propanol (204 mmol, 18.0 g) was added. The mixture was reacted at 0 °C for 2.5 h. After the reaction, the mixture was poured into 4 M HCl (400 mL) and extracted with EtOAc (300 mL). The organic layer was washed with saturated $NaHCO_3$ aqueous solution and brine, and dried over Na_2SO_4. The filtrate was concentrated using an evaporator. The residue was dissolved in isopropanol (100 mL) at 60 °C and recrystallized in a refrigerator overnight. The precipitate was collected by filtration and dried in a vacuum oven at 50 °C overnight to obtain pure 1-neopentylsulfonyl-2,5-dichlorobenzene (**1**) as white powder. (24.8 g, yield 82.2 %).

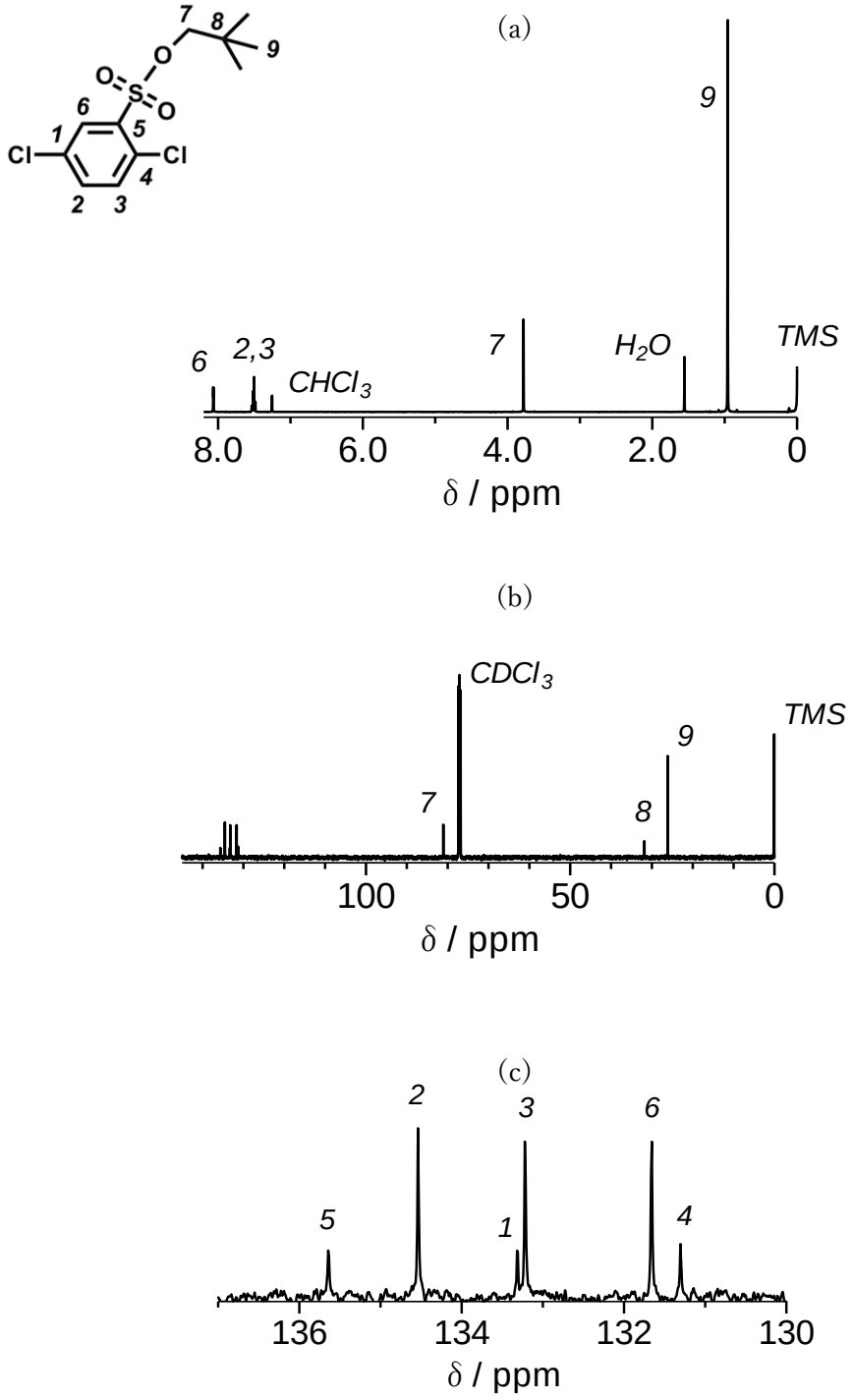

Figure 3-1. (a) ^{1}H and (b) (c) ^{13}C NMR

spectra of 1-neopentylsulfonyl-2,5 dichlorobenzene (**1**).

3.2.4 Copolymerization Reaction

A typical procedure is as follows. A 100 mL three neck flask equipped with a reflux condenser, a Dean-Stark trap, a mechanical stirrer, and a nitrogen inlet/outlet was charged with oligo(phenylene ether sulfone) (0.111 mol, 0.503 g), $NiBr_2$ (6.27 mmol, 1.37 g), NaI (12.5 mmol, 1.88 g), 2,2'-bipyridyl (13.2 mmol, 2.06 g), DMAc (20.0 mL), and toluene (10.0 mL). The mixture was heated at 145 °C for 2 h for azeotropic removal of water. Then, the mixture was cooled to 60 or 80 °C, and Zn powder (31.3 mmol, 2.05 g) and the protected monomer **1** (2.50 mmol, 0.743 g) were added to the mixture. The mixture was stirred with mechanical stirrer for 3 h. After the copolymerization reaction, the mixture was poured into a large excess of methanol to precipitate a product. The crude product was washed with 6 M HCl and water. The obtained copolymer (**2**) was dried in a vacuum oven at 60 °C overnight.

3.2.5 Deprotection Reaction

A 100 mL three neck flask equipped with a reflux condenser, a magnetic stirring bar, and a nitrogen inlet/outlet was charged with the copolymer (0.400 g), LiBr (3.77 mmol, 0.328 g), and DMAc (5.0 mL). The mixture was reacted at 100 °C for 22 h. After the reaction, the mixture was poured into 1 M HCl (70 mL). The resulting yellow suspension was dialyzed with a regenerated cellulose film tubing (cutoff molecular weight: 1000). The dialyzed solution was evaporated and dried in a vacuum oven at 80 °C overnight to recover a deprotected copolymer (**3**).

3.2.6 Membrane Preparation

The deprotected copolymer (0.15 g) was dissolved in 4 mL of DMSO and cast onto a flat glass plate. The solution was dried at 80 °C to obtain a thin membrane. The membrane was further dried at 80 ° C in a vacuum oven at least for 3 h. Then, the membrane was treated with 1 M H_2SO_4 at least for 12 h, washed with water several times, and dried at 25 °C.

3.3 Result and discussion

The copolymerization reaction of the sulfonated monomer (2,5-dichlorobenzenesulfonic acid) with oligo(phenylene ether sulfone) (Scheme 3-1) was investigated under several different conditions. I first used sodium salt of the monomer, however, the copolymers were obtained in relatively low yield (62%) and were of low molecular weight (M_w = 50.8 kDa and M_n = 18.3 kDa, No. 1 in Table 1). The copolymer was soluble in polar organic solvents (*e.g.*, DMSO and NMP), and casting from the solution did not provide self-standing membrane because of the insufficient molecular weight. Longer polymerization time (24 h) or replacing sodium iodide (NaI) with tetraethylammonium iodide (Et_4NI) as additive (promoting the reduction reaction of Ni^{2+} with Zn) did not improve the reaction (Nos. 2 and 3, respectively). The ^1H NMR spectra of the obtained copolymers suggested that the composition of the sulfophenylene component was much smaller than the feed ratio (as evidenced by low IEC values), indicating low reactivity of the monomer in the polymerization system.

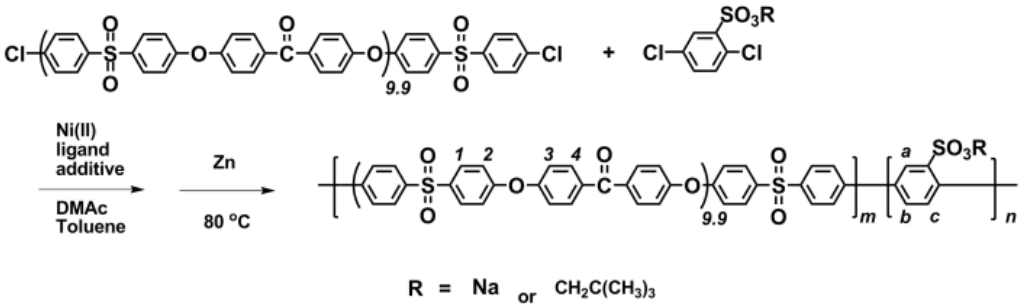

Scheme 3-1. Synthesis of copolymers.

Table 3-1. Copolymerization of the sulfonated monomer 1 with aromatic oligomer.[a]

No.	R	Reaction time (h)	Additive	Yield (%)	M_n (kDa)	M_w (kDa)	Membrane	IEC by NMR (meq. g^{-1})	IEC by titration (meq. g^{-1})
1	Na	3	NaI	62	18.3	50.8	×	0.67	−
2	Na	24	NaI	74	13.6	32.2	×	0.52	−
3	Na	3	Et_4NI	60	31.0	74.9	×	0.32	−
4	Neopentyl	3	NaI	54	60.1	150	○	0.90[c]	1.37
5	Neopentyl	3	Et_4NI	41	51.2	117	○	0.08[c]	−
6[b]	Neopentyl	3	NaI	85	60.1	133	○	2.00[c]	2.36
7[b]	Neopentyl	3	NaI	93	41.2	158	○	2.11[c]	2.45

[a] Five equimolar Zn to $NiBr_2$ was used. [b]The protected monomer (1) was added to the mixture after the azeotropic dehydration. [c]Estimated from the protected samples.

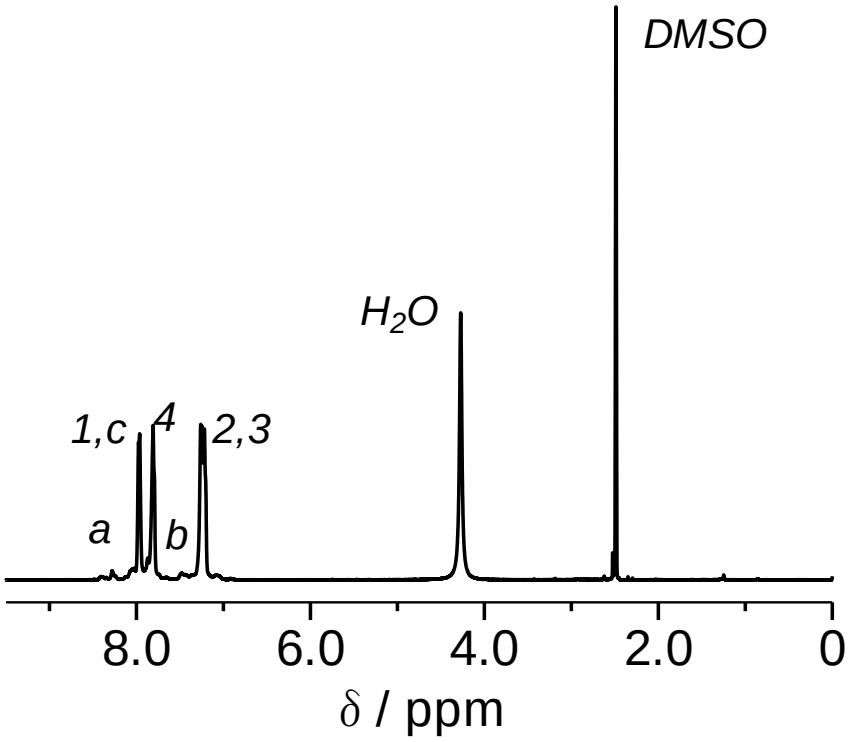

Figure 3-2. ^{1}H NMR spectra of the copolymer No. 4

The sulfonate groups were then protected with 2,2-dimethyl-1-propyl (neopentyl) groups (see Supporting Information for the preparation). The copolymerization reaction of the monomer (1) protected with neopentyl sulfonate ester proceeded better than that of the unprotected (sodium sulfonate) monomer. The copolymers were obtained in 54% and 41% yields (still not high) but their molecular weights were much higher with M_w = 150 kDa and M_n = 60.1 kDa with NaI for No. 4 and M_w = 117 kDa and M_n = 51.2 kDa with Et_4NI for No. 5, respectively. The copolymers were soluble in polar organic solvents and provided bendable and transparent membranes by solution casting. In the ^{1}H NMR spectrum of the copolymer No. 4, the peaks assignable to neopentyl groups were hardly observed (Figure 3-2). The results suggest that the neopentyl protecting groups were eliminated presumably during the

azeotropic removal of water carried out at high temperature (145 °C). The ion exchange capacity (IEC) of the membrane No. 4 determined by titration was 1.37 meq. g^{-1}, significantly lower than that calculated from the comonomer composition (2.82 meq. g^{-1}), implying that the deprotected monomer was less reactive and did not participate well in the copolymerization reaction as discussed above for Nos.1-3.

To prevent the thermal decomposition of the neopentyl protecting groups, the polymerization conditions were slightly modified and the protected monomer (1) was added after the dehydration process in Nos. 6 and 7. The copolymerization reaction was carried out at 80 °C for No. 6 and 60 °C for No. 7, respectively. In both cases, the copolymers were obtained in high yields (85% and 93%) and of high molecular weights (M_w = 133-158 kDa and M_n = 41.2-60.1 kDa). In the ^{1}H NMR spectrum of the copolymer No. 6, the peaks assignable to neopentyl groups were well-observed (Figure 3-3(a)). The possible IEC value of the copolymer No. 6 estimated from the integral ratios in the ^{1}H NMR spectrum was 2.00 meq. g^{-1} and significantly higher than those of the copolymers Nos. 1-5. The copolymer No. 7 showed similar ^{1}H NMR spectrum (not shown) and high IEC value (2.11 meq. g^{-1}). It is concluded that the addition of the protected monomer after the dehydration process is very effective in improving the copolymerization reaction. Since the copolymerization was carried out with hydrophobic oligomer and sulfonated monomer, the obtained products were semi-block copolymers. Although the main objective of the present study was not to conduct the polymerization under catalytic conditions, the polymerization was carried out with half equimolar or less $NiBr_2$ to the terminal chlorine groups. The polymerization did not proceed well and only gave low molecular weight products probably because Zn could reduce $NiBr_2$

but not Ni(I)Cl as an intermediate.

The deprotection reaction of the neopentyl sulfonate groups was carried out for the copolymers Nos. 6 and 7 as shown in Scheme 3-2. The solubility of the copolymer did not change after the deprotection reaction. Complete deprotection reaction was suggested by the ^{1}H NMR spectrum (Figure 3-3(b)), where the peaks of neopentyl groups were not detected and the aromatic peaks did not change. The molecular weights of the copolymer also did not practically change and the small molecular weight portion was removed during the purification procedure after the deprotection reaction (Figure 3-3(c)). The deprotected copolymer Nos. 6 and 7 provided bendable and transparent membranes by solution casting (Figure 3-4). The thickness of the self-standing membrane could be lower than 30 μm without mechanical failure. The IEC values of the membranes obtained by titration were higher than those estimated from the ^{1}H NMR spectra, suggesting that some deprotection reaction might have occurred even at lower temperatures (60 and 80 °C) during the polymerization reaction, which could have caused underestimation of the IEC values by the NMR spectra.

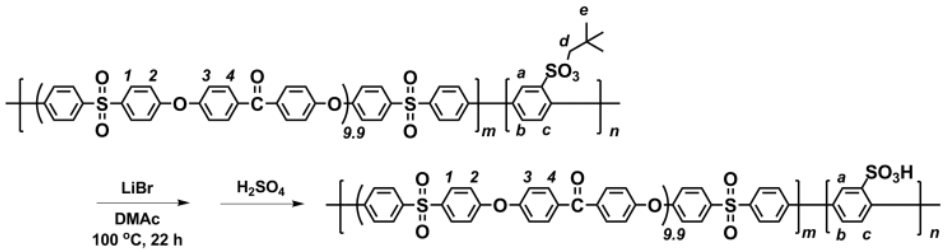

Scheme 3-2. Deprotection reaction.

(a)

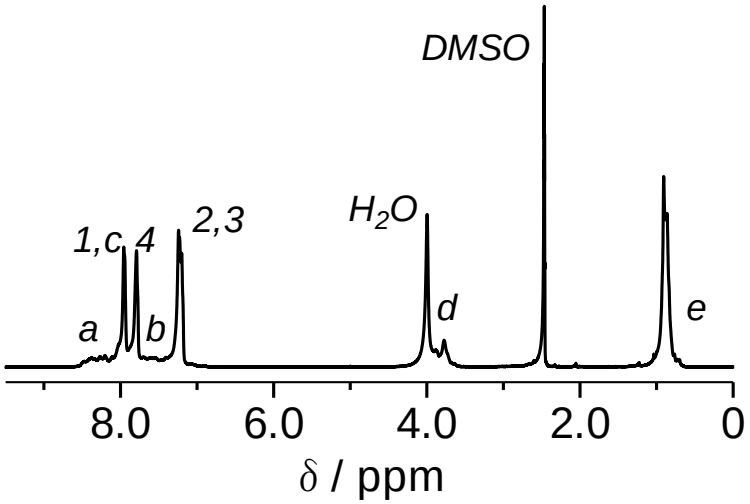
DMSO
H2O
1,c
4
2,3
a
b
d
e
8.0
6.0
4.0
2.0
0
δ / ppm

(b)

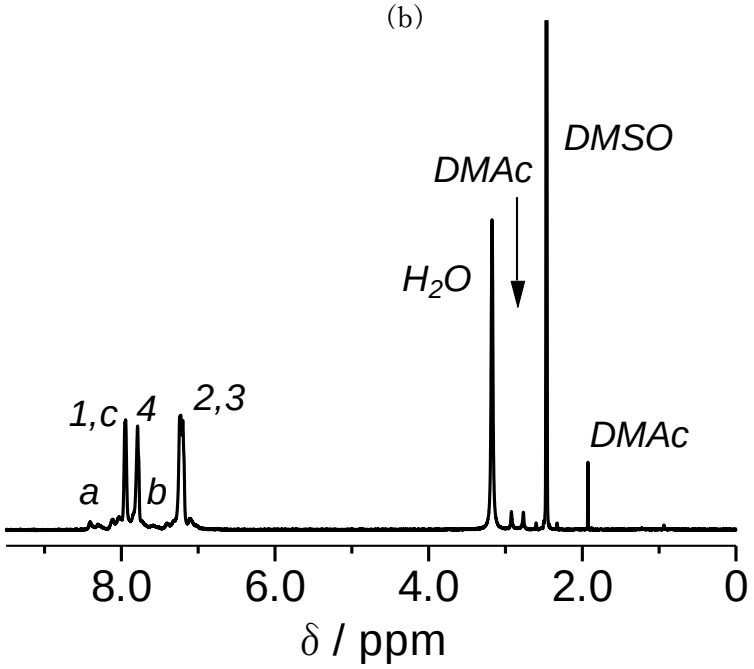
DMSO
DMAc
H2O
1,c
4
2,3
a
b
DMAc
8.0
6.0
4.0
2.0
0
δ / ppm

(c)

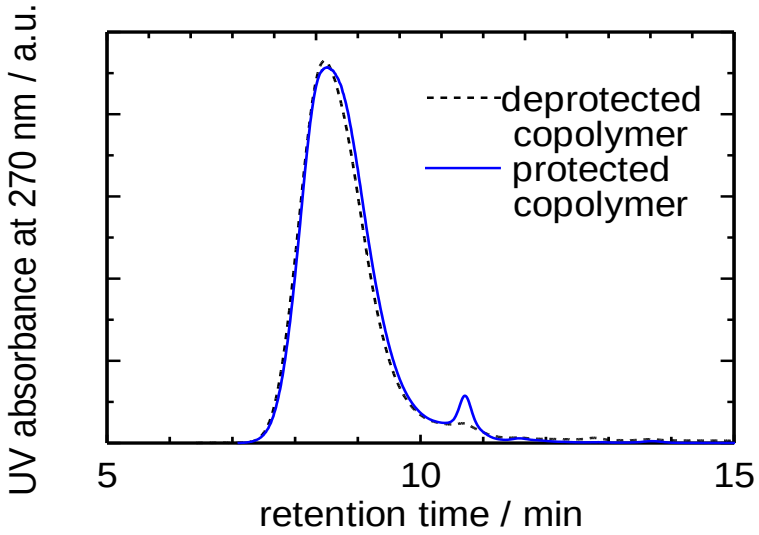

Figure 3-3. (a) ^{1}H NMR spectrum of the copolymer No. 6, (b) ^{1}H NMR spectrum of the deprotected copolymer No. 6 and (c) GPC profiles of the copolymers No. 6 before and after the deprotecting reaction.

Figure 3-4. Picture of the deprotected copolymer membrane No. 6

Figure 3-5 shows the humidity dependence of water uptake and proton conductivity of the copolymer No. 6 membrane at 80 °C. For comparison, data for a reference SPP-*bl*-1 copolymer membrane with the same chemical structures (n = 5, IEC = 2.67 meq. g^{-1}) synthesized using $Ni(cod)_2$ are also shown.[7] The copolymer No. 6 membrane and the reference polymer membrane showed similar water uptake and its humidity dependence from 20 to 95% relative humidity (RH). However, No.6 membrane exhibited slightly lower proton conductivity than that of the reference polymer membrane at any humidity condition investigated probably because of its lower IEC value. The results confirmed that the versatile copolymerization method using $NiBr_2$ via *in-situ* reduction of Ni(II) to Ni(0) provided sulfonated aromatic copolymers with similar chemical structure, molecular weight, and proton conducting behavior.

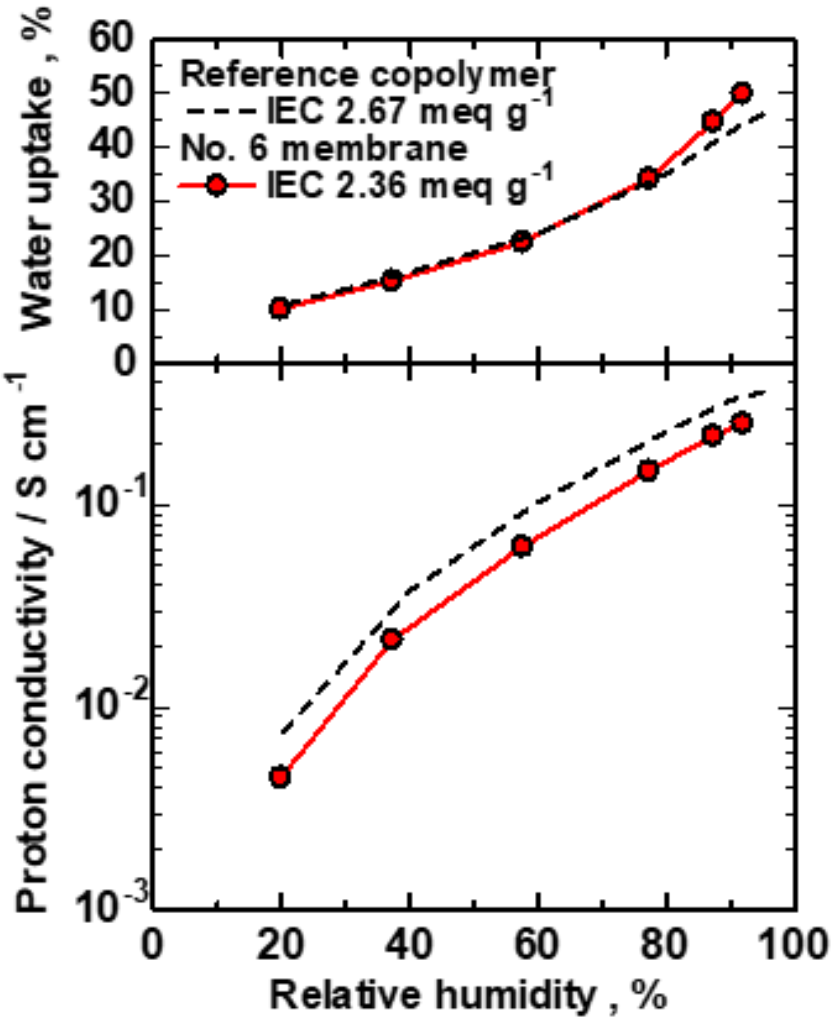

Figure 3-5. Water uptake and proton conductivity of copolymer No. 6 membrane and the reference SPP-*bl*-1 copolymer membrane at 80 °C as a function of relative humidity (RH).

3.4 Conclusion

In conclusion, I have successfully applied the versatile synthetic method of aromatic polymers using $NiBr_2$ via *in-situ* reduction of Ni(II) to Ni(0) to our sulfonated copolymers. The obtained copolymer had similar molecular weight, chemical structure, membrane-forming capability, and proton conductivity compared with those of the copolymers prepared by the previous method using costly and air-sensitive Ni(0). The results not only strengthen the advantages of aromatic polymer-based ionomers for fuel cell applications but also may open applicability of this versatile polymerization method to other functional aromatic polymers.

3.5 Reference

1 M. A. Hickner, H. Ghassemi, Y. S. Kim, B. R. Einsla, J. E. McGrath, *Chem. Rev.* **2004**, *104*, 4587.

2 S. Shi, A. Z. Weber, A. Kusoglu, *J. Membr. Sci.* ***2016***, 516, 123

3 K. D. Kreuer, *Chem. Mater.* **2014**, *26*, 361.

4 N. Li, M. D. Guiver, *Macromolecules* **2014**, *47,* 2175

5 A. Kraytsberg, Y. Ein-Eli, *Energy Fuels* **2014**, *28*, 7303

6 H. Lade, V. Kumar, G. Arthanareeswaran, A. F. Ismail,

Int. J. Hydrogen Energy, **2017**, *42*, 1063

7 J. Miyake, T. Mochizuki, K. Miyatake *ACS Macro Lett.* **2015**, *4*, 750.

8 T. Yamamoto, K. Osakada, T. Wakabayashi, A. Yamamoto, *Makromol. Chem. Rapid Commun.* **1985**, *6*, 671.

9 M. Ueda, F. Ichikawa, *Macromolecules* **1990**, *23*, 926.

10 I. Tonozuka, M. Yoshida, K. Kaneko, Y. Takeoka, M. Rikukawa, *Polymer* **2011**, *52*, 6020.

11 K. Umezawa, T. Oshima, M. Yoshizawa-Fujita, Y. Takeoka, M. Rikukawa, *ACS Macro Lett.* **2012**, *1*, 969.

12 T. Oshima, M. Yoshizawa-Fujita, Y. Takeoka, M. Rikukawa, *ACS Omega* **2016**, *1*, 939.

13 S. Chen, K. Chen, X. Zhang, R. Hara, N. Endo, M. Higa, K. Okamoto, L. Wang, *Polymer* **2013**, *54*, 236.

14 J. Miyake, T. Mochizuki, K. Miyatake *ACS Macro Lett.* **2015**, *4*, 750.

Chapter 4: Differences in the Synthetic Method Affected Copolymer Sequence and Membrane Properties of Sulfonated Polymers

4.1 Introduction

For energy-device applications such as fuel cells, sulfonated hydrocarbon ionomer membranes seem attractive candidates to replace state-of-the-art perfluorosulfonic acid-based ionomers due to easy synthesis, potentially low cost, wide variety of molecular structure, and environmental compatibility.[1-3] A number of sulfonated aromatic copolymers were reported in the literature.[4,5] Recently, sulfonated aromatic polymers without heteroatom linkages in the main chains have been claimed to exhibit excellent membrane properties (high proton conductivity, superior mechanical properties, gas barrier properties, and high chemical stability).[6,7] For example, Holdcroft et al. reported that a sulfophenylated terphenylene copolymer membrane with ion exchange capacity (IEC) of 3.70 meq g^{-1} showed high proton conductivity (338 mS cm^{-1} at 80 ºC and 95% RH) and displayed no practical weight loss and chemical degradation in the oxidative stability test (at 80 ºC in Fenton's reagent).[8] We have also developed a series of sulfonated aromatic copolymers composed of sulfo-1,4-phenylene group as the hydrophilic component, and arylene ether oligomer (SPP-*bl*-1),[9] hexafluoroisopropylidene (SBAF),[10] quinquephenylene (SPP-QP),[11] or perfluoroalkylene (SPAF)[12] group as the hydrophobic component. The copolymer membranes exhibited high proton conductivity (360 mS cm^{-1} for SPP-*bl*-1 with IEC = 2.67 meq g^{-1}, 218 mS cm^{-1} for SBAF with IEC = 2.50 meq g^{-1}, 166 mS cm^{-1} for SPP-QP with IEC = 2.43 meq g^{-1} and 220

mS cm^{-1} for SPAF with IEC = 1.60 meq g^{-1} at 80 ºC and 95% RH). Among these membrane, SBAF and SPP-QP membranes had significantly high chemical stability in the oxidative stability test. Other membrane properties such as mechanical strength and gas permeability were tunable depending on the hydrophobic components and their composition. These sulfonated aromatic copolymers required costly, air- and moisture-sensitive Ni(0) complex, bis(1,5-cyclooctadiene)nickel(0) ($Ni(COD)_2$), as a promoter for efficient C-C coupling copolymerization reactions to obtain high molecular weight polymers, which undermines the advantages of potentially inexpensive hydrocarbon-based materials. To overcome this issue, we preliminary proposed more versatile synthetic method without using Ni(0) complex for SPP-*bl*-1, where $NiBr_2$ was used as the promoter in the presence of Zn powder.[13] The obtained SPP-*bl*-1 copolymer synthesized with $NiBr_2$ showed high molecular weight (M_n: 60.1 kDa, M_w: 133 kDa) and provided thin and self-standing membrane. The result suggests that *in-situ* reduction of Ni(II) to Ni(0) by Zn occurred efficiently during the copolymerization reaction.

The objective of the present research is to apply the newly developed polymerization method using $NiBr_2$ and Zn to other series of the sulfonated aromatic copolymers to confirm its versatility. We have investigated in detail copolymer structure including composition and sequence of the components and compared the structure, morphology, membrane properties with those of the copolymers synthesized with Ni(0).

4.2 Experimental

4.2.1 Materials

2,5-Dichlorobenzenesulfonyl chloride, 2,2-dimethyl-1-propanol, 1,4-phenylenediboronic acid, 1-bromo-3-iodobenzene, tri(*o*-tolyl)phosphine, palladium acetate, perfluoro-1,6-diiodohexane, 1-chloro-3-iodobenzene, and 4,4'-(hexafluoroisopropylidene)diphenol were purchased from TCI, Inc. and used as received. 3-Chlorophenylboronic acid, pyridine, Cu powder (particle size 75–150 μm), 2,2'-bipyridyl, sodium sulfate (Na_2SO_4), sodium carbonate (Na_2CO_3), sodium hydrogen carbonate ($NaHCO_3$), sodium chloride (NaCl), lithium bromide (LiBr), activated carbon, ethanol, methanol, 2-propanol, ethyl acetate, dichloromethane, toluene, toluene dehydrated, N,N-dimethylformamide, dimethyl sulfoxide (DMSO), deuterated dimethyl sulfoxide (DMSO-d_6), 0.01 M sodium hydroxide aqueous solution, nitric acid, and hydrochloric acid were purchased from Kanto Chemical Co. and used as received. Nickel(II) bromide ($NiBr_2$) and sodium iodide (NaI) were purchased from Wako and used as received. Dichlorotriphenylphosphorane was purchased from Sigma-Aldrich and used as received. N,N-Dimethylacetamide (DMAc) was purchased from Kanto Chemical Co. and dehydrated over solvent purification system (Nikko Hansen & co., LTD) prior to use. Zn powder was purchased from Wako and washed with 1.0 M hydrochloric acid, ethanol, and acetone prior to use. The protected monomer (SP-p) was synthesized according to the literature.[1]

4.2.2 Measurements

^{1}H NMR spectra were obtained on a JEOL JNM-ECA 500 using deuterated dimethyl sulfoxide (DMSO-d_6) as a solvent and tetramethylsilane (TMS) as an internal reference. Molecular weight of the copolymers was measured with gel permeation chromatography (GPC) equipped with a Jasco 805 UV detector and a Shodex K-805L column. DMF containing 0.01 M LiBr was used as eluent. Molecular weight was calibrated with standard polystyrene samples. Ion exchange capacity (IEC) of the copolymer membranes was determined by back-titration. A piece of the membrane (ca. 30 mg) was equilibrated in 60 mL of 2 M NaCl aqueous solution for 12 h. HCl released from the membrane by the ion exchange reaction was titrated with standard 0.01 M NaOH aqueous solution at r.t.

Water uptake and proton conductivity of the membranes were measured at 80 °C with a solid electrolyte analyzer system (MSBAD-V-FC, Bel Japan Co.) equipped with a temperature/humidity-controllable chamber. Weight of the membrane was measured by magnetic suspension balance at a given humidity, then water uptake was calculated using the following equation. [(weight of hydrated membrane - weight of dry membrane) / weight of dry membrane × 100] Vacuum drying for 3 h at 80 °C gave the weight of dry membranes and exposure to a given humidity for at least 2 h gave the weight of hydrated membranes. Proton conductivity was measured using a four-probe conductivity cell equipped with Solartron 1255B and SI1287 impedance analyzers in the same chamber. Ion conducting resistances (R) were determined from the impedance plot obtained in the frequency range from 1 to 10^5 Hz. The proton conductivity (σ) was calculated from the equation $\sigma = l/(A \times R)$, where A and l are the conducting area and the electrode distance, respectively.

Morphology of the membranes was analyzed by transmission electron microscopy (TEM). For TEM observation, the membranes were stained with lead ions (Pb^{2+}) by ion exchange of the sulfonic acid groups in 0.5 M $Pb(OAc)_2$ aqueous solution, rinsed with deionized water, and dried in a vacuum oven overnight. The stained samples were embedded in epoxy resin, sectioned into 50 nm slices with a Leica microtome Ultracut UCT, collected by Cu grids, and then investigated with a Hitachi H-9500 TEM at an acceleration voltage of 200 kV.

SAXS measurement was conducted using a Rigaku NANO-Viewer diffractometer equipped with a temperature/humidity-controllable chamber. The membrane was equilibrated for at least 2 h under each humidity condition from 30% to 90% relative humidity (RH) at 80 °C.

Tensile strength testing was carried out with a Shimadzu universal testing instrument Autograph AGS-J500N equipped with a temperature/humidity-controllable chamber. A membrane sample in proton form was cut into a dumbbell shape (35 × 6 mm (total) and 12 × 2 mm (test area)). Stress versus strain curves were obtained at 80 °C and 60% RH at a stretching rate of 10 mm min^{-1} after equilibrating the membrane for at least 3 h.

4.2.3 Copolymerization Reaction

Oligomer **1** and monomers **2**, **3**, and **4** were synthesized according to the literature.[9-13] A typical polymerization procedure is as follows. A 100 mL three neck flask equipped with a reflux condenser, a Dean-Stark trap, a mechanical stirrer, and a nitrogen inlet/outlet was charged with **1** or **2** or **3** or **4**, $NiBr_2$ (1.2 equivalent to total amount of Cl), NaI (2.1 equivalent to the amount of $NiBr_2$), 2,2'-bipyridyl (2.1 equivalent to the amount of $NiBr_2$), DMAc (molar concentration of the total amount of the monomers in DMAc was 0.379 M), and toluene (the

same volume as DMAc). The mixture was heated at 145 °C for 2 h for azeotropic removal of water. Then, the mixture was cooled to 60 °C, and Zn (5.0 equivalent to the amount of $NiBr_2$) and the protected monomer (SP-p) were added to the mixture. The mixture was stirred with mechanical stirrer for 3 h. After the copolymerization reaction, the mixture was poured into a large excess of methanol to precipitate the product. The crude product was washed with 6 M HCl and water. The obtained protected copolymers were dried in a vacuum oven at 60 °C overnight.

4.2.4 Deprotection Reaction

A 100 mL three neck flask equipped with a reflux condenser, a magnetic stirring bar, and a nitrogen inlet/outlet was charged with the protected copolymer, LiBr (4.0 equivalent to the amount of neopentyl groups), and DMAc (the concentration of the protected copolymer was 0.10 w/v). The mixture was heated at 100 °C for 24 h. After the reaction, the mixture was poured into 1 M HCl (70 mL). The resulting yellow suspension was dialyzed with a regenerated cellulose film tubing (cut-off molecular weight: 1000). The dialyzed solution was evaporated and dried in a vacuum oven at 80 °C overnight to recover a deprotected copolymer.

4.2.5 Membrane Preparation

A 5 mL of 10 wt% copolymer solution in DMAc was cast on a flat glass plate and dried at 60 ° C overnight. The resulting membranes were treated with 1 M H_2SO_4 aqueous solution for 1 d, and washed in deionized water several times to remove residual H_2SO_4.

4.3 Result and discussion

4.3.1 Synthesis and Characterization

A series of sulfonated aromatic hydrocarbon copolymers were synthesized from the neopentyl-protected sulfophenylene monomer (SP-p) and monomers **1-4** via the previously reported C-C coupling reaction using $NiBr_2$ (Scheme 1).[13] For reference, the same series of the copolymers were also prepared using $Ni(COD)_2$ as a promoter (Scheme 2).[9-12] The feed comonomer ratio was controlled to obtain copolymers with different IEC values. After the deprotecting reaction, the resulting copolymers (denoted as (B)) showed similar solvent solubility to those prepared with $Ni(COD)_2$ (denoted as (C)); soluble in polar aprotic solvents such as DMSO, DMAc and NMP. Copolymers (B) had slightly lower molecular weights (M_n = 4.83-60.1 kDa, M_w = 24.9-133 kDa) compared with those of the copolymers (C) (M_n = 22.3-66.2 kDa, M_w = 76.4-240 kDa) (Table 4-1). Nevertheless, the resulting copolymers (B) provided bendable and transparent membranes by solution casting. The results indicate that the copolymerization method via the *in-situ* reduction of Ni^{2+} with Zn functioned well and was versatile, providing sulfonated aromatic hydrocarbon copolymers with a wide variety of molecular structures including arylene ether, partially fluorinated, all-phenylene, or perfluoroalkylene groups. The chemical structure of the copolymers (B) and (C) was analyzed by ^1H NMR spectra. A typical example is shown in Figure 4-1(b) for SPP-QP(C) with SPP-QP(B) for comparison. Lack of the protons of neopentyl groups (e.g., 3.7 ppm for protons *d*) supports complete deprotection reaction using LiBr. At the lowest magnetic field (8.2 - 8.4 ppm) in the aromatic region, differences were observed between SPP-QP(C) and SPP-QP(B). These peaks were most likely assignable to the protons (*a*) in the sulfo-2,5-phenylene

groups. From the literature that reported ^{1}H NMR chemical shifts of some model biphenyl compounds having sulfonic acid groups at different positions,[14-16] we reasonably assigned three peaks of protons *a*, as a_1 for SP unit with unsubstituted phenylene groups at both ends, a_2 for two-connected SP units with one unsubstituted phenylene group, and a_3 for three-connected SP units (Figure 4-1(a)). (Note that the peak a_3 overlapped with the peak 2 in this case) We defined the integral ratio of $(a_1/a_1+a_2+a_3)$ as the randomness of SP unit or the isolated hydrophilic component (SP) ratio in the copolymer backbone. The randomness was calculated for all copolymers by ^{1}H NMR spectra (Figure 4-1(c)-(e)) and included in Table 4-1. The copolymers (B) showed randomness ranging from 26% to 79%, much higher than that of the copolymers (C) (12% to 38%). In other words, the copolymers (B) contained less sequenced structure in the hydrophilic components. The result suggests that the non-ionic, protected SP-p monomer with low polarity as the hydrophilic component had similar reactivity to the hydrophobic oligomer **1** and monomers (**2**, **3**, and **4**) and caused increased randomness of the comonomer sequence in the polymer chains. The randomness of SP unit was likely to be higher (SBAF (C) with 1.50 meq g^{-1} > SBAF (C) with 2.50 meq g^{-1} > SPAF (C) with 1.60 meq g^{-1} > SPP-QP (C) > SPP-*bl*-1(C), SBAF (B) with 1.43 meq g^{-1} > SPP-QP (B) > SBAF (B) with 2.60 meq g^{-1} > SPAF (B) with 1.50 meq g^{-1} > SPP-*bl*-1(B)) when the smaller hydrophobic comonomer was used for the copolymerization.

Table 4-1. Copolymerization results for sulfonated polyphenylene derivatives using $NiBr_2$ or $Ni(COD)_2$.

Copolymer	A	Promoter[a]	Yield (%)	M_n (kDa)	M_w (kDa)	IEC theo.[b] (meq. g^{-1})	IEC by titration (meq. g^{-1})	Randomness of SP unit[c] (%)	Dimensional change, in-plane[d] (%)	Dimensional change, through-plane[d] (%)
SPP-*bl*-1(B)	**1**	$NiBr_2$	85	60.1	133	2.82	2.36	26	8	42
SBAF(B)	**2**	$NiBr_2$	93	27.7	63.0	2.00	1.43	79	1	1
SBAF(B)	**2**	$NiBr_2$	99	25.6	57.9	3.00	2.60	32	13	21
SPP-QP(B)	**3**	$NiBr_2$	96	27.2	67.3	2.82	2.31	47	10	24
SPAF(B)	**4**	$NiBr_2$	90	28.6	69.4	2.00	1.50	26	28	11
SPAF(B)	**4**	$NiBr_2$	82	23.3	59.8	2.50	1.92	27	16	13
SPAF(B)	**4**	$NiBr_2$	98	4.83	24.9	3.50	2.75	34	51	11
SPP-*bl*-1(C)	**1**	$Ni(COD)_2$	79	22.3	240	3.60	2.67	12	13	26
SBAF(C)	**2**	$Ni(COD)_2$	94	42.3	158	1.70	1.50	38	10	3
SBAF(C)	**2**	$Ni(COD)_2$	94	66.2	180	3.00	2.50	30	15	23
SPP-QP(C)	**3**	$Ni(COD)_2$	97	32.2	76.4	3.10	2.43	19	10	17
SPAF(C)	**4**	$Ni(COD)_2$	95	57.6	146	1.90	1.60	21	11	24

[a]See Schemes 1 and 2 for details with $NiBr_2$ and $Ni(COD)_2$, respectively.

[b]Calculated from the feed comonomer ratio.

[c]Randomness of SP unit: the integral ratio of ($a_1/a_1+a_2+a_3$) in the NMR spectra (see Figure 1 for example).

[d]In water at r.t. for 2 h. Calculated from the equation: $(L_{wet}-L_{dry})/L_{dry}\times 100$, where L is the length (in-plane) or thickness (through-plane) of the membranes.

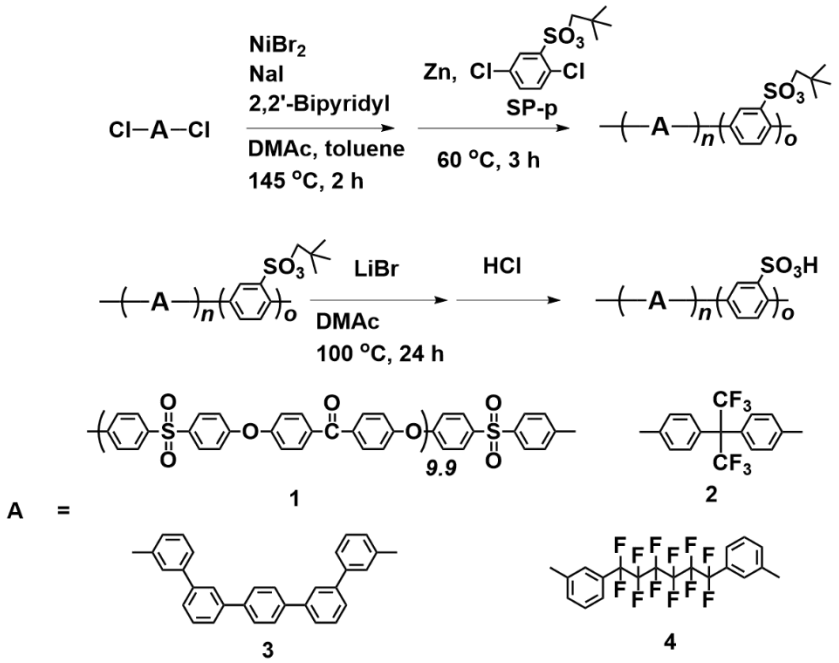

Scheme 4-1. Synthesis of sulfonated polyphenylene derivatives using $NiBr_2$

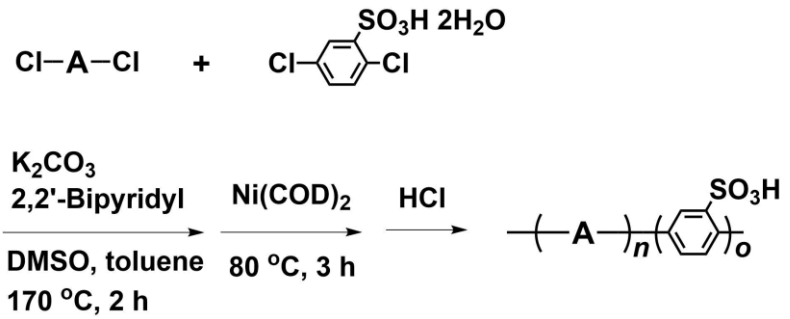

Scheme 4-2. Synthesis of sulfonated polyphenylene derivatives using $Ni(COD)_2$.

(a)

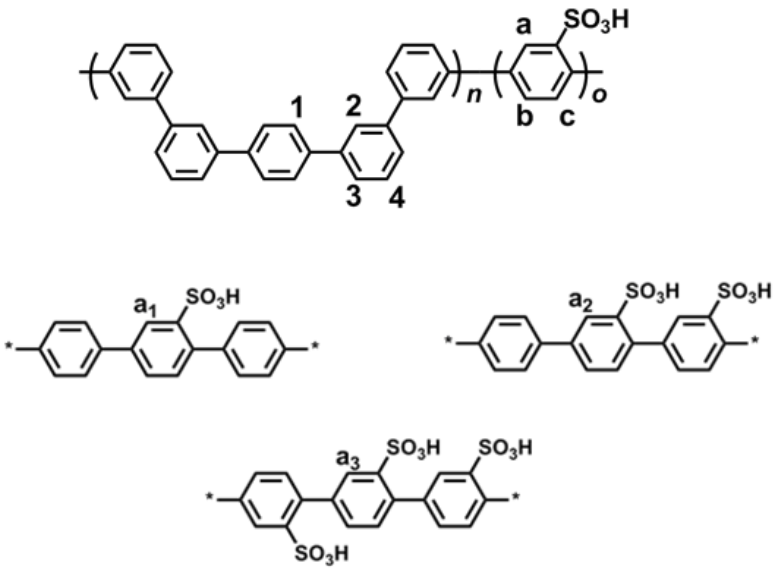
a
SO3H
n
o
b
c
1
2
3
4
a1
SO3H
a2
SO3H
SO3H
a3
SO3H
SO3H
SO3H

(b)

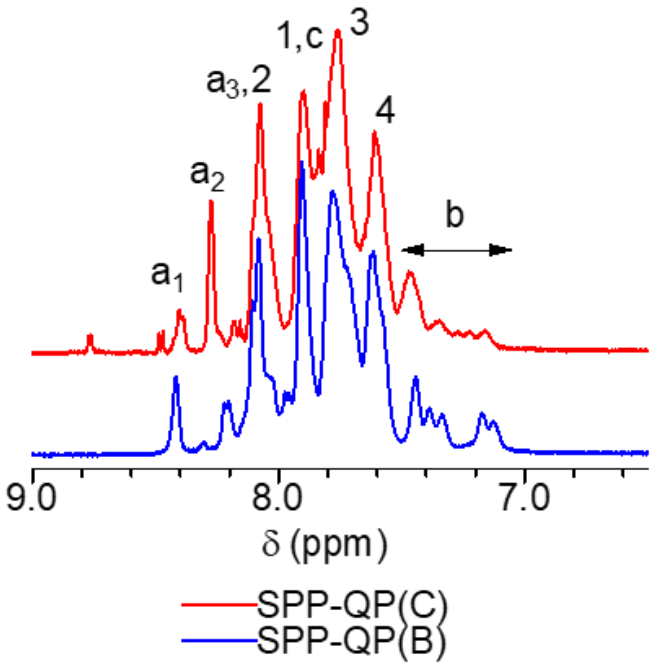
1,c
3
a3,2
4
a2
b
a1
9.0
8.0
7.0
δ (ppm)
SPP-QP(C)
SPP-QP(B)

(c)

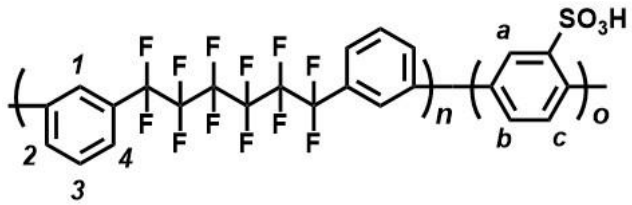
SO3H
a
1
F
F
F
F
F
F
F
F
F
F
F
F
n
2
4
3
b
c
o

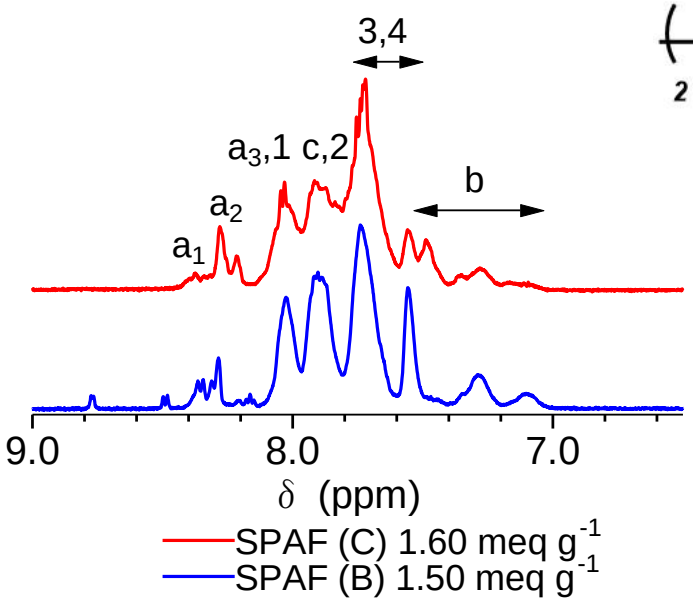
3,4
a3,1 c,2
b
a2
a1
9.0
8.0
7.0
δ (ppm)
SPAF (C) 1.60 meq g-1
SPAF (B) 1.50 meq g-1

(d)

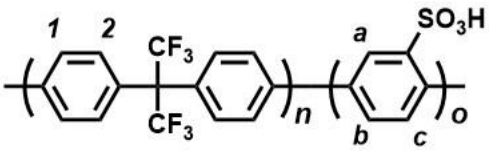
SO3H
1
2
CF3
CF3
a
n
b
c
o

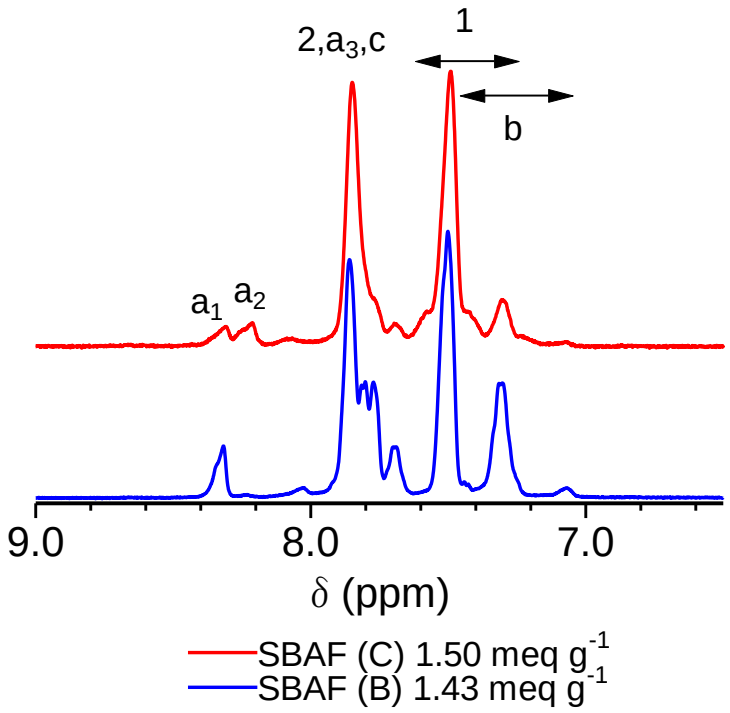
2,a3,c
1
b
a1
a2
9.0
8.0
7.0
δ (ppm)
SBAF (C) 1.50 meq g-1
SBAF (B) 1.43 meq g-1

(e)

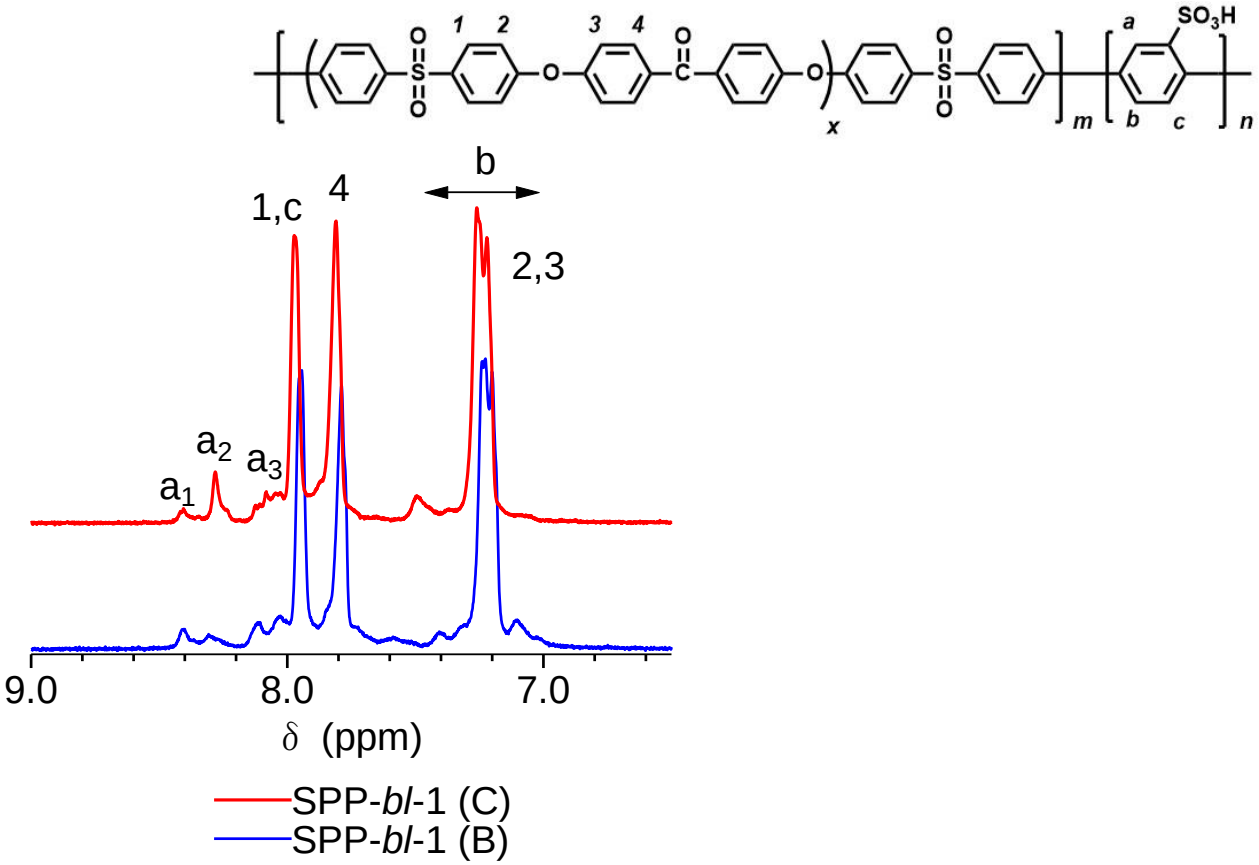

Figure 4-1. (a) Chemical structure of SPP-QP and possible sequences containing SP units, ^{1}H NMR spectra of (b) SPP-QP (B) with IEC = 2.31 meq. g^{-1} and (C) with 2.43 meq. g^{-1} (c) SPAF (B) with IEC = 1.50 meq. g^{-1} and (C) with IEC = 1.60 meq. g^{-1}, (d) SBAF (B) with IEC = 1.43 meq. g^{-1} and (C) with IEC = 1.50 meq. g^{-1}, and (e) SPP-*bl*-1(B) with IEC =2.36 meq. g^{-1} and (C) with IEC = 2.67 meq. g^{-1} copolymers in DMSO-d_6 at 80 ºC.

4.3.2. Morphology

To investigate the effect of the comonomer sequence on the morphology of the copolymers (B) and (C) membranes, TEM and SAXS analyses were carried out. As a representative example, TEM images of SPP-QP (B) and (C) membranes stained with Pb^{2+} ions are shown in Figure 4-2. These membranes showed quite similar morphology, i.e., well-developed hydrophobic (bright) / hydrophilic (dark) nanophase separation with the size of approximately 2 nm for both clusters. SBAF and SPAF membranes also exhibited a similar nanophase separation and cluster size between (B) and (C) series (Figure 4-2). The hydrophilic and hydrophobic cluster sizes were ca. 1.2 nm for SBAF and ca. 1.1 nm for SPAF, respectively. Based on these results, the difference in the comonomer sequence or the randomness of SP unit did not affect the phase-separated morphology under the dry conditions.

Then, the membrane morphology was further investigated via SAXS measurements under controlled humidity conditions from 30% to 90% relative humidity (RH) at 80 °C. Figure 4-3 shows the scattered intensity with respect to the scattering vector (q). SPP-QP (C) membrane exhibited a scattering peak at ca. q = 0.79 nm^{-1} or d = 7.9 nm at 30% RH, which became smaller as increasing the humidity. The results suggest that wetting disturbed the formation of uniform-sized ionic clusters. Similar behavior was observed with our sulfonated aromatic polymer membranes in which the water would be absorbed not only in the hydrophilic domains but also in the hydrophobic ones causing randomization of the ionic clusters.[17] In contrast, SPP-QP (B) membrane exhibited no scattering peaks at any humidity investigated indicating that uniform-sized ionic clusters did not form under wet conditions.

The SPP-QP (C) with low randomness or sequenced structure of the SP units tended to form uniform-sized ionic clusters with high periodicity. SPAF (B) and (C) membranes showed a peak, of which *d* spacing was 5.45 and 10.9 nm for (B) and (C) membranes, respectively (Figure 4-3). Humidity dependence of the SAXS peak for SPAF membrane was contrary to that of SPP-QP (C) membrane, but similar to that of perfluorosulfonic acid ionomer membranes such as Nafion; the peak developed as increasing the humidity.[17] The presence of highly hydrophobic perfluoroalkyl groups in the main chain possibly caused distinct hydrophilic/hydrophobic phase-separation and promoted the selective water absorption in the hydrophilic clusters. SBAF (B) and (C) membranes with IEC = 1.50 meq g^{-1} did not show the scattering peaks at any humidity conditions. Rigid but smaller molecular size of BAF groups than QP and PAF moieties (0.72 nm for BAF, 1.53 nm for QP and 1.42 nm for PAF, respectively, estimated by B3LYP 6-31G*) would not promote the formation of a periodic structure.

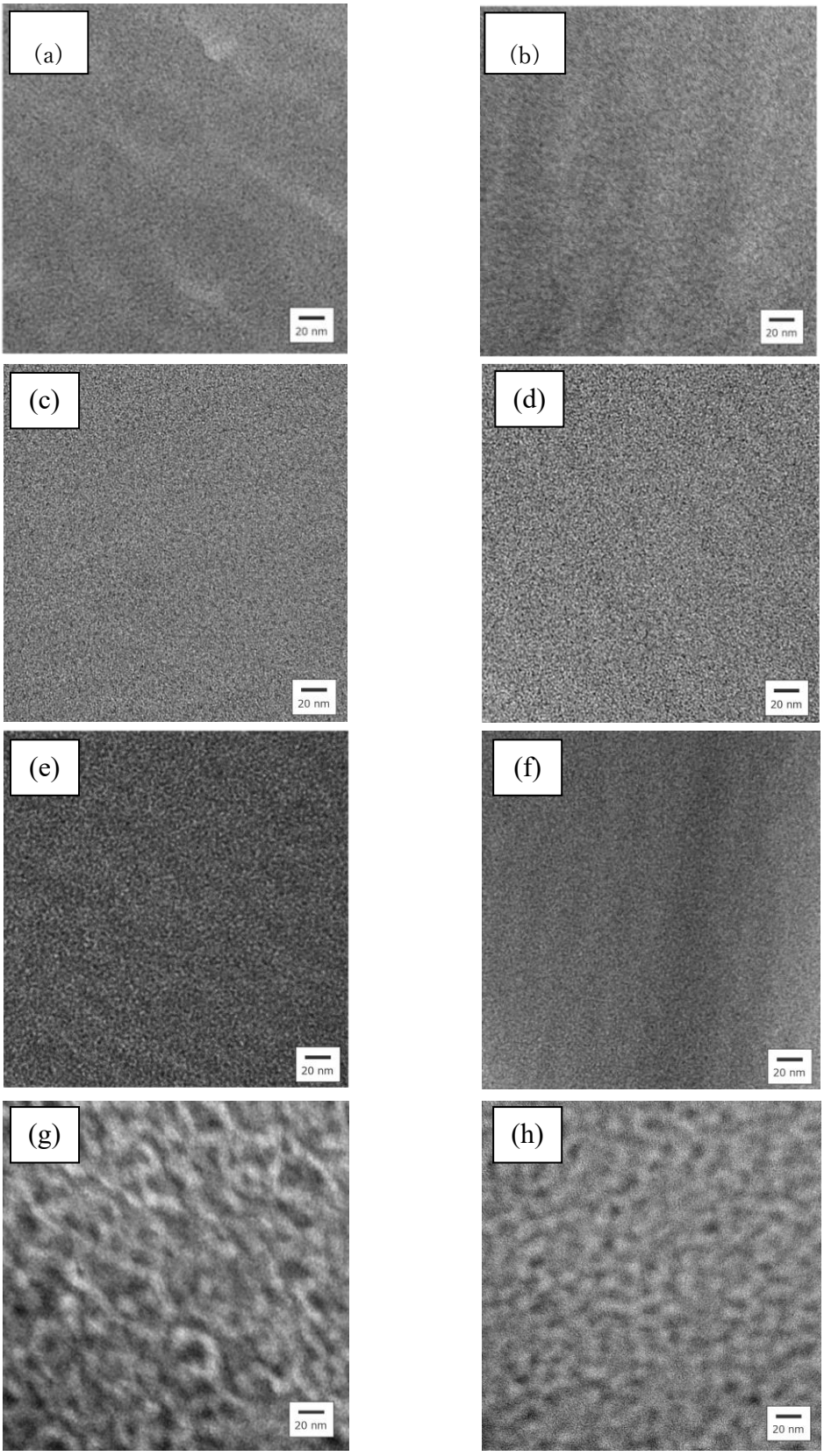

Figure 4-2. TEM images of (a) SPP-QP (B) with IEC = 2.31 meq. g^{-1} and (b) SPP-QP (C) with 2.43 meq. g^{-1}, (c) SPAF (B) with IEC = 1.50 meq. g^{-1} (d) SPAF (C) IEC = with 1.60 meq. g^{-1}, (e) SBAF (B) with IEC = 1.43 meq. g^{-1} (f) SBAF (C) with IEC = 1.50 meq. g^{-1}, (g) SPP-*bl*-1 (B) with IEC = 2.36 meq. g^{-1} and (h) SPP-*bl*-1 (C) with IEC = 2.67 meq. g^{-1} membrane. The samples were ion-exchanged with lead (Pb^{2+}) ions prior to the observation so as to stain the hydrophilic domains in black.

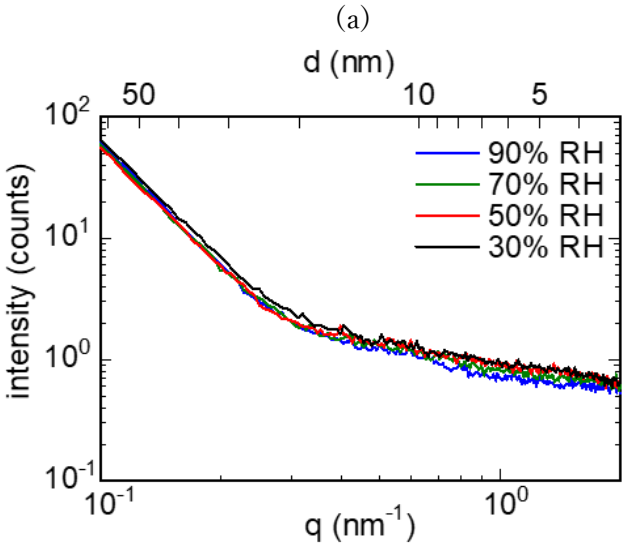
(a)
d (nm)
50
10
5
intensity (counts)
q (nm^{-1})
90% RH
70% RH
50% RH
30% RH

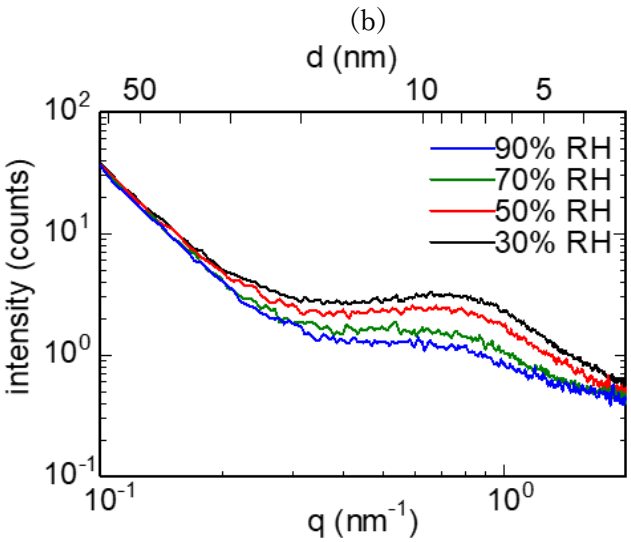
(b)
d (nm)
50
10
5
intensity (counts)
q (nm^{-1})
90% RH
70% RH
50% RH
30% RH

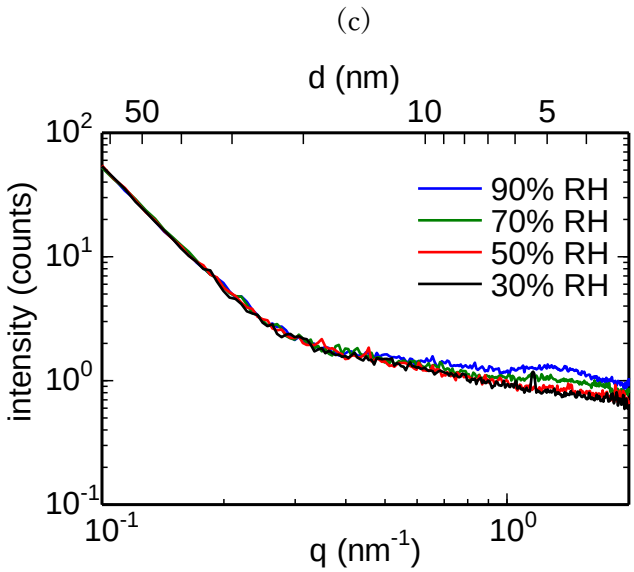
(c)
d (nm)
50
10
5
intensity (counts)
q (nm^{-1})
90% RH
70% RH
50% RH
30% RH

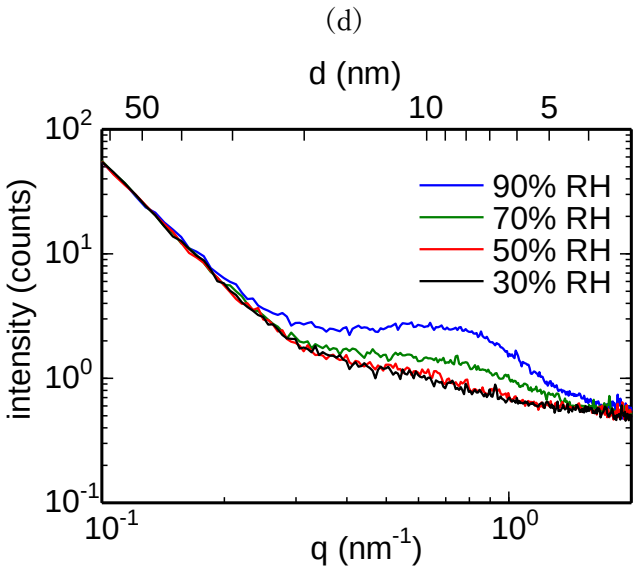
(d)
d (nm)
50
10
5
intensity (counts)
q (nm^{-1})
90% RH
70% RH
50% RH
30% RH

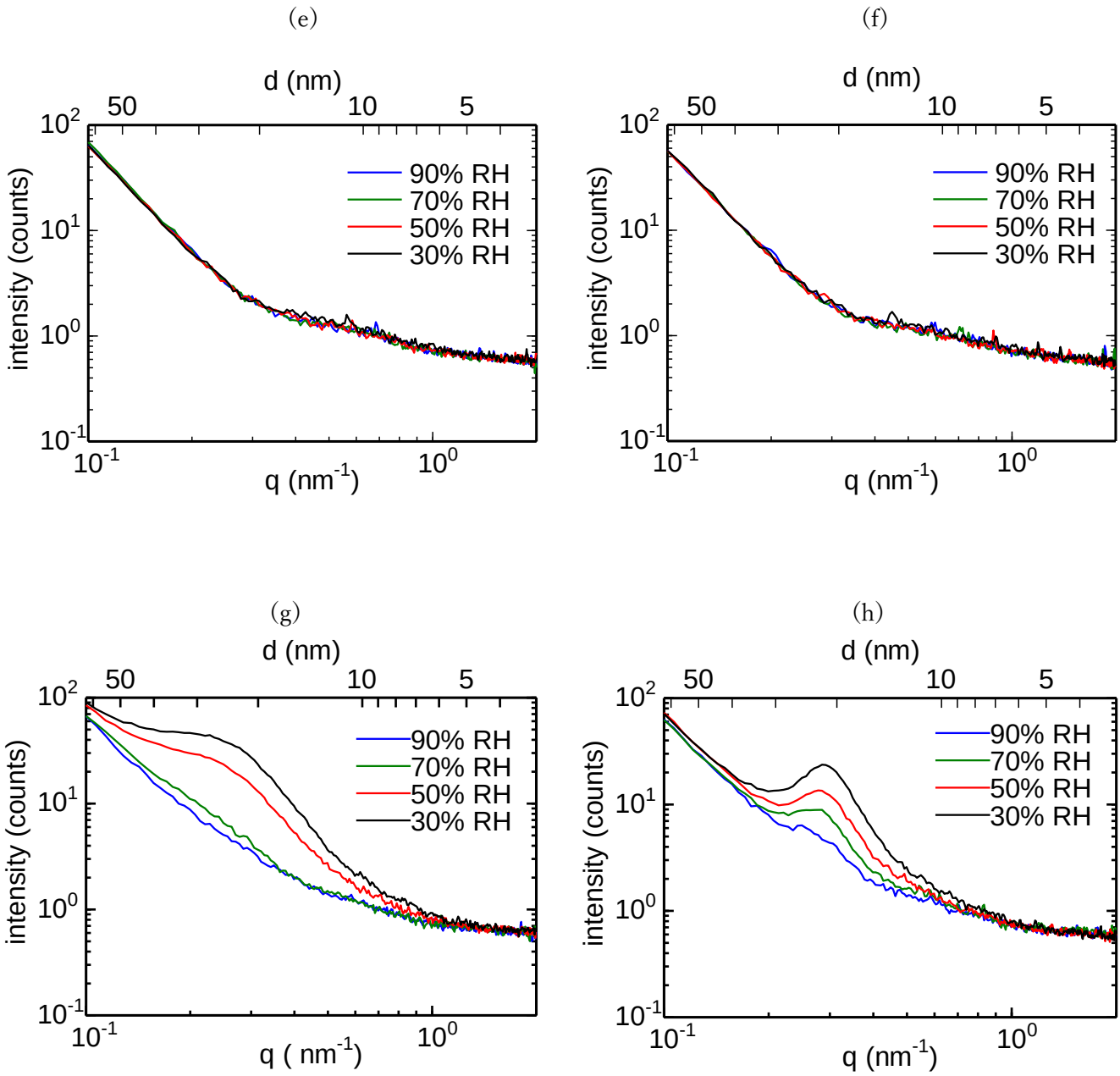

Figure 4-3. SAXS profiles for (a) SPP-QP (B) with IEC = 2.31 meq. g^{-1} and (b) SPP-QP (C) with 2.43 meq. g^{-1}, (c) SPAF (B) with IEC = 1.50 meq. g^{-1} (d) SPAF (C) IEC = with 1.60 meq. g^{-1}, (e) SBAF (B) with IEC = 1.43 meq. g^{-1} (f) SBAF (C) with IEC = 1.50 meq. g^{-1}, (g) SPP-*bl*-1 (B) with IEC = 2.36 meq. g^{-1} and (h) SPP-*bl*-1 (C) with IEC = 2.67 meq. g^{-1} membrane as a function of the *q* value at humidity from 30% to 90% RH and 80 °C.

4.3.3 Water Uptake and Ion Conductivity

Water uptake and proton conductivity of the SPP-QP membranes were measured at 80 ºC and plotted as a function of the relative humidity (Figure 4-4). The water uptake of SPP-QP (B) membrane was comparable to that of SPP-QP (C) membrane. Nevertheless, SPP-QP (B) membrane showed slightly lower proton conductivity compared with SPP-QP (C). The proton conductivity was re-plotted as a function of λ which is defined as number of the absorbed water molecules per sulfonic acid group (Figure 4-5). At any λ value, proton conductivity of SPP-QP (B) membrane was lower than that of SPP-QP (C) membrane indicating that SPP-QP (C) membrane could efficiently use the water molecules for proton transport. Similar behavior was also observed in SPAF, SBAF and SPP-*bl*-1 membranes (Figures 4-5); i.e., SPAF (C), SBAF (C) and SPP-*bl*-1 (C) membranes were more proton conductive compared with the corresponding (B) membranes. At 20% RH, for example, the conductivity of (C) membranes was 3 times higher for SPAF with IEC = 1.60 meq g^{-1}, 9 times higher for SBAF with IEC = 1.50 meq g^{-1}, and 1.6 times higher for SPP-*bl*-1 with IEC = 2.67 meq g^{-1}, respectively, than those of the corresponding (B) membranes. In general, proton conductivity of proton exchange membranes depends significantly on the morphology, in particular, size and connectivity of ionic domains as proton transporting pathway. It is well-recognized for the block copolymer-based proton exchange membranes that longer block length both in the hydrophilic and hydrophobic components resulted in more developed phase-separated morphology and higher proton conductivity.[18,19] As discussed above, SPP-QP (B) had higher randomness of SP unit (higher degree of isolated hydrophilic component) and less uniform-sized ionic clusters. Therefore, the hydrophilic clusters of SPP-QP (B)

membrane were less-developed compared with those of SPP-QP (C) membrane, which must be responsible for the lower proton conductivity of SPP-QP (B) membrane. For detailed discussion, the relative water uptake and proton conductivity defined as (C)/(B) values at 20% RH were plotted as a function of the randomness. (Figure 4-6) The relative water uptake was approximately constant, indicating that the water uptake was not affected by the randomness of the hydrophilic component and the membrane morphology but simply dependent on the concentration of the ionic groups (*e.g.*, IEC value). A similar trend was observed in dimensional change (in water at r.t. for 2 h). The dimensional changes increased with increasing the IEC value (or water uptake) but had no correlation with the randomness of SP unit (Table 1). In contrast, the relative proton conductivity increased with decreasing the randomness of SP units. The tendency was more pronounced for the SPAF and SBAF membranes with partially fluorinated hydrophobic components. Lower randomness of SP units presumably caused well-developed ionic channels resulting in improved proton conductivity.

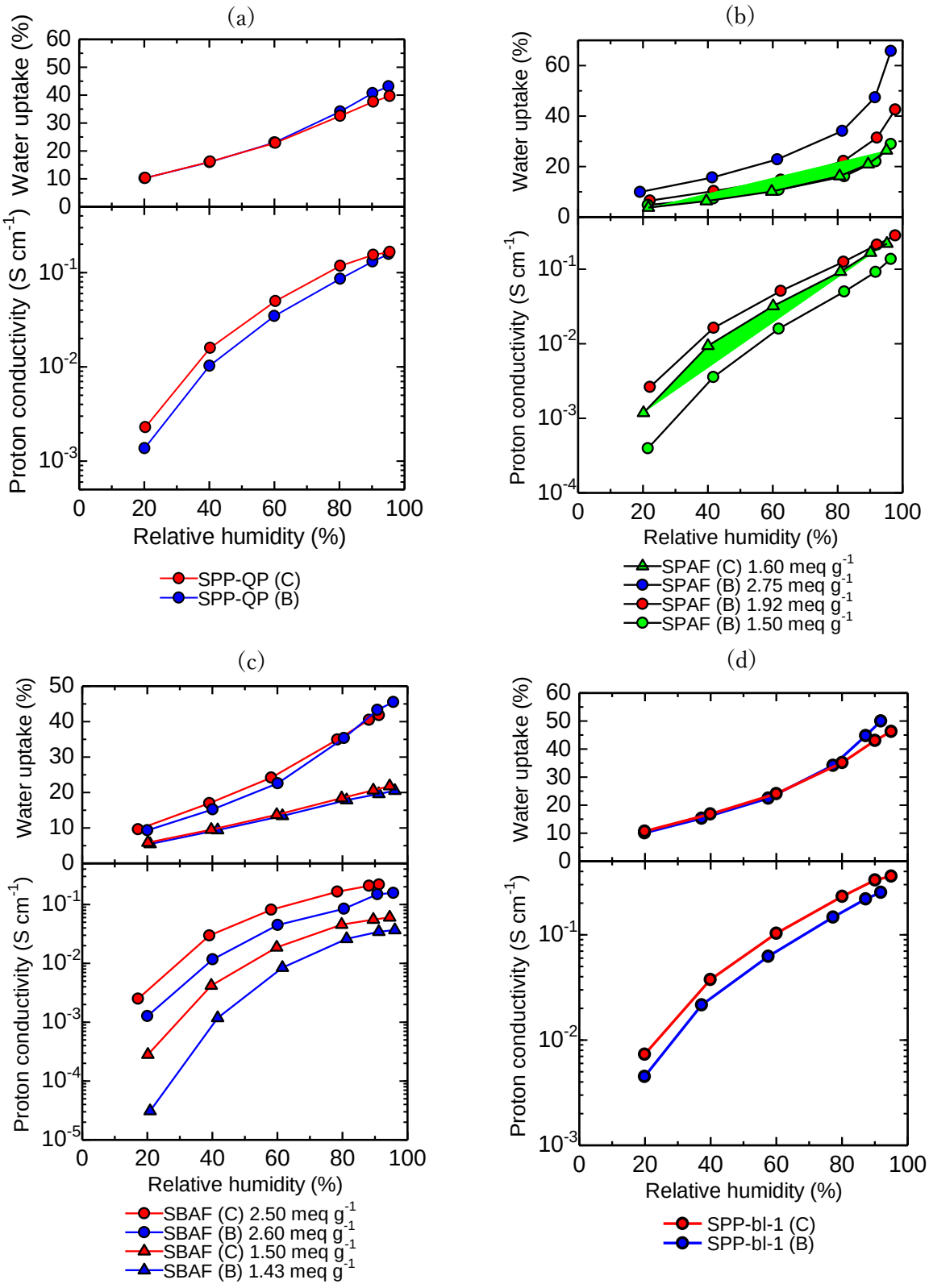

Figure 4-4. Water uptake and proton conductivity of (a) SPP-QP series (b) SPAF series membranes, (c) SBAF series membranes and (d) SPP-*bl*-1 series membranes at 80 °C as a function of relative humidity.

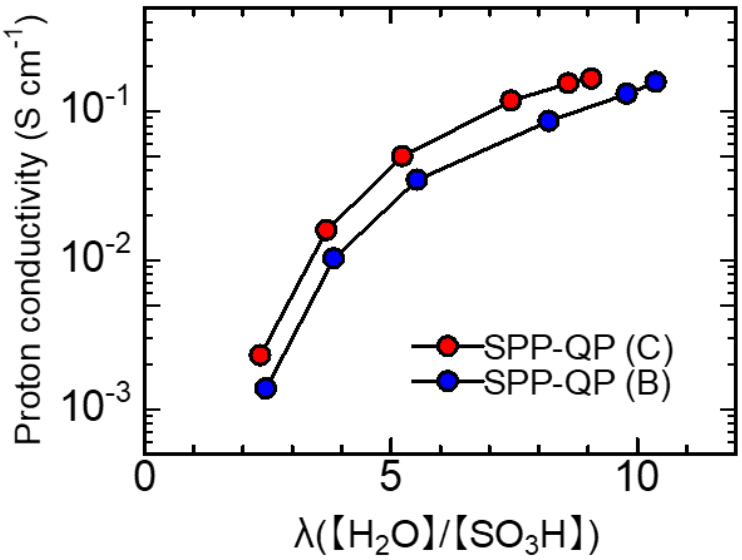

Figure 4-5. Proton conductivity of SPP-QP (B) and (C) membranes at 80 °C as a function of λ.

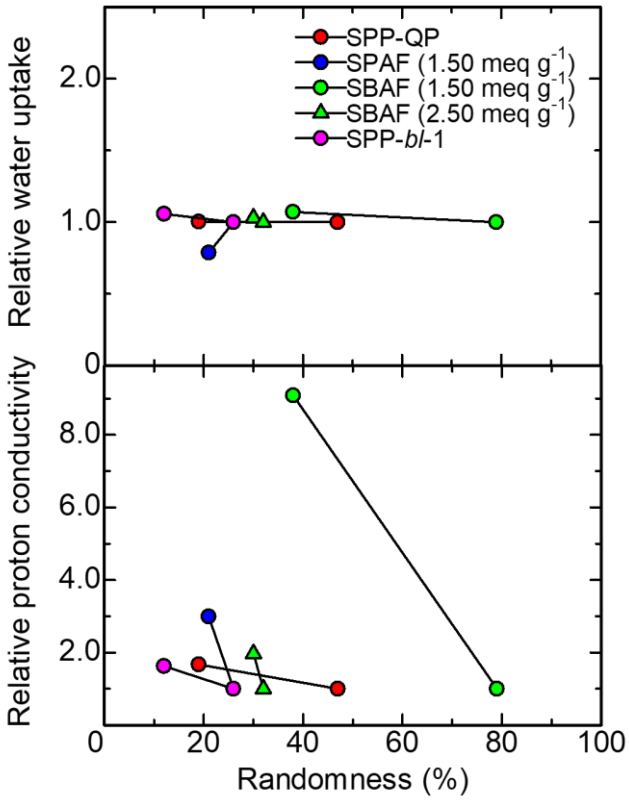

Figure 4-6. Relative water uptake and proton conductivity (defined as (C)/(B) values) of the membranes at 80 °C, 20% RH as a function of the randomness.

4.3.4 Mechanical Properties

The mechanical properties of SPP-QP (B) and (C) membranes were evaluated by tensile tests at 80 °C and 60% RH as shown in Figure 4-7. SPP-QP (B) membrane exhibited lower mechanical properties, in particular smaller elongation, than those of SPP-QP (C) membrane: Young's modulus (0.72 GPa for (B) and 1.19 GPa for (C)), maximum stress (29.6 MPa for (B) and 39.1 MPa for (C)), and elongation at break (2.57% for (B) and 68.5% for (C)). Since SPP-QP (B) and (C) were comparable in molecular weights (Table 4-1), the large differences in the tensile properties were caused by other factors. In fact, the increase of the randomness of SP unit from 19% to 47% caused significant decrease of the elongation by a factor of 1/27. For the other three copolymer membranes, similar results were observed (Figure 4-7). Increase of the randomness of SP units caused decrease in elongation by a factor of 1/8.3, 1/1.8, 1/8.3 and 1/2.6 for SPP-*bl*-1 with IEC = 2.36 meq g^{-1}, SBAF with IEC = 1.43 and 2.60 meq g^{-1}, and SPAF with IEC = 1.50 meq g^{-1}, respectively (Figure 4-8 and Table 4-2). (please note that, in these copolymer membranes, differences in the molecular weight must also be contributable.). It is assumed that the tensile properties are mostly related with the hydrophobic domains. With smaller randomness of SP units, the hydrophobic components (QP, arylene ether oligomer, BAF, and PAF) were also likely to have more sequenced structure with better connection to account for better mechanical properties of the resulting thin membranes.

Table 4-2. The tensile properties of SPP-*bl*-1, SBAF, SPP-QP and SPAF copolymer membranes at 80 °C and 60% RH

Copolymer	Young's modulus (GPa)	Maximum stress (MPa)	Elongation at break (%)
SPP-*bl*-1(B)	0.45	15.5	8.91
SPP-*bl*-1(C)	0.99	35.7	74.9
SBAF (B) 1.43	0.71	34.2	30.1
SBAF (C) 1.50	1.77	79.4	53.3
SBAF (B) 2.60	0.60	27.2	7.39
SBAF (C) 2.50	0.72	35.8	61.6
SPP-QP (B)	0.72	29.6	2.57
SPP-QP (C)	1.19	39.1	68.5
SPAF (B)	0.12	7.76	59.1
SPAF (C)	0.05	13.4	152

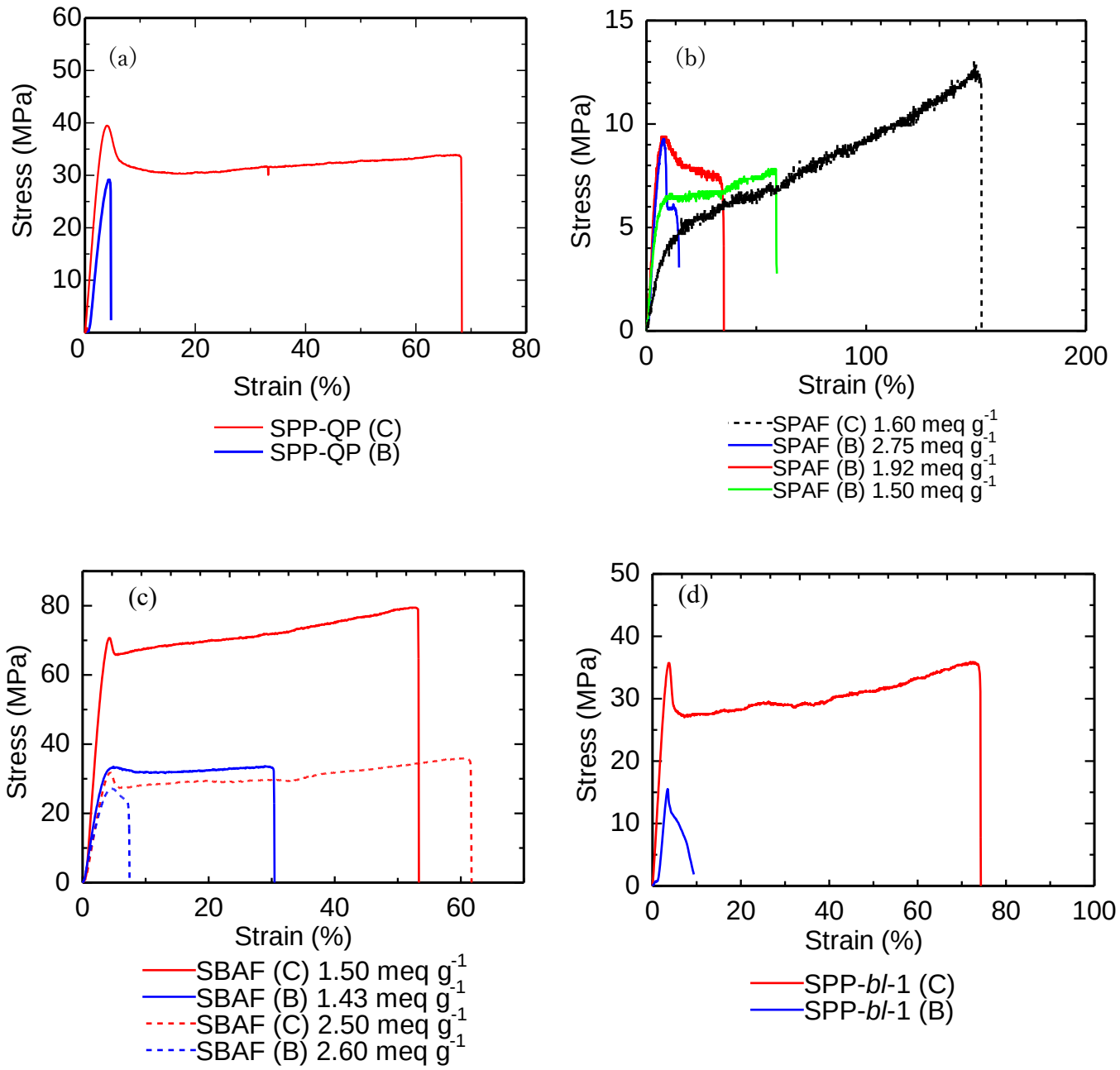

Figure 4-7. Stress versus strain curves of (a) SPP-QP series (b) SPAF series membranes, (c) SBAF series membranes and (d) SPP-*bl*-1 series membranes at 80 ºC and 60% RH.

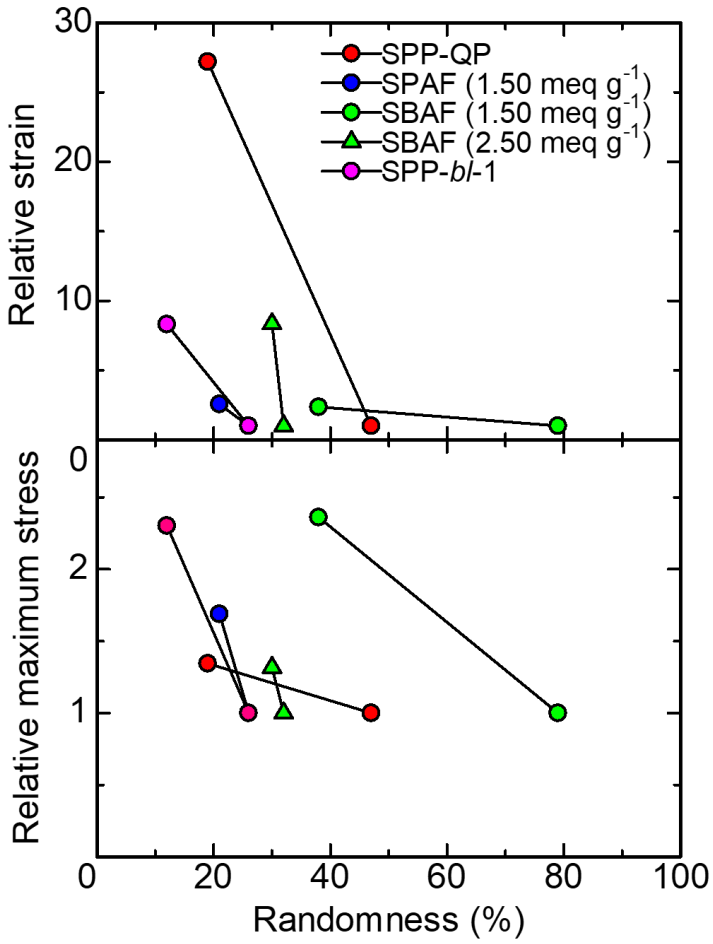

Figure 4-8. Relative strain and relative maximum stress (defined as (C)/(B) values) of the membranes at 80 °C, 60% RH as a function of randomness.

4.4 Conclusion

A series of sulfonated aromatic copolymers including arylene ether oligomer, hexafluoroisopropylidene, quinquephenylene, or perfluoroalkylene groups as hydrophobic components were successfully synthesized using $NiBr_2$ as a polycondensation promoter via the *in-situ* reduction of Ni^{2+} with Zn. The results suggest that this synthetic method is highly versatile and effective for sulfonated aromatic copolymers. The copolymers synthesized with $NiBr_2$ (B series) showed higher randomness of sulfophenylene (SP) unit in the polymer main chains compared with that prepared with $Ni(COD)_2$ (C series) due to the use of the non-ionic, protected SP monomer with low polarity as the hydrophilic component in the copolymerization reaction. The TEM images revealed that the (B) and (C) series membranes showed similar nanophase separated morphologies with ionic and non-ionic clusters under the dry conditions in spite of the large differences in the randomness of SP unit. On the other hand, the differences in the morphology were observed under the wet conditions from the SAXS analyses that the (C) series membranes possessed higher uniformity in the ionic cluster sizes compared with those of the (B) series membranes. The randomness of SP unit affected some membrane properties. The proton conductivity of the (C) series membranes with lower randomness was higher than that of the (B) series membranes, because lower randomness caused well-developed (or inter-connected) ionic channels resulting in improved proton conductivity. In the tensile tests, the (C) series membranes exhibited much larger elongations than those of the (B) series membranes. The smaller randomness of SP unit in the (C) series membranes would have caused longer sequence of the hydrophobic components, resulting in the improved mechanical properties.

4.5 Reference

1 M. M. Whiston, I. L. Azevedo, S. Litster, K. S. Whitefoot, C. Samaras, J. F. Whitacre, *PNAS* **2019**, *116*, 4899.

2 C. Arntsen, J. Savage, Y.-L. S. Tse, G. A. Voth, *Fuel Cells* **2016**, *16*, 695.

3 N. Esmaeili, E. MacA. Gray, C. J. Webb, *ChemPhysChem* **2019**, *20*, 2016.

4 J. Ran, L. Wu, Y. He, Z. Yang, Y. Wang, C. Jiang, L. Ge, E. Bakangura, T. Xu*, J. Membr. Sci.* **2017**, *522*, 267.

5 H. Lade, V. Kumar, G. Arthanareeswaran, A. F. Ismail, *Int. J. Hydrog. Energy* **2017**, *42*, 1063.

6 K. H. Lee, J. Y. Chu, A. R. Kim, D. J. Yoo, *ACS Appl. Mater. Interfaces* **2018**, *10*, 20835.

7 Y. Zhang, J. Li, L. Ma, W. Cai, H. Cheng, *Energy Technol.* **2015**, *3*, 675.

8 Y. Zhao, X. Li, S. Wang, W. Li, X. Wang, S. Chen, J. Chen, X. Xie, *Int. J. Hydrog. Energy* **2017**, *42*, 30013.

9 T. J. G. Skalski, M. Adamski, B. Britton, E. M. Schibli, T. J. Peckham, T. Weissbach, T. Moshisuki, S. Lyonnard, B. J. Frisken, S. Holdcroft, *ChemSusChem* **2018**, *11*, 4033.

10 J. Miyake, T. Mochizuki, K. Miyatake, *ACS Macro Lett.* **2015**, *4*, 750.

11 J. Ahn, R. Shimizu, K. Miyatake, *J. Mater. Chem. A* **2018**, *6*, 24625.

12 J. Miyake, R. Taki, T. Mochizuki, R. Shimizu, R. Akiyama, M. Uchida, K. Miyatake, *Sci. Adv.* **2017**, *3*, eaao0476.

13 T. Mochizuki, M. Uchida, K. Miyatake, *ACS Energy Lett.* **2016**, *1*, 348.

14 I. Hosaka, M. Kusakabe, K. Miyatake, *Chem. Lett.* **2018**, *47*, 257.

15 J. Zhao, X. He, Y. Zhang, J. Zhu, X. Shen, D. Zhu, *Cryst. Growth Des.* **2017**, *17*, 5524.

16 L.-J. Zhou, W.-H. Deng, Y.-L. Wang, G. Xu, S.-G. Yin, Q.-Y. Liu, *Inorg. Chem.* **2016**, *55*, 6271.

17 Y. Dong, G. Liu, *Chem. Commun.* **2013**, *49*, 8066

18 T. Mochizuki, K. Kakinuma, M. Uchida, S. Deki, M. Watanabe, K. Miyatake, *ChemSusChem* **2014**, *7*, 729.

19 B. Bae, T. Hoshi, K. Miyatake, M. Watanabe, *Macromolecules* **2011**, *44*, 3884.

20 Y. Hu, X. Li, L. Yan, B. Yue, *Fuel Cells* **2017**, *17*, 3.

Chapter 5: General conclusion and Future proposal

5.1 General conclusion

Sulfonated aromatic ionomer membranes are greatly demanded as alternatives to the PFSA ionomers, however, chemically stable sulfonated aromatic ionomer with cost-effectiveness has not been developed yet. Therefore, the objective of this PhD research is to develop a highly proton conductive sulfonated aromatic ionomer with high chemical stability in consideration of mass production and dissemination. To accomplish this objective, two approaches, i.e., effect of radical quencher and elimination of ether linkage, have been tried and investigated.

In chapter 2, a new type of aromatic block copolymer (PP) containing dense sulfonated triphenylphosphine oxide moieties in the hydrophilic blocks was successfully prepared, and the effect of triphenyl phosphine oxide on oxidative stability was investigated. Introduction of sulfonated triphenylphosphine oxide moieties to hydrophilic component is effective in improving the oxidative stability of the membranes. However, detailed comparison with the PK membrane sharing similar hydrophobic blocks but a smaller content of sulfonated triphenylphosphine oxide moieties revealed that the dense introduction of sulfonated triphenylphosphine oxide moieties led to higher water uptake, resulting in the decrease in the oxidative stability of the membranes. Thus, the position and content of the sulfonated triphenylphosphine oxide moieties should be optimized for further improving the properties. The Proton conductivity of PP membrane was significantly lower than general aromatic hydrocarbon membrane. There seemed two reasons for low proton conductivity. The First is difficult to obtain the membrane containing the phosphine oxide moieties with high IEC. The copolymer containing phosphine oxide moiety in the hydrophilic part showed the high

solubility in water because of large polarization between phosphine and oxygen double bonding. The PP copolymer with high IEC dissolved into the water during the purification process and couldn't be isolated as the membrane form. The second reason is inhibition of proton conduction by triphenylphosphine oxide moiety. In general, phosphine oxide serves as the Lewis bases, resulting in the neutralization with proton of sulfonic acid. Thus, amount of active proton species for proton conduction decrease, which cause the decrease of proton conductivity.

In chapter 3, the versatile synthetic method of aromatic polymers using $NiBr_2$ via *in-situ* reduction of Ni(II) to Ni(0) have been successfully applied to several sulfonated copolymers. The obtained copolymer had similar molecular weight, chemical structure, membrane-forming capability, and proton conductivity compared with those of the copolymers prepared by the previous method using costly and air-sensitive Ni(0). The results not only strengthen the advantages of aromatic polymer-based ionomers for fuel cell applications but also may open applicability of this versatile polymerization method to other functional aromatic polymers. Moreover, effect of difference in the synthetic route between conventional method with Ni(0) complex and new method with $NiBr_2$ on the membrane properties such as proton conductivity, mechanical property and membrane morphology was also investigated in detail in Chapter 4. The copolymers synthesized with $NiBr_2$ (B series) showed higher randomness of sulfophenylene (SP) unit in the polymer main chains compared with that prepared with $Ni(COD)_2$ (C series). The differences in the morphology were observed under the wet conditions from the SAXS analyses that the (C) series membranes possessed higher uniformity in the ionic cluster sizes compared with those of the (B) series membranes. The

proton conductivity of the (C) series membranes with lower randomness was higher than that of the (B) series membranes, because lower randomness caused well-developed (or inter-connected) ionic channels resulting in improved proton conductivity. In the tensile tests, the (C) series membranes exhibited much larger elongations than those of the (B) series membranes. The smaller randomness of SP unit in the (C) series membranes would have caused longer sequence of the hydrophobic components, resulting in the improved mechanical properties.

5.2 Future proposal

Based on these results, elimination of ether linkages from the polymer backbone via new versatile synthetic method with $NiBr_2$ investigated in PhD. thesis is significantly effective compared with introducing of phosphine oxide to polymer main chain as radical quencher in membrane to obtain the proton exchange membrane with high oxidative stability and cost-effectiveness. One of the new challenges is to apply the new versatile synthetic method with $NiBr_2$ to the general method using the sulfonic acid monomer. New versatile synthetic method using $NiBr_2$ is required the low polarization monomer by protection to sulfonic acid group, causing the complex synthetic procedure. Therefore, the reaction condition for synthesis aromatic hydrocarbon ionomer is needed for further improvement of versatility for new synthetic method. Up to this thesis, the amount and selection of Ni (II) were optimized. However, investigation of effect of the ligand on the molecular weight for aromatic ionomer is not carried out yet. To improve the versatile synthetic method with $NiBr_2$, the optimization of the amount and selection of ligand are required. Specifically, monodentate ligand such as

triphenylphosphine, trimethylphosphine and triethylphosphine will be used for C-C coupling reaction, and the effect of deference in the monodentate and bidentate ligand on molecular weight will be studied in detail.

In chapter 4, it is clarified that primary-structure of polymer greatly affects the membrane property such as proton conductivity and mechanical property. For further improvements of membrane performance, the sequence of polymer main chain should be considered in future works. It is expected that longer sequenced structure in polymer main chain shows the superior proton conductivity and excellent mechanical property. However, it should be noted here that too large-scale phase-separated morphology resulted in the decrease of utilization of Pt, causing the performance decrement of fuel cell.[1] To prepare the proton exchange with longer sequenced structure, two approaches are suggested as follows.

1: Changing the reaction scheme

In the new synthetic method investigated in PhD. thesis, hydrophobic and hydrophilic monomer were added to reaction system at the same time, which provided the random copolymer with high randomness of SP unit. To prepare the copolymer with longer sequenced structure i.e. low randomness of SP unit, new reaction scheme is suggested as follow (Figure 5-1). Hydrophobic monomer is polymerized at first, and then hydrophilic monomer is added to reaction system and polymerized with hydrophobic component. This newly reaction procedure might provide the copolymer with low randomness of SP unit. Moreover, the randomness of SP unit could be controlled by changing the polymerization time of hydrophobic monomer, which can clarify the effect of primary-structure on membrane property in particular proton conductivity and mechanical property in detail.

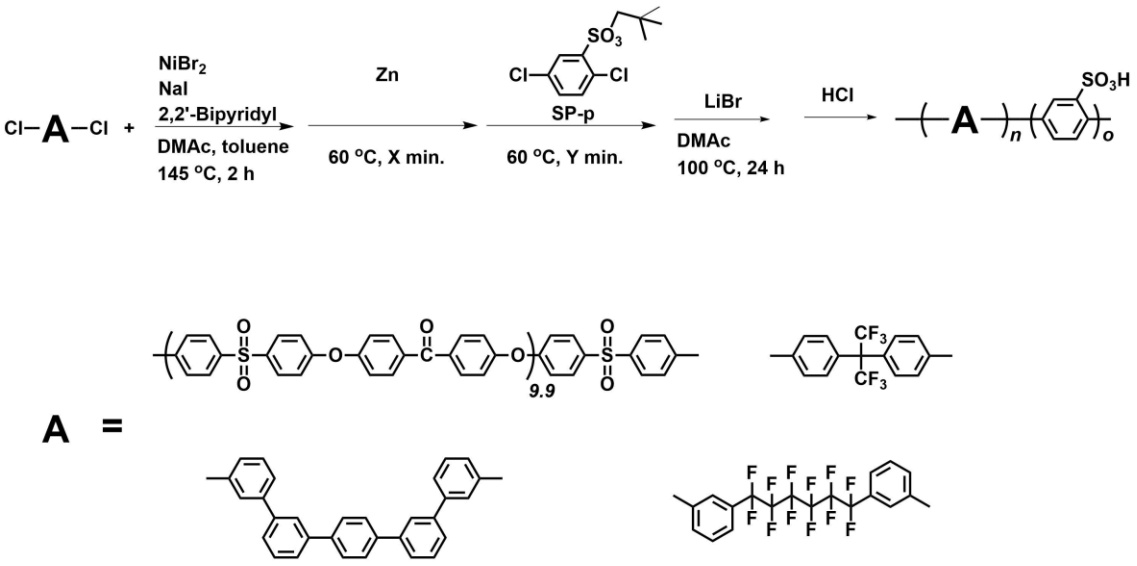

Figure 5-1. New reaction procedure to prepare copolymer with low randomness of SP

2: Synthesis of new hydrophobic monomer

Sulfonated longer sequenced perfluoroalkylene and hexafluoroisopropylidene polymer (SDPAF and SDBAF) is suggested to understand the effect of the length of polymer sequence on membrane property (Scheme 5-1). These copolymers may clarify the detail of correction between primary-structure in polymer main chain and membrane property, which will give the guideline for proton exchange membrane with superior properties.

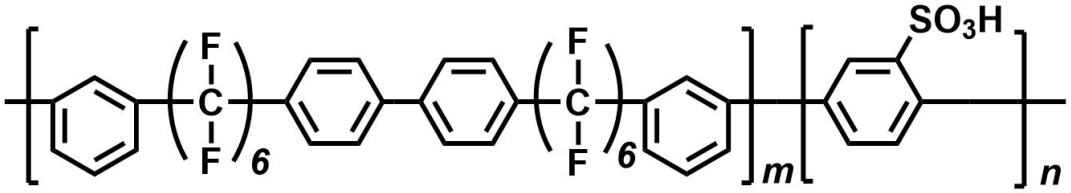

SDPAF

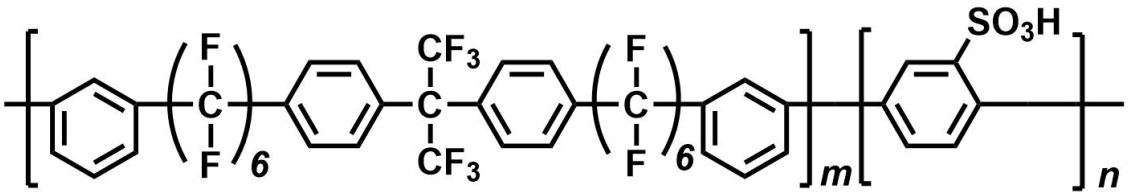

SDBAF

Figure 5-2. Chemical structures of SDPAF and SDBAF copolymer.

1 T. Mochizuki, M. Uchida, H. Uchida, M. Watanabe, K. Miyatake, ACS Appl. Mater. Interfaces **2014**, *6*, 13894

List of publications

1. Effect of Sulfonated Triphenylphosphine Oxide Groups in Aromatic Block Copolymers as Proton-exchange Membranes

   J. Miyake, I. Hosaka, and K. Miyatake, *Chem. Lett.* **2016**, *45*, 33

2. Versatile Synthesis of Sulfonated Aromatic Copolymers Using NiBr2

   I. Hosaka, M. Kusakabe, and K. Miyatake, *Chem. Lett.* **2018**, *47*, 257

3. Differences in the Synthetic Method Affected Copolymer Sequence and Membrane Properties of Sulfonated Polymers

   I. Hosaka, T. Sawano, T. Kimura, A. Matsumoto, J. Miyake, and K. Miyatake

   Bull. Chem. Soc. Jpn.

Meeting Abstracts

1. 64th SPSJ Annual Meeting, Sapporo, Japan (2015.5)

I. Hosaka, F. T. Hartanti, Z. Yaojian, R. Akiyama, J. Miyake, M. Watanabe, K. Miyatake

2. The 4th International seminar on Green Energy Conversion Summer School for Young Scientists, Kofu, Japan (2015.8)

I. Hosaka, F. T. Hartanti, Z. Yaojian, R. Akiyama, J. Miyake, M. Watanabe, K. Miyatake

3. The 7th International Fuel Cell Workshop, Kofu, Japan (2015.8)

I. Hosaka, F. T. Hartanti, Z. Yaojian, R. Akiyama, J. Miyake, M. Watanabe, K. Miyatake

4. The 5th International Seminar on Green Energy Conversion Summer School for Young Scientists, Koumi, Japan (2016.8)

I. Hosaka, R. Akiyama, J. Miyake, K. Miyatake

5. The 11th SPSJ International Polymer Conference, Fukuoka, Japan (2016.12)

I. Hosaka, R. Akiyama, J. Miyake, K. Miyatake

6. The 7th International Seminar on Green Energy Conversion Summer School for Young Scientists, Kofu, Japan (2018.8)

I. Hosaka, M. Kusakabe, K. Miyatake

7. The 8th International Fuel Cell Workshop, Kofu, Japan (2018.8)

I. Hosaka, M. Kusakabe, K. Miyatake

8. 68th SPSJ Annual Meeting, Osaka, Japan (2019.5)

I. Hosaka, T. Sawano, M. Kusakabe, J. Miyake, K. Miyatake

9. Workshop on Ion Exchange Membranes for Energy Applications, Bad Zwischenahn, Germany (2019. 6)

I. Hosaka, T. Sawano, M. Kusakabe, J. Miyake, K. Miyatake

10. The 8th International Seminar on Green Energy Conversion Fall School for Young Scientists, Kofu, Japan (2019.10)

I. Hosaka, T. Sawano, M. Kusakabe, J. Miyake, K. Miyatake

Awards

1. ISE Poster Award

The 7th International Fuel Cell Workshop, Kofu, Japan (2015.8)

"Effect of phosphine oxide groups in the sulfonated aromatic multiblock copolymers as proton exchange membrane"

I. Hosaka, F. T. Hartanti, Z. Yaojian, R. Akiyama, J. Miyake, M. Watanabe, K. Miyatake

2. Poster Award

5th International Seminar on Green Energy Conversion Summer School for Young Scientists, Koumi, Japan (2016.8)

"Synthesis and characterization of sulfonated aromatic copolymers containing phosphine oxide groups as chemically stable proton exchange membrane"

I. Hosaka, R. Akiyama, J. Miyake, K. Miyatake

3. IPC 2016 Young Scientist Poster Award

The 11th SPSJ International Polymer Conference, Fukuoka, Japan (2016.12)

"Sulfonated aromatic polymers containing phosphine oxide groups as chemically stable proton exchange membranes"

I. Hosaka, R. Akiyama, J. Miyake, K. Miyatake

Acknowledgments

This present thesis is the summary of studies at Clean Energy Research Center, Fuel Cell Nanomaterials Center, and Interdisciplinary Graduate School of Medicine and Engineering in University of Yamanashi from 2014-2020. This research was supported by funds for the "Research on Nanotechnology for High Performance Fuel Cell" (Hiper-FC) project and "Superlative, Stable, and Scalable Performance Fuel Cell" (Sper-FC) project from the New Energy and Industrial Technology Development Organization (NEDO).

I would like to express my deepest gratitude to Professor Kenji Miyatake of University of Yamanashi for this academic supervisor of this work, for his continuous guidance, invaluable suggestion, and warm encouragement throughout the study.

I also would like to express my gratitude to Professor Masahiro Watanabe, Professor Akihiro Iiyama, and Professor Hiroyuki Uchida and Assistant Professor Junpei Miyake for his invaluable advice and encouragement.

Sincere gratitude is expressed to Professor Shigehito Deki, Professor Junji Inukai, Professor Makoto Uchida, Professor Kazutoshi Higashiyama, Professor Tomio Omata, Professor Takao Tsuneda, Professor Mitsuru Wakisaka, Professor Toshihiro Miyao, Associate Professor Shinji Nohara, Associate Professor Hiroshi Yano, Associate Professor Shinji Nohara, Associate Professor Masanori Hara, and Assistant Professor Hanako Nishino for their suggestions, advice and discussions as well as continuous encouragement throughout the work.

I would like to express my gratitude to Professor Donald Alexander Tryk and Professor Manuel E. Brito for your kindness, helpful English support and useful advices.

Sincere gratitude is also expressed to all staffs of Clean Energy Research Center, Fuel Cell Nanomaterials Center, and Special Doctoral Program for Green Energy Conversion Science and Technology for their kind help.

I am grateful to Ms. Toshiko Gomyo and Ms. Setsuko Mori for assistance of the and TEM measurements.

I would like to thank Dr. Takayuki Hoshi, Dr. Morio Chiwata, Dr. Yuji Chino, Dr. Yuya Yamashita, Dr. Kazuhiro Takanohashi, Mr. Masaki Saito, Dr. Ryo Shimizu, Dr. Hideaki ohno, Ms. Chisato Arata, Mr. Ryunosuke Taki, Mr. Shigefumi Shimada, Mr. Masuda, Takashi, Mr. Jun Fukasawa, Mr. Ikkei Arima, Mr. Takumi Kuroda, Mr. Takuya Nakamura, Mr. Seiya Kosaka, Mr. shun Kobayashi, Mr. Taro Kimura and Mr. Yuma Shimizu and Mr. Keisuke Shino for their kindly support.

I would like to thank deeply Dr. Ryo Akiyama, Dr. Naoki Yokota, Dr. Akinobu Matsumoto, Dr. Masaru Sakamoto. Dr. Manai Shimada, Dr. Hideaki Ono, Dr. Takashi Mochizuki, Dr. Zhang Yaojian, Dr. Jinju Ahn, Ms. Febrina Tri Hartanti, Ms. Natsumi Yoshimura, Mr. Long Zhi, Mr. Daniel Koronka, Ms. Mizuki Ozawa, Ms. Reika Oida, Mr. Toshiki Tanaka, Mr. Kanji Otsuji, Ms. Liu Fanghua, Mr. Takayuki Watanabe, Mr. Takatoshi Sawano, Mr. Yasunari

Ogawa and Mr. Yuto Shirase for their grateful support.

I am grateful to Professor Chulsung Bae, Dr. Stefan Turan, Dr. Sangtaik Noh, Dr. Kihyun Kim, Dr. Junyoung Han, Dr. Jong Yeob Jeon, Mr. Ding Tian, Mr. Mike Pagels and Chandula Walgama of Rensselaer Polytechnic Institute (RPI) for for their kindly support and invaluable discussion.

Once again, I would like to thank all members in laboratory of Clean Energy Research Center and Fuel Cell Nanomaterials Center for their help.

I would like to express my heartily gratitude to my parents, Mr. Masaki Hosaka and Mrs. Yoko Hosaka and to my sister, their support and sincere
encouragement.

Finally, I would like to express my heartily gratitude to the best wife in the world, Ms. Saki Hosaka, their support and sincere.

March 2020

Ibuki Hosaka